NASA CONTRACTOR REPORT

NASA CR-592

MATRIX HOLZER ANALYSES FOR FULLY-COUPLED VIBRATIONS OF CLUSTERED LAUNCH-VEHICLE CONFIGURATIONS INCLUDING APPLICATIONS TO THE TITAN IIIC AND UNCOUPLED SATURN I CASES

by Robert G. Loewy and Mukund M. Joglekar

Prepared by
UNIVERSITY OF ROCHESTER
Rochester, N. Y.
for

NATIONAL AERONAUTICS AND SPACE ADMINISTRATION • WASHINGTON, D. C. • DECEMBER 1966

NASA CR-592

MATRIX HOLZER ANALYSES FOR FULLY-COUPLED VIBRATIONS OF CLUSTERED LAUNCH-VEHICLE CONFIGURATIONS INCLUDING APPLICATIONS TO THE TITAN IIIC AND UNCOUPLED SATURN I CASES

By Robert G. Loewy and Mukund M. Joglekar

Prepared under Grant No. NsG-469 by
UNIVERSITY OF ROCHESTER
Rochester, N.Y.

for

NATIONAL AERONAUTICS AND SPACE ADMINISTRATION

For sale by the Clearinghouse for Federal Scientific and Technical Information
Springfield, Virginia 22151 – Price $3.00

Preface

This study has been conducted under the direction of Messers. Harry Runyan, Homer Morgan, and Elwood Peele of the Langley Research Center, NASA. The computer programming was performed by Mr. Norman Plyter of the University of Rochester Computing Center Staff.

SUMMARY

A general matrix-Holzer method is developed for predicting the free vibration modes of clustered launch vehicles. The problem is so formulated that it can be adapted to the analysis of clustered structures capable of vibrating in various types of modes. A complete theoretical analysis of the fully-coupled vibrations of the Titan IIIC launch vehicle is followed by analysis of the transverse bending vibrations of the Saturn I. The latter is a simplification of the fully-coupled case specialized to the Saturn cluster boundary conditions. The first six transverse bending modes of the NASA Saturn I 1/5 scale model are calculated and compared with test results. A procedure for predicting the longitudinal vibration modes of Saturn I is also presented, and represents a second specialization of the fully coupled case.

The formulation minimizes numerical operations by invoking symmetry where possible and by postponing satisfaction of compatability of deflections at cluster attachments until the last steps. Any kind of cluster boundary conditions can be represented in such a matrix-Holzer analysis, as illustrated by the two examples studied. Not only do the cluster boundary conditions of the Titan IIIC differ significantly from those of the Saturn I, but different cluster boundary conditions are also encountered in the same vehicle (Saturn I) depending on the direction of motion considered.

The method developed here can account for (1) cluster body motion, longitudinal as well as in and out of plane of the centerbody motion; (2) cluster attachment flexibility; (3) various clusterbody end conditions, differing amoung cluster bodies from end to end and between bending planes; (4) steady axial loads; (5) liquid sloshing; (6) shear deflections and rotary mass moments of inertia; (7) structural elements overhanging from the main body of the vehicle such as rocket engines and cluster body overhangs forward of the forward cluster attachments and aft of the aft cluster attachments; (8) discontinuities in bending and torsion properties at staging joints.

TABLE OF CONTENTS

LIST OF TABLES

LIST OF FIGURES

LIST OF FIGURES (cont'd)

LIST OF FIGURES (cont'd)

LIST OF FIGURES (cont'd)

LIST OF FIGURES (cont'd)

INTRODUCTION

The importance of the dynamic deformations of large missiles, and in particular knowledge of the natural frequencies and mode shapes, can be related to several continuing problems. Structural natural frequencies should be placed, for example, so as not to excite fuel-sloshing, or premature rocket engine cut-off could occur. The minimum bending slope points should be known so that control system gyros can be placed where they will sense rigid pitch and yaw, which are indicative of the vehicle's course, rather than flexible body motion. Structural loads resulting from response to dynamic excitation, such as wind shears, must be predicted for design purposes, and the natural modes are basic inputs in such structural calculations, as they are for control system stability analyses. Methods for predicting the natural frequencies of launch vehicles at the earlies possible design stage, therefore, continue to be actively pursued.

Clustered configurations, where a number of tanks are arranged in a concentric ring or in a "piggy-back" arrangement on a central tank, have recently come into use, and will be of interest whenever it seems profitable to gang existing boosters to achieve still higher thrusts. Such arrangements, from a structural viewpoint, comprise closed, branched-beam systems, and there is relatively little experience with the dynamics of such systems.

It is usual to assume that launch vehicles have symmetry about a plane through the longitudinal axis of the configuration. The cross sections of individual bodies, in fact, are very close to being polar symmetric, and the array of cluster-bodies is generally symmetric about the center-body. The attachment of clustered bodies to the center-body, however, is usually such that deflections relative to the center-body in the radial direction differ, in general, from those in the tangential direction. As a result, unless the motion of a cluster-body support point is solely in a radial or tangential plane, that cluster-body will respond in two planes. This has been evident in reports of shake tests conducted at NASA, Langley (References 1 and 2). If, however, one or more of the bodies lacks axial symmetry or if the cluster array is unsymmetrical, then the entire array may not only experience oscillatory bending in two planes, but couple with torsional and extensile vibrations, as well. Even in the simpler, symmetric case, the lateral offset of the clustered body's neutral axis from the vehicle center-line suggests that longitudinal compression and extension are essential to the mathematical model, whether or not additional degrees of freedom need to be included for such motion. It follows that flexibility of cluster-body supporting structure must also be accounted for, and that the special joints often used at such attachments must be properly represented.

In addition to characteristics unique to clustered configurations, other effects encountered in the design of more conventional vehicles must still be considered. First stage booster rockets, for example, can deliver high longitudinal accelerations near burn-out. The resulting longitudinal compression loads can have an appreciable effect on the first stage effective stiffness characteristics, and hence on the vehicle's natural modes and frequencies. In addition, cluster-body supporting structures are likely to have rotary mass moments of inertia sufficiently large to require that the analysis be capable of accounting for such mass properties. Further, the depth to length ratio of certain sections of the vehicle such as the "barrel" in the Saturn model (see figure 1a), strongly suggests that transverse shear deflections may not be ignored. Finally, the coupling effects of fundamental fuel sloshing and rocket engine natural frequencies considered as subsystems mounted to "ground" should be represented.

All these "secondary" effects are more likely to affect branched systems than their simpler counterparts. There is a tendency for one or more of the system natural frequencies to fall relatively close to a natural frequency of a cluster-body or center-body considered separately from the rest of the vehicle. Small changes, then, due to any of the usually small effects discussed above, can in such cases have appreciable influence on the system natural frequency and often result in really substantial differences in the associated mode shape. This pertains particularly to the motions which might normally be assumed uncoupled by virtue of neglecting small disymmetries.

One of the earliest published theoretical attacks on this problem is in a paper by Hung and Stone (Reference 3). The Myklestad method was applied in matrix form to the vibrations, in a single plane, of a beam with two branches mounted on a center tank. Shear deflections were taken into account, but extensile loads and motions of the bodies off the neutral axis, flexibility of attachment structure, and subsystem degrees of freedom, were not.

The special case of four uniform beams of circular cross section, coupled symmetrically at their ends thru pinned joints, and undergoing torsional oscillations about a longitudinal axis thru the center of the cluster, was analyzed by Lianis and Fontenot (Reference 4). They used a continuous system approach. The uncoupled, differential equations for bending and torsion were coupled by the boundary conditions and led to a 40 x 40 transcendental characteristic determinant for natural frequencies of modes in which torsional oscillations are coupled with radial and tangential bending. A lumped parameter approach was also described briefly. Apparently influence coefficients were obtained and a Dynamic Matrix (The "D" matrix in the notation of Bisplinghoff, Ashley and Halfman, Reference 5) set up, which yields the natural frequencies of four non-uniform bodies in the same arrangement.

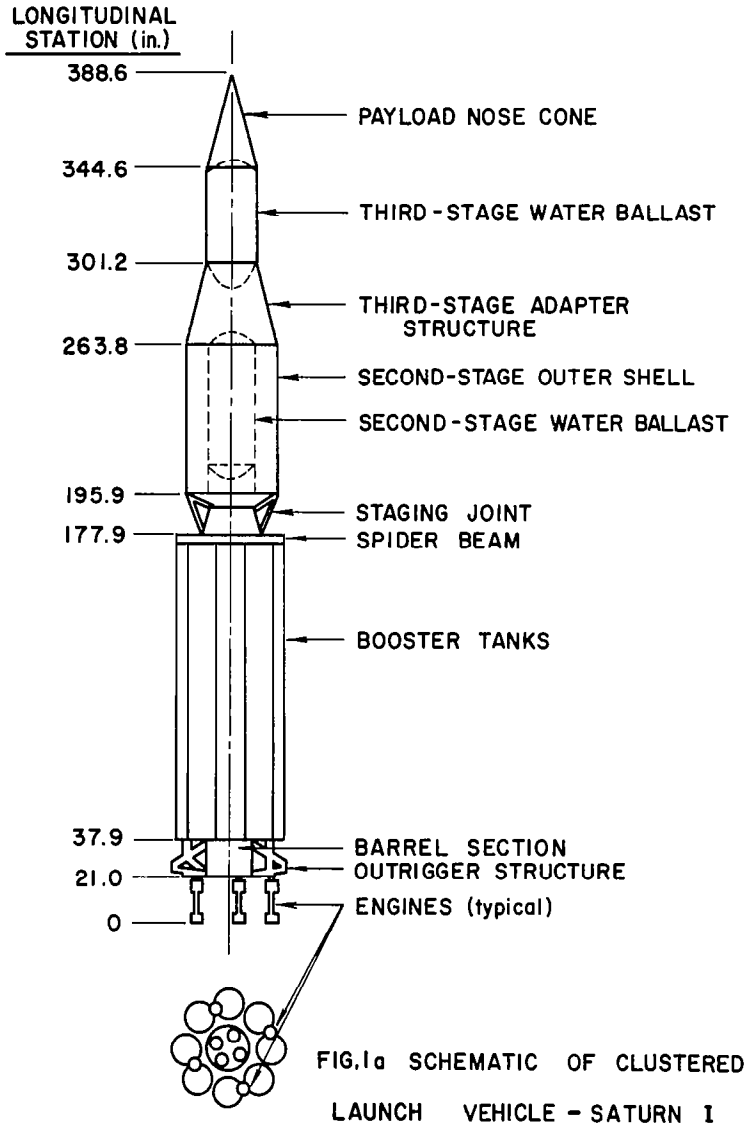

FIG. 1a SCHEMATIC OF CLUSTERED LAUNCH VEHICLE - SATURN I

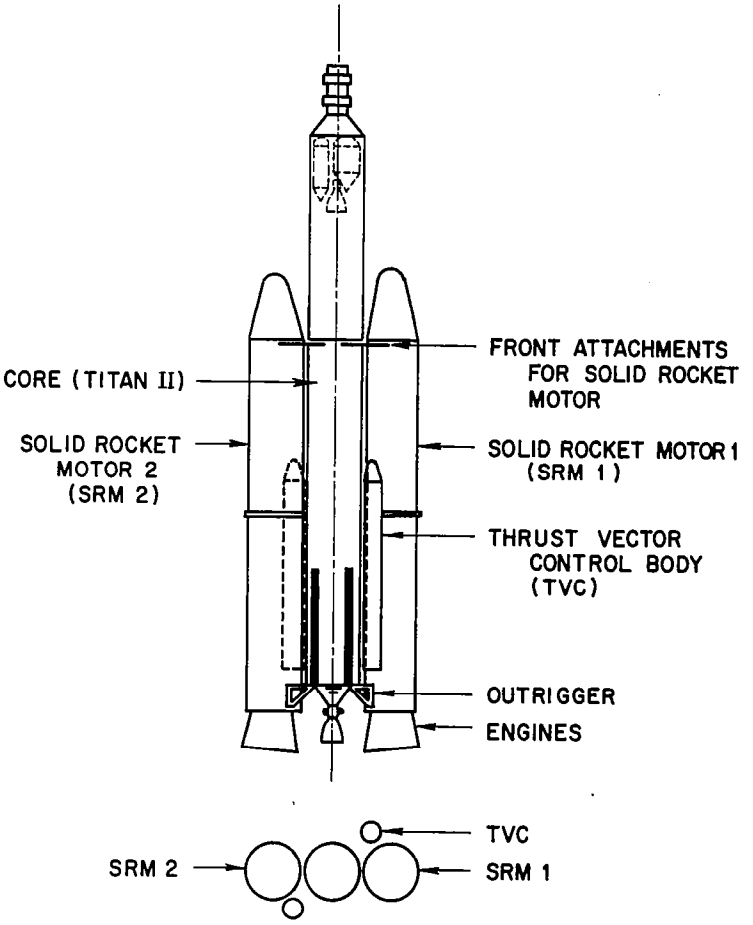

FIGURE 1b SCHEMATIC OF CLUSTERED LAUNCH VEHICLE - TITAN III C

Analysis of the Titan IIIC (Fig. 1b) three-body configuration*, emphasizing the effects of attachment flexibility, was carried out by Storey (Reference 6). Offsets of the centers of gravity of cross sections of individual bodies from their centerlines were neglected. The oscillatory behavior of the system could thus be simplified to three uncoupled motions; (1) bending of the centerbody in the plane of the clustered bodies coupled to extensile motion of the cluster-bodies plus their bending in the same plane; (2) twisting and bending of the cluster-bodies normal to the plane of their attachment, in concert, plus similar bending of the center-body; and (3) opposed bending of the clustered bodies, normal to the plane of their attachment, plus torsion coupled to center-body torsion. This formulation calculates flexibility influence coefficients by energy methods, eliminates redundant loads by requiring compatibility of deflections at joints, and forms a Dynamic Matrix which is used to calculate the eigen-values. The order of this matrix, of course, is the total number of degrees of freedom in the representations; e.g. even presuming symmetry, using 10 mass points for bending and 5 for longitudinal motion of the cluster-body, and 20 for bending of the center-body, leads to a 35 x 35 dynamic matrix for this case of two clustered bodies.

Milner (Reference 7) carried out a multiple-beam analysis of the Saturn I, using a Rayleigh-Ritz approach, and a generalized coordinate approach to clustered configureations was recently published by J.S. Keith et al (Reference 8). In an appendix of the latter reference, the NASA 1/5 Scale Saturn I model is analyzed for lateral vibrations using the suggested approach. Although complexity in analysis is like beauty, i.e. it exists only in the eye of the beholder, the number of subformulations required, and the number of modes which must be used as coordinates to insure accuracy, detracts from this method as a means of analyzing clustered configurations.

All of the usual methods for analyzing non-uniform systems can be thought of as either (1) requiring the assumption or precalculation of deflection shapes for the system or its subsystems (e.g. Rayleigh-Ritz, Lagrange's equations with normal modes as generalized coordinates); (2) setting up a Dynamic Matrix through the calculation of either stiffness or flexibility influence coefficients; or (3) establishing transfer matrices preparatory to applying the holzer technique. As mentioned regarding References 7 and 8, a rather large number of modes must be used for clustered configurations in the first approach. Perhaps more important, this method is best adapted to situations for which there is a background of considerable experience. The number of variations possible with clustered arrangements exposes the analysist using the first of these approaches to the danger of neglecting some significant but inobvious mode of motion.

---

*Throughout this report reference to "Titan III" implies the clustered "C" configuration.

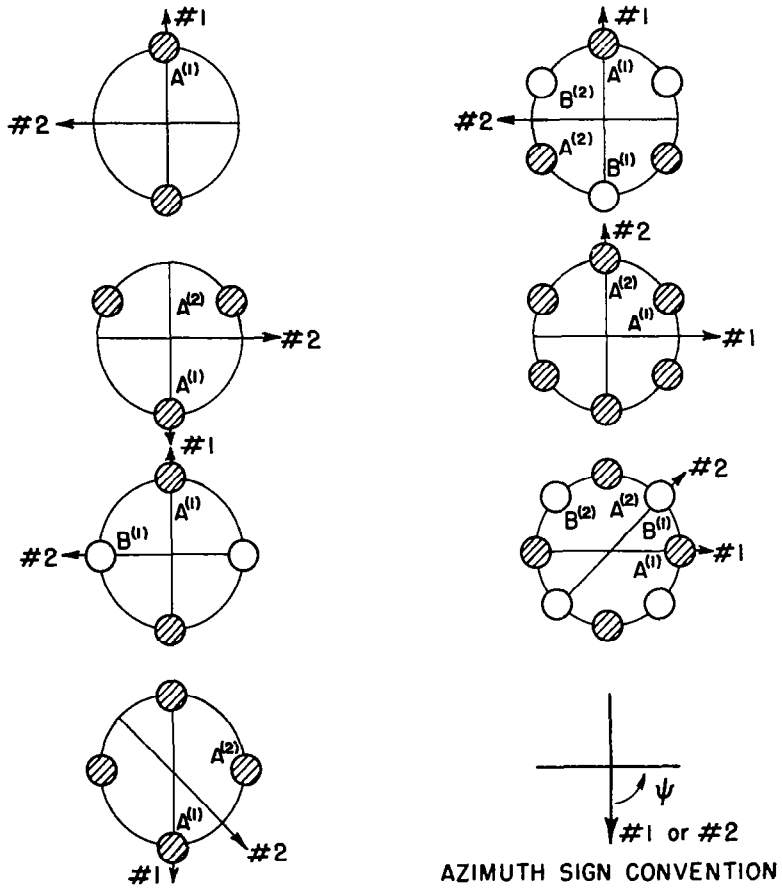

Figure 2. Cluster Configurations and Principal Axis Convention

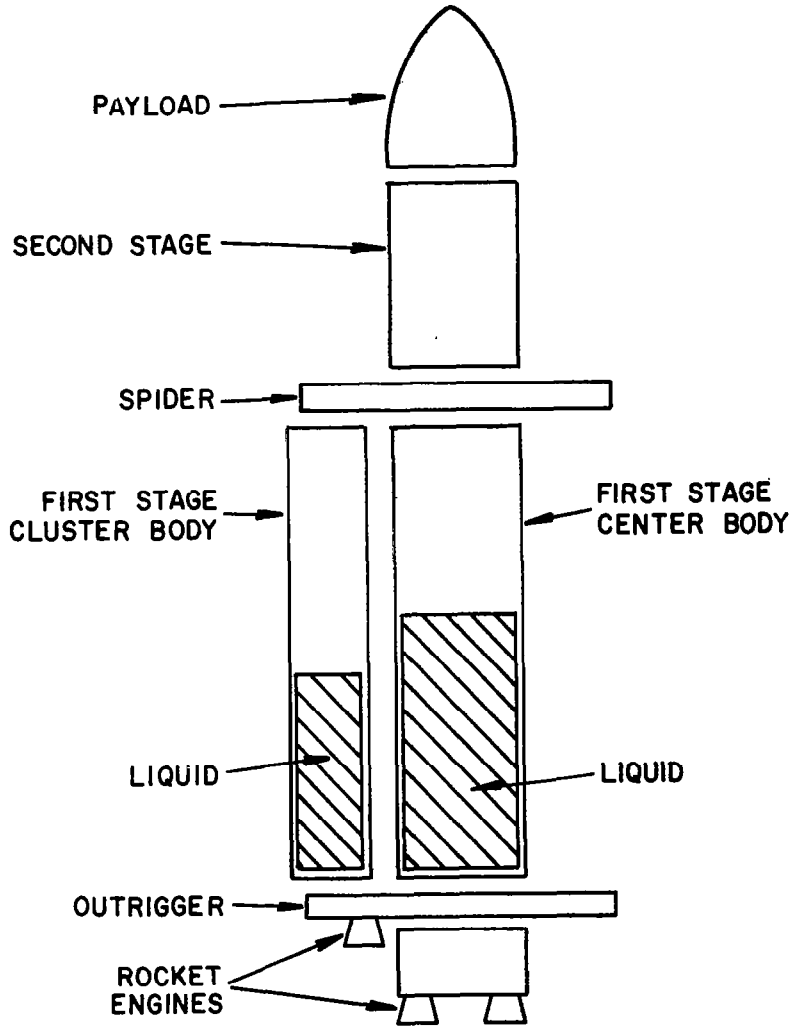

FIG. 3a. CLUSTERED LAUNCH VEHICLE BREAKDOWN FOR ANALYSIS (SATURN TYPE)

Comparison of the relative advantages of the last two methods fills the literature, but it is profitable to review the important points here. The Dynamic Matrix method is adapted to an iteration procedure which quickly converges to the first mode. The first mode results must be used, however, if the same iteration scheme is to work for higher modes. This is often cited as a disadvantage, since the errors of the lower modes creep successively into larger errors for succeeding modes. Actually, the higher modes could be solved from the original dynamic matrix by other schemes, such as determinant expansions with a series of trial values assumed for the unknown frequency. In this way, the evaluation of each frequency would be independent of the other, as it is in the Matrix-Holzer method.

A more pertinent benefit in using the Matrix-Holzer approach stems from the fact that the bulk of the numerical work can be performed independent of boundary conditions. Imposing boundary conditions at the last steps of the calculation, has a distinct advantage for systems where more than one set of boundary conditions may be of interest. Furthermore, where bodies are duplicated, and/or have polar symmetry and are free to move in two planes, the "transfer" from one end of such bodies to the other need only be done once. The reduction in labor achieved by using this technique for clustered configurations will become apparent. Most important, the ease with which representation of very complex systems can be formulated using the Matrix-Holzer approach is a powerful argument in its favor.

In the following sections, the general approach is described; transfer relations are written in matrix form, drawing on previously published material where possible; and application is made to two clustered launch vehicles, the Titan IIIC and Saturn I. The Titan III case is a fully-coupled formulation, specialized to that vehicle. Sufficient symmetry exists on Saturn I so that no significant increase in complexity is entailed in presenting an analysis capable of handling configurations with from two to eight clustered bodies, either all the same or consisting of two kinds, (see figure 2). In this case lateral bending vibrations of the center-body in one of two planes of symmetry is emphasized. The analyses are capable of accounting for the effects of:

1. independent bending motions of clustered elements in and out of the plane of motion of the center-body, torsion and longitudinal motion .
2. flexibility of clustered element attachments.
3. various end conditions of cluster-body attachment, differing among clustered element types, from one bending plane to another , and from one end of the clustered bodies to another.
4. steady axial loads in all elements due to either accelerations or preload.
5. coupling due to fundamental sloshing and rocket engine natural frequencies.
6. shear deflections and rotary mass moments of inertia.
7. discontinuities in bending and torsion properties at staging joints .
8. structural elements overhanging from the points of support of the clustered bodies.

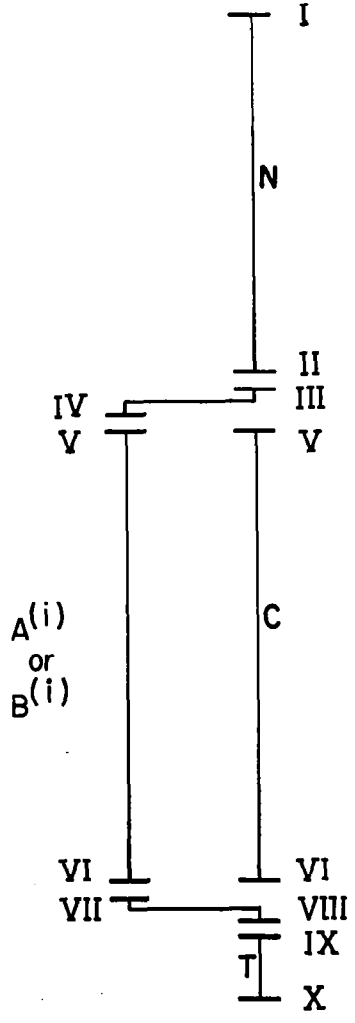

Fig. 3b MATHEMATICAL MODEL FOR SATURN I

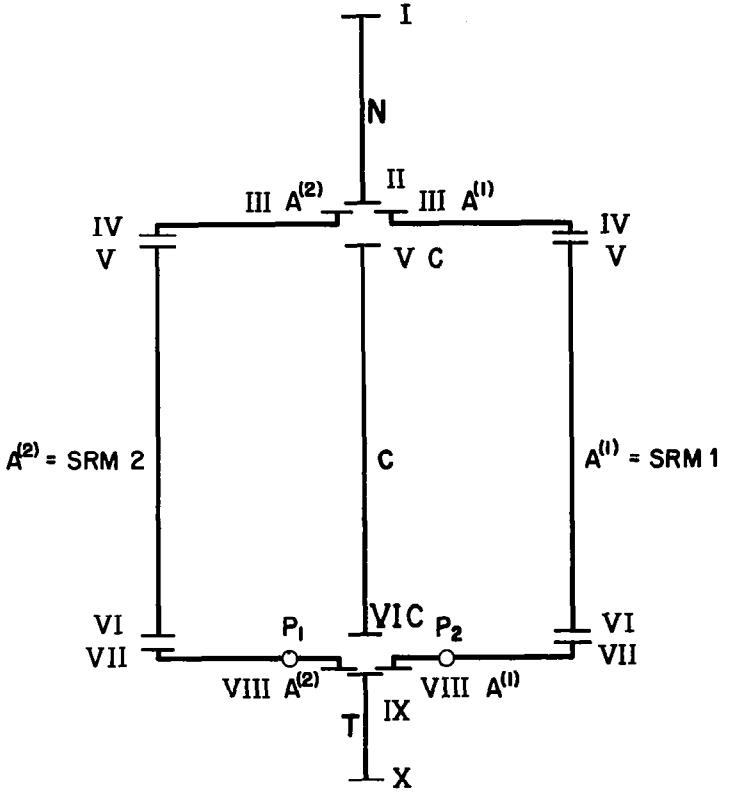

FIG. 3c MATHEMATICAL MODEL FOR TITAN III C

I. ANALYTICAL DEVELOPMENT

A. General

In review, it is noted that the Matrix-Holzer or transfer-matrix procedure (References 9, 10, 11) is simply an adaptation of the Holzer or Myklestad method in matrix form. The first step in the approach is to "break down" the continuous system into (a) mass properties considered infinitesimal in length i.e. "lumped", (b) lengths of massless, elastic members of various flexibilities, and (c) special concentrated elastic elements such as may occur at staging joints. "Transfer matrices" are written for each such element, relating the pertinent quantities (deflections, forces, moments) on the left of the element to those on the right, or relating bottom to top, in the case of launch vehicles. These quantities are usually arranged in columns, sometimes called "state matrices". The"state" of the left hand side of one element is, of course, also that of the right hand side of the next element to the left. Thus, by continuous substitution for these common "state matrices", in the case of an unbranched system, one relates the important quantities at one end of the system to those at the other. At this point the known boundary conditions can be applied and the unknown quantities evaluated if the equations are non-homogeneous. If natural frequencies are sought, the set is homogeneous and the natural frequency appears as an eigen-value. The procedure, then, is to assume values for the natural frequency; the boundary conditions provide a test to show whether the assumed value is correct.

In adapting the method to clustered launch vehicle analysis, the points where the clustered bodies join the center-body are at first thought of as the ends of unbranched systems (See Figure 3b,c). The"assembly" then proceeds as follows: starting from Station I in figure 3b,c and traversing downward, the system "branches" at Station II. The deflections at the upper (or right-hand) end of all of the branches, Station III A, B or C are, of course, equal to the center-body deflections at Station II. A certain number of unknown forces and moments ("redundants", if you like) must be introduced here, however, since the clustered bodies will carry as yet unknown portions of the loads from the part of the system between Stations I and II. Whatever the number of these "intermediate unknowns", the requirement that there be compatibility of deflections at Station VIII provides sufficient simultaneous algebraic equations to eliminate them. The procedure then continues as though the system were unbranched.

Suppose it is presumed at the outset that there will be coupling of some kind among all the motions possible. Cross sections of each of the bodies making up the vehicle, however, will be assumed to retain their shapes, so that shell effects are neglected. The motion of a cross section can then be assumed to include that due to

(1) radial bending involving the quantities:

$$|\mathcal{B}| \triangleq \begin{vmatrix} V \\ M \\ \phi \\ y \end{vmatrix}$$

where: V = transverse shear force (#), positive down

M = bending moment (# in.), positive with upper fibers in tension

ϕ = bending slope (radians), positive when it causes an increase in y_{i+1} compared to y_i

y = bending displacement (in.), positive down

(2) tangential bending, with the same four quantities, but differentiated from radial effects by a prime; i.e.

$$|\mathcal{B}'| \triangleq \begin{vmatrix} V' \\ M' \\ \phi' \\ y' \end{vmatrix}$$

where: relationships with radial quantities are shown in figure 4

(3) torsion, described by

$$|\mathcal{T}| \triangleq \begin{vmatrix} T \\ \theta \end{vmatrix}$$

where: T = torsion moment (# in.) positive forward, considered as a vector

θ = torsion angle (rad.) positive forward, considered as a vector

and

(4) extensile motion, involving

$$|\mathcal{L}| \triangleq \begin{vmatrix} F \\ z \end{vmatrix}$$

where: F = longitudinal force (#) positive forward

z = longitudinal displacement (in.) positive forward

No significant loss of generality will be suffered if one restriction regarding the coupling between these different motions is made; namely that elastic coupling will exist only in the attachments of the clustered bodies. This is a consequence of the near polar symmetry of the elastic characteristics of the individual bodies about their longitudinal axes, and the fact that all deflections are assumed to be small, first order.

B. Basic Longitudinal Transfers

Using Targoff's Notation (Reference 9), the change in all the quantities of interest across a length of one of the component bodies, considered as a massless, elastic element of uniform properties, can be written as

$$\begin{vmatrix} \mathcal{B} \\ \mathcal{B}' \\ \mathcal{T} \\ \mathcal{L} \end{vmatrix}_{i+1} = \underbrace{\begin{bmatrix} [E_b] & & & \\ & [E_b] & & \\ & & [E_t] & \\ & & & [E_\ell] \end{bmatrix}_i}_{[\mathcal{E}]_i} \begin{vmatrix} \mathcal{B} \\ \mathcal{B}' \\ \mathcal{T} \\ \mathcal{L} \end{vmatrix}_{i+\frac{1}{2}} \qquad \text{Eq. (1)}$$

Where:

$$[E_b]_i = \begin{bmatrix} 1 & & & \\ \ell & 1 & \ell a & \\ \frac{\ell^2}{2EI} & \frac{\ell}{EI} & 1 & \\ \frac{\ell^3}{3EI}\left(\frac{1}{2}-\eta\right) & \frac{\ell^2}{2EI} & \ell & 1 \end{bmatrix}_i$$

$$[E_t]_i = \begin{bmatrix} 1 & \\ -\frac{\ell}{GJ} & 1 \end{bmatrix}_i$$

$$[E_\ell]_i = \begin{bmatrix} 1 & \\ -\frac{\ell}{AE} & 1 \end{bmatrix}_i$$

ℓ = length of the elastic element (in)
a = steady axial load (#), positive in tension
η = $3EI/Ght\ell^2$
E = Young's modulus ($\#/in^2$) of the material
G = shear modulus ($\#/in^2$) of the material
ht = effective shear area of cross section (in^2)
I = second moment of area of the cross section referred to the neutral bending axis (in^4)
J = torsional stiffness characteristic of the cross section (in^4)
A = effective compressive-tensile area of the cross section (in^2)

Here and throughout the paper, zero matrix elements will be omitted unless there is danger of confusion. The diagonal nature of this partitioned matrix reflects the lack of elastic coupling. The bending elastic matrix is an approximate form for small axial loads, i.e. where

$$\frac{\ell^2 a}{EI} << 1$$

In general, most elements of the array become hyperbolic or trignometric functions of

$$\left[\frac{\ell^2 a}{EI}\right]^{1/2}$$

depending on whether a is positive or negative, respectively. The vehicle breakdown will usually be fine enough to make $[E_b]$ a good approximation; however, the complete bending tranfer is derived in Appendix A.

The transfer of quantities across a mass element, considered to be infinitesimal in length, can be written by inspection using Figure 4.

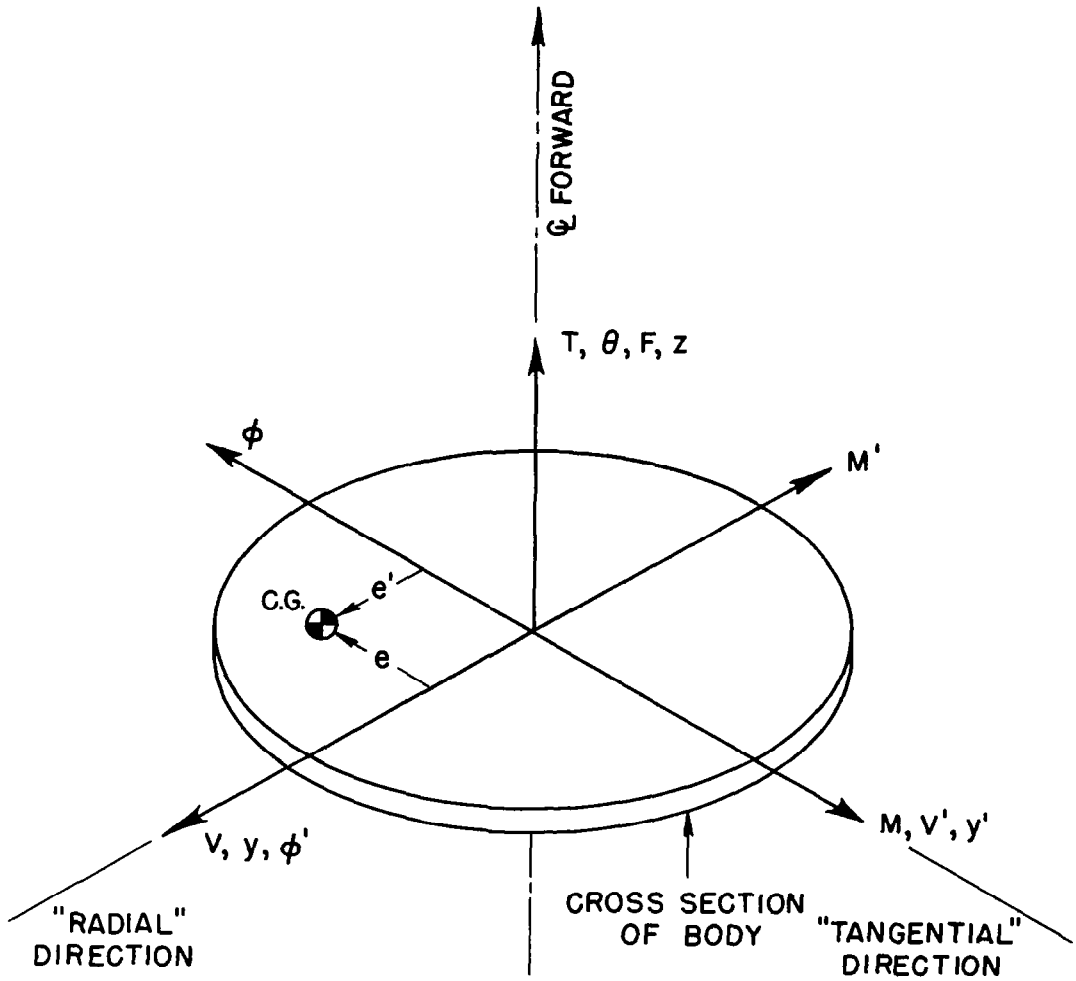

FIG. 4 SIGN CONVENTIONS; STATE QUANTITIES AND MASS OFFSETS

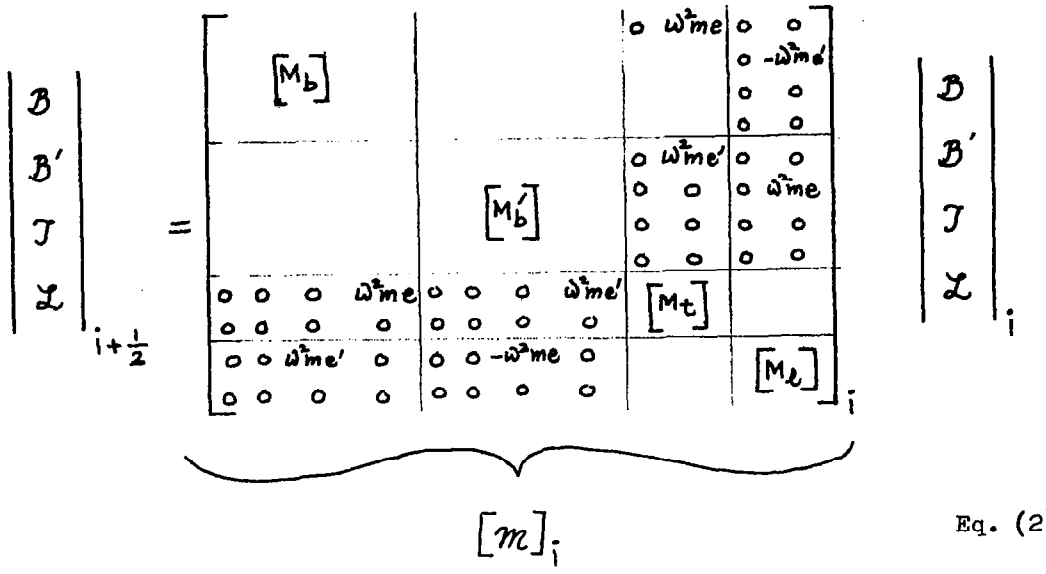

Eq. (2)

where:

$$[M_b]_i \triangleq \begin{bmatrix} 1 & & & \omega^2 m_i \\ & 1 & -\omega^2 I_{\phi_i} & \\ & & 1 & \\ & & & 1 \end{bmatrix}$$

$$[M_b']_i \triangleq \begin{bmatrix} 1 & & & \omega^2 m_i \\ & 1 & -\omega^2 I'_{\phi_i} & \\ & & 1 & \\ & & & 1 \end{bmatrix}$$

$$[M_t]_i \triangleq \begin{bmatrix} 1 & \omega^2 I_{t_i} \\ & 1 \end{bmatrix}$$

$$[M_\ell]_i \triangleq \begin{bmatrix} 1 & \omega^2 m_{\ell_i} \\ & 1 \end{bmatrix}$$

ω = the vibratory frequency (radians/sec)

m_i = mass at the i^{th} station (lbs sec^2/in.) acting in bending

I_{ϕ_i} = rotational mass moment of inertia at the i^{th} station (lb.in. sec^2) about the radial bending axis

I'_{ϕ_i} = rotational mass moment of inertia at the i^{th} station (lb.in. sec^2) about the tangential bending axis

I_{t_i} = torsional mass moment of inertia at the i^{th} station (lb. in. sec^2)

m_{ℓ_i} = mass at the i^{th} station (lbs sec^2/in) acting longitudinally

The quantities m_i, I_{ϕ_i}, I'_{ϕ_i}, and I_{t_i} and m_{ℓ_i} can all be thought of, when it is convenient to do so, as "effective" or frequency-dependent mass properties. In the simplest cases, there may be a flexible local attachment so that part of the total mass m_{t_i} is mounted at station i thru a spring. If the natural frequency of that soft-mounted mass, m_{n_i}, is ω_{n_i}, when the station i is considered fixed, then

$$m_i = m_{t_i} + \frac{\left(\frac{\omega}{\omega_{n_i}}\right)^2 m_{n_i}}{1 - \left(\frac{\omega}{\omega_{n_i}}\right)^2}$$

The mass term in the longitudinal sub-matrix, m_{ℓ_i}, is purposely differentiated from m_i, since liquid mass would not generally be included, except for stations where there is a transverse bulkhead. All the liquid mass between a transverse bulkhead station and the next one forward, would be considered as lumped at the aftmost one. Similarly, liquid contributions to I_{t_i} would be largely neglected, except where there are segmented tanks. Portions of the liquid near a free surface, and"overhung" parts of the structure such as the rocket engines in Figure 1a and the clustered body noses in Figure 1b require special treatment, and are discussed in later sections. The transfer across the i^{th} mass and elastic length on any of the bodies comprising the clustered vehicle is thus written as

$$\begin{vmatrix} \mathcal{B} \\ \mathcal{B}' \\ \mathcal{T} \\ \mathcal{L} \end{vmatrix}_{i+1} = \left[\mathcal{E}\right]_i \left[m\right]_i \begin{vmatrix} \mathcal{B} \\ \mathcal{B}' \\ \mathcal{T} \\ \mathcal{L} \end{vmatrix}_i$$

Referring to Fig. 3b, transfer and state matrices can be associated with specific parts of the launch vehicle by using the subscript N for quantities associated with the length between Stations I and II; C for those between Stations V and VI on the center-body; T for those between Stations IX and X; and $A^{(i)}$ or $B^{(i)}$ on the i^{th} cluster-body of one or the other of two types between Stations V and VI. Clearly then

$$\begin{vmatrix} \mathcal{B} \\ \mathcal{B}' \\ \mathcal{J} \\ \mathcal{L} \end{vmatrix}_{(II, VIC, VIA^{(i)}, VIB^{(i)}, X)} = [\sigma]_{(N,C,A,B,T)} \begin{vmatrix} \mathcal{B} \\ \mathcal{B}' \\ \mathcal{J} \\ \mathcal{L} \end{vmatrix}_{(I, VC, VA^{(i)}, VB^{(i)}, IX)} \qquad \text{Eq. (3)}$$

where:

$$[\sigma] \triangleq \prod_{i=1}^{n} [\mathcal{E}]_i [m]_i$$

The summation in Eq. 3 assumes that the first mass in each body is identified as $i=1$. It should also be noted that the number of masses, n, may be different from one section of the system to another. Most important, however, $[\sigma]$ need only be obtained once for each kind of cluster-body, regardless of how many of such bodies there are. Furthermore, for a free-free condition of the launch vehicle

$$\begin{vmatrix} V \\ M \\ V' \\ M' \\ T \\ F \end{vmatrix}_{(I,X)} = \begin{vmatrix} 0 \\ 0 \\ 0 \\ 0 \\ 0 \\ 0 \end{vmatrix} \qquad \text{Eq. (4)}$$

Thus $[m]_{i_N}$ may be taken as a 12 x 6 matrix consisting only of those columns of the general mass matrix multiplying the deflections; i.e. columns 3, 4, 7, 8, 10, and 12. Similarly $[\mathcal{E}]_{n_T}$ may be taken as a 6 x 12 matrix consisting

of the rows corresponding to the zero forces and moments; namely rows 1, 2, 5, 6, 9, and 11. By postmultiplying (from the right) to obtain $[\sigma]_N$ and premultiplying (from the left) to get $[\sigma]_T$ this application of the boundary conditions saves half the numerical steps which might otherwise have been carried out in obtaining these two products.

C. Joining the Branches

At Station III the structural attachments of the clustered bodies may individually experience transverse shears, extensile loads, bending moments and torques, irrespective of the particular motion assumed for the center-body. If, for example, the center-body is undergoing only bending in one plane, the shears and moments in a normal plane can exist on individual attachment "arms", so long as those components cancel among them. One can, of course, state unequivocably and quite generally that

$$\begin{vmatrix} V \\ M \\ V' \\ M' \\ T \\ F \end{vmatrix}_{V\,C} = \begin{vmatrix} V \\ M \\ V' \\ M' \\ T \\ F \end{vmatrix}_{II} - \sum_i \begin{vmatrix} V \\ M \\ V' \\ M' \\ T \\ F \end{vmatrix}_{III\,A^{(i)}} - \sum_i \begin{vmatrix} V \\ M \\ V' \\ M' \\ T \\ F \end{vmatrix}_{III\,B^{(i)}} \qquad \text{Eq. (5)}$$

Similarly

$$\begin{vmatrix} V \\ M \\ V' \\ M' \\ T \\ F \end{vmatrix}_{IX\,T} = \begin{vmatrix} V \\ M \\ V' \\ M' \\ T \\ F \end{vmatrix}_{VI\,C} + \sum_i \begin{vmatrix} V \\ M \\ V' \\ M' \\ T \\ F \end{vmatrix}_{VIII\,A^{(i)}} + \sum_i \begin{vmatrix} V \\ M \\ V' \\ M' \\ T \\ F \end{vmatrix}_{VIII\,B^{(i)}} \qquad \text{Eq. (6)}$$

The forces, moments and torques at Stations $\text{III}_{A^{(i)},B^{(i)}}$ are the "intermediate" unknowns of this problem. It is important to note that Eqs. (5) and (6) imply that these quantities are in the same axis system as the center-body; if, as shown in figure 2, the cluster-body axis system is reached by rotating thru an angle, Ψ, this must be reflected in the transfer from stations $\text{III}_{A^{(i)},B^{(i)}}$ to $\text{IV}_{A^{(i)},B^{(i)}}$ and from $\text{VII}_{A^{(i)},B^{(i)}}$ to $\text{VIII}_{A^{(i)},B^{(i)}}$. The "intermediate" unknowns ultimately are eliminated for the most part by equations which are companions to Eq. (6), expressing the compatibility of displacements at the aft attachment of the clustered bodies. That is

$$\left|\begin{matrix}\phi\\ y\\ \phi'\\ y'\\ \theta\\ z\end{matrix}\right|_{\text{VI C}} = \left|\begin{matrix}\phi\\ y\\ \phi'\\ y'\\ \theta\\ z\end{matrix}\right|_{\text{VIII A}^{(i)}} = \left|\begin{matrix}\phi\\ y\\ \phi'\\ y'\\ \theta\\ z\end{matrix}\right|_{\text{VIII B}^{(i)}} \qquad \text{Eq. (7)}$$

Exceptions to making complete use of these equations will be clear in specific cases. The conditions at Station VIC will be expressible in terms of the unknown deflections at the nose of the vehicle and the "intermediate" unknowns thru the use of Eqs. (3) and (5). Thus, Eqs. (6) and (7) may be rewritten as

$$\left|\begin{matrix}V\\ M\\ V'\\ M'\\ T\\ F\end{matrix}\right|_{\text{IX}} = [\gamma_1] \left|\begin{matrix}\phi\\ y\\ \phi'\\ y'\\ \theta\\ z\end{matrix}\right|_{\text{I}} - [\sigma_1']_C \left\{ \sum_i \left|\begin{matrix}V\\ V'\\ T\\ M\\ M'\\ F\end{matrix}\right|_{\text{III A}^{(i)}} + \sum_i \left|\begin{matrix}V\\ V'\\ T\\ M\\ M'\\ F\end{matrix}\right|_{\text{III B}^{(i)}} \right\}$$

$$+ \sum_i \left|\begin{matrix}V\\ M\\ V'\\ M'\\ T\\ F\end{matrix}\right|_{\text{VIII A}^{(i)}} + \sum_i \left|\begin{matrix}V\\ M\\ V'\\ M'\\ T\\ F\end{matrix}\right|_{\text{VIII B}^{(i)}}$$

Eq. (8)

$$\left|\begin{matrix}\phi\\ y\\ \phi'\\ y'\\ \theta\\ z\end{matrix}\right|_{IX} = [\nu_2] \left|\begin{matrix}\phi\\ y\\ \phi'\\ y'\\ \theta\\ z\end{matrix}\right|_{I} - [\sigma_2']_c \left\{ \sum_i \left|\begin{matrix}V\\ V'\\ T\\ M\\ M'\\ F\end{matrix}\right|_{III\,A^{(i)}} + \sum_i \left|\begin{matrix}V\\ V'\\ T\\ M\\ M'\\ F\end{matrix}\right|_{III\,B^{(i)}} \right\}$$

$$= \left|\begin{matrix}\phi\\ y\\ \phi'\\ y'\\ \theta\\ z\end{matrix}\right|_{VIII\,A^{(i)}} = \left|\begin{matrix}\phi\\ y\\ \phi'\\ y'\\ \theta\\ z\end{matrix}\right|_{VIII\,B^{(i)}} \qquad \text{Eq. (9)}$$

where

$[\nu_1] \triangleq$ rows 1, 2, 5, 6, 9, 11 of $[\nu]$

$[\nu_2] \triangleq$ rows 3, 4, 7, 8, 10, 12 of $[\nu]$

$[\nu] \triangleq [\sigma^1]_c [\sigma_1]_N + [\sigma^2]_c [\sigma_2]_N$

$[\sigma^1]_c \triangleq$ columns 1, 5, 9, 2, 6, 11(in that order) of $[\sigma]_c$

$[\sigma^2]_c \triangleq$ columns 3, 4, 7, 8, 10, 12 of $[\sigma]_c$

$[\sigma_1]_N$ rows 1, 5, 9, 2, 6, 11 (in that order)of $[\bar{\sigma}]_N$

$[\bar{\sigma}]_N$ columns 3, 4, 7, 8, 10, 12 of $[\sigma]_N$

$[\sigma_2]_N$ rows 3, 4, 7, 8, 10, 12, of $[\bar{\sigma}]_N$

$[\sigma_1']_c \triangleq$ rows 1, 2, 5, 6, 9, 11 of $[\sigma^1]_c$

$[\sigma_2']_c \triangleq$ rows 3, 4, 7, 8, 10, 12 of $[\sigma^1]_c$

The arbitrary rearrangement of forces and moments at Stations $III_{A^{(i)}}$ and $III_{B^{(i)}}$ will prove convenient in later steps. Now if the quantities at $VIII_{A^{(i)},B^{(i)}}$ can be similarly expressed in terms of the unknown deflections at Station I and the intermediate unknowns, there will be as many sets of Eqs. (8) as there are cluster-bodies $A^{(i)}$ or $B^{(i)}$. This provides a total number of equations equal to the number of intermediate unknowns, so that the latter can be eliminated in terms of the nose deflections. To relate quantities at $VIII_{A^{(i)},B^{(i)}}$ to those at Station $III_{A^{(i)},B^{(i)}}$ requires transfer matrices for the forward and aft structural attachments.

These expressions may take different forms depending on the kind of attachment configuration encountered, and depending on whether test data or data from previous static structural calculations is available. Rather than attempt to generalize, several examples are given in presenting the analysis of the Titan IIIC and Saturn I vehicles in the sections to follow.

1. Titan IIIC Fully Coupled Motion

a. General

Titan IIIC consists of two large Solid (propellant) Rocket Motors (SRM's) clustered about a modified Titan II liquid rocket. Thus, using the general notation, the $A^{(1)}$ and $A^{(2)}$ bodies correspond to SRM 1 and SRM 2, respectively, and there are no $B^{(i)}$ bodies. Figure 1b shows two Thrust Vector Control bodies (TVC's) attached to the two solid rocket motors. It may be noted that in the convention shown in Fig. 3c the $A^{(1)}$ (i.e. SRM 1) properties are identical to those of $A^{(2)}$ (i.e. SRM 2). Nevertheless, the presence of the TVC bodies has the important effect of coupling the torsion of the cluster bodies with their bending in both the radial (yaw) and tangential (pitch) planes. Thus torsion is a mechanism for coupling between the two kinds of bending. In addition, there may be mass coupling between pitch bending and torsion in the center-body, due to apparent asymmetry of upper stage tanks. (See Figure 1b).

The cluster arrangement is such that regardless of the mass offset of individual bodies from their elastic axes, antisymmetric longitudinal motion of the cluster bodies couples with yaw-bending of the vehicle. Similarly if their tangential motion is in-phase in the convention of Fig. 3c (i.e. in opposite directions), the effect is to excite center-body torsion. If the tangential motion of the cluster tanks is out-of-phase (i.e. in the same directions), it excites bending of the center-body in pitch.

Suppose, as in Ref. 6, eccentricities in the individual bodies are ignored. Uncoupled analyses could then be conducted and would result in four distinct kinds of modes, all of which involve center-body motion, viz.:

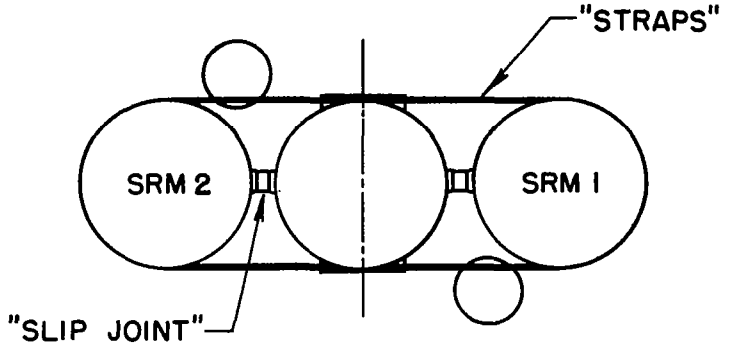

(a) FORWARD ATTACHMENT
(looking aft)

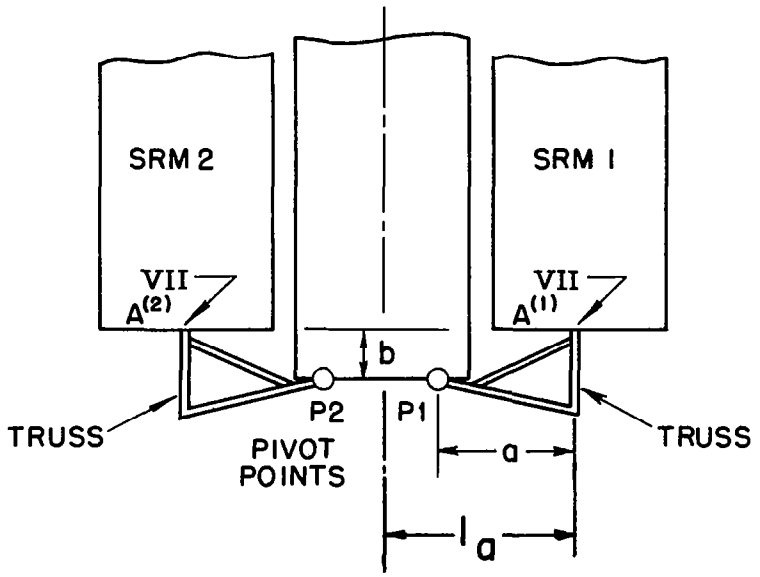

(b) AFT ATTACHMENT

FIG. 5 SCHEMATIC OF TITAN III C CLUSTER - BODY ATTACHMENTS

a) Center-body torsion, coupled with in-phase cluster-body tangential bending-torsion.

b) Center-body yaw-bending, coupled with out-of-phase cluster-body radial bending and extensile motion.

c) Center-body pitch-bending, coupled with out-of-phase cluster-body extensile motion and yaw bending.

d) Center-body extensile motion coupled with in-phase cluster-body extensile motion and yaw bending.

It is not clear that the mass-offset couplings can be ignored, however, and the resulting analysis cannot take advantage of symmetry. All twelve state quantities must therefore be carried on center-body and clusters, and distinction between state matrices on $A^{(1)}$ from those on $A^{(2)}$ must be made.

b. Cluster-body attachments

The forward attachments of the cluster-bodies on Titan IIIC differ significantly from those aft. The forward "strap and slip-joint" arrangement can transmit shear loads and torsion, but not axial loads or bending moments in either the pitch or the yaw sense (See Fig. 5a). However, the aft truss is capable of carrying not only shears and torsion, but also bending in the pitch direction, and longitudinal force at the truss attachments points (P1 and P2 in Fig. 5b). Since F, M or M' cannot be transmitted at the forward attachments, the system variables z, ϕ, ϕ' on the $A^{(i)}$ bodies will be discontinuous with respect to the corresponding quantities on the center-body at those points. These quantities on $A^{(1)}$ and $A^{(2)}$, therefore, replace the six "intermediate unknowns" $(F, M, M')_{III\,A^{(i)}}$, which are known to be zero in this case. This explains why the forces and moments at Stations $III_{A^{(i)}B^{(i)}}$ were rearranged and the corresponding state matrices partitioned as they are in Eqs. 8 and 9. Similarly, since no moment, M, can be sustained at the points P1 and P2 in Fig. 5b, the slope, ϕ, may be discontinuous here. These points do require, however, that the displacements y and z be compatible with those on the center-body.

We can thus summarize the intermediate unknowns of this formulation as $(V, V', T)_{III\,A^{(1)},A^{(2)}}$ and $(\phi, \phi', z)_{IV\,A^{(1)},A^{(2)}}$ for a total of twelve quantities.

There will also be twelve conditions to be satisfied by the state variables, after traversing the branched part of the system. These are the compatibility of the six displacements $(\phi, y', \theta)_{VIII\,A^{(1)},A^{(2)}}$ contained in Eq. 8. However, instead of the remaining six, $(\phi, y, z)_{VII\,A^{(1)},A^{(2)}}$, it will be more convenient to match (y, z) P1, P2 with corresponding quantities on the center-body and require the vanishing of the two yaw-moments M_{P1}, M_{P2}. These twelve equations will allow eliminating the twelve "intermediate unknowns" for the Titan IIIC.

At this point the flexibility of the attachment structure must be represented for those loads which can be carried. Load deflection data does exist for the forward and aft cluster-body structural attachments and was provided by NASA Langley. This information is available in a form which presumes the center-body fixed and the cluster-bodies loaded, that is the flexibility of the upper attachments fixed and the cluster-bodies loaded; may be written with the aid of Fig. 3c, as

$$\underset{IV}{\left|\begin{matrix} y' \\ \theta \end{matrix}\right|_{A^{(1)}}} - \begin{bmatrix} 1 & \ell_a \\ 0 & 1 \\ -1 & \ell_\omega \\ 0 & 1 \end{bmatrix} \underset{III}{\left|\begin{matrix} y' \\ \theta \end{matrix}\right|_{N}} = \begin{bmatrix} \left[\frac{1}{k}\right]_{11} & \left[\frac{1}{k}\right]_{12} \\ \left[\frac{1}{k}\right]_{12} & \left[\frac{1}{k}\right]_{11} \end{bmatrix} \underset{IV}{\left|\begin{matrix} V' \\ T \end{matrix}\right|_{A^{(1)}}}$$

where

$$\left[\frac{1}{k}\right]_{11} = \begin{bmatrix} \frac{1}{k_{y'v'}} & \frac{1}{k_{y'T}} \\ \frac{1}{k_{y'T}} & \frac{1}{k_{\theta T}} \end{bmatrix}_{11}$$

$$\left[\frac{1}{k}\right]_{12} = \begin{bmatrix} \frac{1}{k_{y'v'}} & \frac{1}{k_{y'T}} \\ \frac{-1}{k_{y'T}} & \frac{1}{k_{\theta T}} \end{bmatrix}_{12}$$

$$\left[\frac{1}{k}\right]_{12} = \begin{bmatrix} \frac{1}{k_{y'v'}} & \frac{-1}{k_{y'T}} \\ \frac{1}{k_{y'T}} & \frac{1}{k_{\theta T}} \end{bmatrix}_{12}$$

$$\left[\frac{1}{k}\right]_{11} = \begin{bmatrix} \frac{1}{k_{y'v'}} & \frac{-1}{k_{y'T}} \\ \frac{-1}{k_{y'T}} & \frac{1}{k_{\theta T}} \end{bmatrix}_{11}$$

$\frac{1}{k_{y'v'}}_{ij}$ = tangential displacement of Station $\text{IV}_{A^{(i)}}$ with respect to Station $\text{III}_{A^{(j)}}$ per unit tangential shear on Station $\text{IV}_{A^{(j)}}$ [in/lb]

$\frac{1}{k_{y'T}}_{ij}$ = tangential displacement of Station $\text{IV}_{A^{(i)}}$ with respect to Station III per unit torque on Station $\text{IV}_{A^{(j)}}$ [in/lb in]

$\frac{1}{k_{\theta T}}$ = torsional deflection of Station $\text{IV}_{A^{(i)}}$ with respect to Station III per unit torque on Station $\text{IV}_{A^{(j)}}$ [rad/lb in]

l_a = distance from center-body centerline to cluster-body centerline [in]

and

$$\left|\begin{matrix} y \\ y \end{matrix}\right|_{\substack{A^{(1)} \\ A^{(2)} \\ \text{IV}}} - \left|\begin{matrix} 1 \\ -1 \end{matrix}\right| y_{N_{\text{III}}} = \begin{bmatrix} \left(\frac{1}{k_{yv}}\right)_{11} & \left(\frac{1}{k_{yv}}\right)_{12} \\ \left(\frac{1}{k_{yv}}\right)_{12} & \left(\frac{1}{k_{yv}}\right)_{11} \end{bmatrix} \left|\begin{matrix} V \\ V \end{matrix}\right|_{\substack{A^{(1)} \\ A^{(2)} \\ \text{IV}}}$$

where: $\left(\frac{1}{k_{yv}}\right)_{ij}$ = radial displacement of Station $\text{IV}_{A^{(i)}}$ with respect to Station III per unit radial shear on Station $\text{IV}_{A^{(j)}}$ [in/lb]

All of the flexibility numbers

$$\left(\frac{1}{k_{y'T}}, \frac{1}{k_{\theta T}}, \frac{1}{k_{y'v'}}\right)_{ij}$$

are assumed known and Maxwell's reciprocity theorem has been used to minimize the number of distinct symbols.

Now from statics, and accounting for rotation of axes from cluster-body axis system to center-body.

$$\left|\begin{matrix} V \\ V' \\ T \end{matrix}\right|_{\substack{IV \\ A^{(1)}}} = \begin{bmatrix} 1 & 0 & 0 \\ 0 & 1 & 0 \\ 0 & -\ell_a & 1 \end{bmatrix} \left|\begin{matrix} V \\ V' \\ T \end{matrix}\right|_{\substack{III \\ A^{(1)}}}$$

$$\left|\begin{matrix} V \\ V' \\ T \end{matrix}\right|_{\substack{IV \\ A^{(2)}}} = \begin{bmatrix} -1 & 0 & 0 \\ 0 & -1 & 0 \\ 0 & \ell_a & 1 \end{bmatrix} \left|\begin{matrix} V \\ V' \\ T \end{matrix}\right|_{\substack{III \\ A^{(2)}}}$$

Thus the desired transfer can be written, using the above flexibility and equilibrium relations, as:

$$\begin{array}{|c|} \hline V \\ y \\ V' \\ y' \\ T \\ \theta \\ \hline V \\ y \\ V' \\ y' \\ T \\ \theta \\ \hline \end{array}\begin{matrix} \\ \\ \\ \\ \\ A^{(1)} \\ \\ \\ \\ \\ \\ A^{(2)} \end{matrix} = \left[\begin{array}{c} [F_1] \\ \hline [F_2] \end{array}\right] \begin{array}{|c|} \hline \phi \\ y \\ \phi' \\ y' \\ \theta \\ z \\ \hline V \\ V' \\ T \\ \hline V \\ V' \\ T \\ \hline \end{array}\begin{matrix} \\ \\ \\ \\ \\ N\,II \\ \\ \\ A^{(1)} \\ \\ \\ A^{(2)} \\ III \end{matrix}$$

where $\dfrac{[F_1]}{[F_2]}$ are as defined on page 25.

$$\frac{[F_1]}{[F_2]} \triangleq$$

$$\left[\begin{array}{cccccc|cc|c|cc}
 & & & & & & 1 & & & & & \\
 & 1 & & & & & \left(1/k_{yv}\right)_{11} & & & -\left(1/k_{yv}\right)_{12} & & \\
 & & & & & & & 1 & & & & \\
 & & & 1 & l_a & & & \left[1/k_{y'v'}\ \ 1/k_{y'T}\right]_{11}\left[\begin{smallmatrix}1 & 0\\ -l_a & 1\end{smallmatrix}\right] & & & \left[1/k_{y'v'}\ \ 1/k_{y'T}\right]_{12}\left[\begin{smallmatrix}-1 & 0\\ l_a & 1\end{smallmatrix}\right] \\
 & & & & & & & -l_a & 1 & & & \\
 & & & & 1 & & & \left[1/k_{y'T}\ \ 1/k_{\theta T}\right]_{11}\left[\begin{smallmatrix}1 & 0\\ -l_a & 1\end{smallmatrix}\right] & & & \left[-1/k_{y'T}\ \ 1/k_{\theta T}\right]_{12}\left[\begin{smallmatrix}-1 & 0\\ l_a & 1\end{smallmatrix}\right] \\
\hline
 & & & & & & & & & -1 & & \\
 & -1 & & & & & \left(1/k_{yv}\right)_{12} & & & -\left(1/k_{yv}\right)_{11} & & \\
 & & & & & & & & & & & \\
 & & & -1 & l_a & & & \left[1/k_{y'v'}\ \ -1/k_{y'T}\right]_{12}\left[\begin{smallmatrix}1 & 0\\ -l_a & 1\end{smallmatrix}\right] & & & \left[1/k_{y'v'}\ \ -1/k_{y'T}\right]_{11}\left[\begin{smallmatrix}-1 & 0\\ l_a & 1\end{smallmatrix}\right] \\
 & & & & & & & & & & l_a & 1 \\
 & & & & 1 & & & \left[1/k_{y'T}\ \ 1/k_{\theta T}\right]_{12}\left[\begin{smallmatrix}1 & 0\\ -l_a & 1\end{smallmatrix}\right] & & & \left[-1/k_{y'T}\ \ 1/k_{\theta T}\right]_{11}\left[\begin{smallmatrix}-1 & 0\\ l_a & 1\end{smallmatrix}\right]
\end{array}\right]$$

Now substituting from Eq. (3) in the right hand side of the above transfer, we obtain:

$$\left|\begin{matrix} V \\ y \\ V' \\ y' \\ T \\ \theta \end{matrix}\right|_{\substack{\text{IV} \\ A^{(1)}}} = \left[F_1^1\right] \left[\sigma_2\right]_N \left|\begin{matrix} \phi \\ y \\ \phi' \\ y' \\ \theta \\ z \end{matrix}\right|_{I} + \left[F_1^2\right] \left|\begin{matrix} V \\ V' \\ T \\ \hline V \\ V' \\ T \end{matrix}\right| \begin{matrix} \text{III} \\ A^{(1)} \\ \\ \text{III} \\ A^{(2)} \end{matrix}$$

Eq. (10)

$$\left|\begin{matrix} V \\ y \\ V' \\ y' \\ T \\ \theta \end{matrix}\right|_{\substack{\text{IV} \\ A^{(2)}}} = \left[F_2^1\right] \left[\sigma_2\right]_N \left|\begin{matrix} \phi \\ y \\ \phi' \\ y' \\ \theta \\ z \end{matrix}\right|_{I} + \left[F_2^2\right] \left|\begin{matrix} V \\ V' \\ T \\ \hline V \\ V' \\ T \end{matrix}\right| \begin{matrix} \text{III} \\ A^{(1)} \\ \\ \text{III} \\ A^{(2)} \end{matrix}$$

Eq. (11)

where: $\left[F_j^1\right] \triangleq$ Columns 1 through 6 of $\left[F_j\right]$

and $\left[F_j^2\right] \triangleq$ Columns 7 through 12 of $\left[F_j\right]$ ..(j = 1, 2).

Now noting that V, V' and T are transferred from Station IV to Station V, and introducing the new intermediate unknowns $(\phi, \phi', z)_{V\,A^{(1)},A^{(2)}}$, Eqs. (10) and (11) can be used in Eq. (3) to traverse the clustered bodies, so that

$$\left|\begin{matrix}\mathcal{B}\\ \mathcal{B}'\\ \mathcal{T}\\ \mathcal{L}\end{matrix}\right|_{\substack{\text{VII}\\ A^{(1)}}} = \left[\sigma^1\right]_{A^{(1)}}\left[F_1^1\right]\left[\sigma^2\right]_N \left|\begin{matrix}\phi\\ y\\ \phi'\\ y'\\ \theta\\ z\end{matrix}\right|_I + \left[\sigma^1\right]_{A^{(1)}}\left[F_1^2\right] \left|\begin{matrix}V\\ V'\\ T\\ \hline V\\ V'\\ T\end{matrix}\right|_{\substack{A^{(1)}\\ A^{(2)}}} + \left[\sigma^2\right]_{A^{(1)}} \left|\begin{matrix}\phi\\ \phi'\\ z\end{matrix}\right|_{\substack{V\\ A^{(1)}}}$$

Eq. (12)

$$\left|\begin{matrix}\mathcal{B}\\ \mathcal{B}'\\ \mathcal{T}\\ \mathcal{L}\end{matrix}\right|_{\substack{\text{VII}\\ A^{(2)}}} = \left[\sigma^1\right]_{A^{(2)}}\left[F_2^1\right]\left[\sigma^2\right]_N \left|\begin{matrix}\phi\\ y\\ \phi'\\ y'\\ \theta\\ z\end{matrix}\right|_I + \left[\sigma^1\right]_{A^{(2)}}\left[F_2^2\right] \left|\begin{matrix}V\\ V'\\ T\\ \hline V\\ V'\\ T\end{matrix}\right|_{\substack{A^{(1)}\\ A^{(2)}}} + \left[\sigma^2\right]_{A^{(2)}} \left|\begin{matrix}\phi\\ \phi'\\ z\end{matrix}\right|_{\substack{V\\ A^{(2)}}}$$

Eq. (13)

where:

$$\left[\sigma^1\right]_{A^{(i)}} = \text{columns } 1, 4, 5, 8, 9, 10 \text{ of } \left[\sigma\right]_{A^{(i)}}$$

$$\left[\sigma^2\right]_{A^{(i)}} = \text{columns } 3, 7, 12 \text{ of } \left[\sigma\right]_{A^{(i)}}$$

Note that the disappearance of columns 2, 6, and 11 of $[\sigma]_{A^{(i)}}$ from consideration reflects the fact that $(M, M', F)_{IV\,A^{(i)}} = (M, M', F)_{III\,A^{(i)}} = 0$.

To apply the compatibility of displacements at Stations $VIII_{A^{(i)}}$ and P_i and require zero moments M at the latter points requires transfers across the aft attachment structure. Load deflections data at that point is also available for the Titan IIIC with the center body restrained and shear forces and torques applied to the SRM's. This information allows writing (See Fig. 5b)

$$\left|\begin{matrix} y' \\ \phi' \\ \theta \end{matrix}\right|_{A^{(1)}} - \left[\begin{matrix} 1 & -b & l_a \\ 0 & 1 & 0 \\ 0 & 0 & 1 \end{matrix}\right] \left|\begin{matrix} y' \\ \phi' \\ \theta \end{matrix}\right|_{A^{(2)}} = \left[\begin{matrix} \left[\frac{1}{K}\right]_{11} & \left[\frac{1}{K}\right]_{12} \\ \left[\frac{1}{K}\right]_{21} & \left[\frac{1}{K}\right]_{22} \end{matrix}\right] \left|\begin{matrix} V' \\ M' \\ T \end{matrix}\right|_{A^{(1)}} \left|\begin{matrix} V' \\ M' \\ T \end{matrix}\right|_{A^{(2)}}$$

VIII VII

Eq. (14)

Which anticipates that deflections at $A^{(1)}, A^{(2)}$ VIII, VI.C and IX are all going to be the same.

where:

$$\left[\frac{1}{K}\right]_{11} = \left[\begin{matrix} \frac{1}{K_{y'V'}} & \frac{1}{K_{y'M'}} & \frac{1}{K_{y'T}} \\ \frac{1}{K_{y'M'}} & \frac{1}{K_{\phi'M'}} & \frac{1}{K_{\phi'T}} \\ \frac{-1}{K_{y'T}} & \frac{-1}{K_{\phi'T}} & \frac{1}{K_{\theta T}} \end{matrix}\right]_{11}$$

$$\left[\frac{1}{K}\right]_{22} = \left[\begin{matrix} \frac{1}{K_{y'V'}} & \frac{-1}{K_{y'M'}} & \frac{1}{K_{y'T}} \\ \frac{-1}{K_{y'M'}} & \frac{1}{K_{\phi'M'}} & \frac{-1}{K_{\phi'T}} \\ \frac{-1}{K_{y'T}} & \frac{1}{K_{\phi'T}} & \frac{1}{K_{\theta T}} \end{matrix}\right]_{11}$$

$$\left[\frac{1}{K}\right]_{12} = \left[\begin{matrix} \frac{1}{K_{y'V'}} & \frac{1}{K_{y'M'}} & 0 \\ \frac{1}{K_{y'M'}} & \frac{1}{K_{\phi'M'}} & 0 \\ 0 & 0 & 0 \end{matrix}\right]_{12}$$

$\left[\frac{1}{K}\right]_{12}$ is the transpose of $\left[\frac{1}{K}\right]_{21}$

and where:

$\left(\frac{1}{\mathcal{K}_{y'v'}}, \frac{1}{\mathcal{K}_{y'T}}, \frac{1}{\mathcal{K}_{\theta T}}\right)$ correspond to $\left(\frac{1}{k_{y'v'}}, \frac{1}{k_{y'T}}, \frac{1}{k_{\theta T}}\right)$

except that the deflections are at Station VII $_{A^{(i)}}$ with respect to Station IX for unit shears or moments applied to Station VII $_{A^{(j)}}$.

$\frac{1}{\mathcal{K}_{y'M'}}_{ij}$ = tangential displacement of Station VII $_{A^{(i)}}$ with respect to Station IX per unit tangential bending moment on Station VII $_{A^{(j)}}$.

$\frac{1}{\mathcal{K}_{\phi M'}}_{ij}$ = tangential bending slope at Station VII $_{A^{(i)}}$ with respect to Station IX per unit tangential bending moment on Station VII $_{A^{(j)}}$.

$\frac{1}{\mathcal{K}_{\phi' T}}_{ij}$ = tangential bending slope at Station VII $_{A^{(i)}}$ with respect to Station IX per unit torque on Station VII $_{A^{(j)}}$

b = longitudinal distance between Station VII $_{A^{(i)}}$ and Station IX taken as positive when the latter is farther out than the former.

Note that this form of transfer across the aft attachment requires that Station IX be at the same longitudinal station as points P1, P2. For radial load-deflection characteristics, two separate relations are available from the following tests; (1) with the center-body fixed, points P1, P2 are loaded and (2) these points are loaded again but with the centerbody free and an SRM fixed. The resulting information allows writing

$$\left|\begin{matrix} y \\ z \end{matrix}\right|_{\substack{\text{VII} \\ A^{(i)}}} - \left|\begin{matrix} y \\ z \end{matrix}\right|_{P1} = \begin{bmatrix} \frac{1}{\mathcal{K}_{yv}} & \frac{1}{\mathcal{K}_{yF}} \\ \frac{1}{\mathcal{K}_{yF}} & \frac{1}{\mathcal{K}_{zF}} \end{bmatrix} \left|\begin{matrix} V \\ F \end{matrix}\right|_{P1}$$

and

$$\left|\begin{matrix} y \\ z \end{matrix}\right|_{\substack{\text{VII} \\ A^{(2)}}} - \left|\begin{matrix} -y \\ z \end{matrix}\right|_{P2} = \begin{bmatrix} \frac{-1}{\mathcal{K}_{yv}} & \frac{1}{\mathcal{K}_{yF}} \\ \frac{-1}{\mathcal{K}_{yF}} & \frac{1}{\mathcal{K}_{zF}} \end{bmatrix} \left|\begin{matrix} V \\ F \end{matrix}\right|_{P2} \qquad \text{Eq. (15)}$$

from the results of the second test and

$$\left|\begin{matrix} y \\ y \end{matrix}\right|_{P1} - \left|\begin{matrix} y \\ y \end{matrix}\right|_{\substack{A^{(1)} \\ A^{(2)} \\ \text{VIII}}} = \begin{bmatrix} \frac{1}{\mathcal{K}_{yv_{11}}} & \frac{1}{\mathcal{K}_{yv_{12}}} \\ \frac{1}{\mathcal{K}_{yv_{12}}} & \frac{1}{\mathcal{K}_{yv_{11}}} \end{bmatrix} \left|\begin{matrix} V \\ V \end{matrix}\right|_{\substack{P1 \\ P2}} \qquad \text{Eq. (16)}$$

from the results of the first, where:

$\frac{1}{\mathcal{K}_{yv}}$ = radial displacement at Station $\text{VII}_{A^{(i)}}$ with respect to Station $\text{VIII}_{A^{(i)}}$ for a unit radial shear at Station $\text{VII}_{A^{(i)}}$.

$\frac{1}{\mathcal{K}_{yF}}$ = radial displacement at Station $\text{VII}_{A^{(i)}}$ with respect to Station $\text{VIII}_{A^{(i)}}$ for a unit longitudinal force at $\text{VII}_{A^{(i)}}$.

$\frac{1}{\mathcal{K}_{zF}}$ = longitudinal displacement at Station $\text{VII}_{A^{(i)}}$ with respect to Station $\text{VIII}_{A^{(i)}}$ for a unit longitudinal force at $\text{VII}_{A^{(i)}}$.

$\frac{1}{\mathcal{K}_{yv_{ij}}}$ = radial displacement at point P_i with respect to Station $\text{VIII}_{A^{(i)}}$ for a unit radial shear at point P_j.

Note that the change in axis system from cluster-body to center-body is in evidence in these equations. Since the structure is such that there is virtually no flexibility between points P1,P2 and Stations VIII $A^{(1)}$, $A^{(2)}$ for z motions, the following kinematic relationship can be written

$$\begin{vmatrix} z \\ z \end{vmatrix}_{\substack{P1 \\ P2}} = \begin{vmatrix} z \\ z \end{vmatrix}_{\substack{A^{(1)} \\ A^{(2)}}}_{\text{VIII}} + (\ell_a - a) \begin{bmatrix} 1 & \\ & -1 \end{bmatrix} \begin{vmatrix} \phi \\ \phi \end{vmatrix}_{\substack{A^{(1)} \\ A^{(2)}}}_{\text{VIII}} \qquad \text{Eq. (17)}$$

From statics, and again accounting for the rotation of cluster-body axes back into the center-body system, it is clear that

$$\begin{vmatrix} V \\ M \\ V' \\ M' \\ T \\ F \end{vmatrix}_{\substack{\text{VIII} \\ A^{(1)}}} = \begin{bmatrix} 1 & 0 & 0 & 0 & 0 & 0 \\ 0 & 0 & 0 & 0 & 0 & -(\ell_a - a) \\ 0 & 0 & 1 & 0 & 0 & 0 \\ 0 & 0 & 0 & 1 & 0 & 0 \\ 0 & 0 & (\ell_a - a) & 0 & 1 & 0 \\ 0 & 0 & 0 & 0 & 0 & 1 \end{bmatrix} \begin{vmatrix} V \\ M \\ V' \\ M' \\ T \\ F \end{vmatrix}_{\substack{\text{VII} \\ A^{(1)}}} \qquad \text{Eq. (18)}$$

$$\begin{vmatrix} V \\ M \\ V' \\ M' \\ T \\ F \end{vmatrix}_{\substack{\text{VIII} \\ A^{(2)}}} = \begin{bmatrix} 1 & 0 & 0 & 0 & 0 & 0 \\ 0 & 0 & 0 & 0 & 0 & (\ell_a - a) \\ 0 & 0 & -1 & 0 & 0 & 0 \\ 0 & 0 & 0 & -1 & 0 & 0 \\ 0 & 0 & (\ell_a - a) & 0 & 1 & 0 \\ 0 & 0 & 0 & 0 & 0 & 1 \end{bmatrix} \begin{vmatrix} V \\ M \\ V' \\ M' \\ T \\ F \end{vmatrix}_{\substack{\text{VII} \\ A^{(2)}}}$$

and

$$\left|\begin{matrix} V \\ F \end{matrix}\right|_{P1} = \left|\begin{matrix} V \\ F \end{matrix}\right|_{\substack{\text{VII} \\ A^{(1)}}}, \qquad \left|\begin{matrix} V \\ F \end{matrix}\right|_{P2} = \left|\begin{matrix} -V \\ F \end{matrix}\right|_{\substack{\text{VII} \\ A^{(2)}}}$$

From the first of each of the Eqs. (15) and (16), and the last of the static equilibrium relations,

$$\left|\begin{matrix} y \\ y \end{matrix}\right|_{\substack{\text{VIII} \\ A^{(1)} \\ A^{(2)}}} = \left|\begin{matrix} y \\ -y \end{matrix}\right|_{\substack{\text{VII} \\ A^{(1)} \\ A^{(2)}}} - \begin{bmatrix} \frac{1}{\mathcal{K}_{yv}} + \frac{1}{\mathcal{K}_{yv_{11}}} & \frac{1}{\mathcal{K}_{yF}} & \frac{-1}{\mathcal{K}_{y_{12}}} & 0 \\ \frac{1}{\mathcal{K}_{yv_{12}}} & 0 & \frac{1}{\mathcal{K}_{yv}} + \frac{1}{\mathcal{K}_{yv_{11}}} & \frac{1}{\mathcal{K}_{yF}} \end{bmatrix} \left|\begin{matrix} V \\ F \\ \hline V \\ F \end{matrix}\right|_{\substack{\text{VII} \\ A^{(1)} \\ A^{(2)}}}$$

Eq. (19)

From (17) and the second of each of the two Eqs. (15) we can write

$$\left|\begin{matrix} z \\ z \end{matrix}\right|_{\substack{\text{VIII} \\ A^{(1)} \\ A^{(2)}}} = \left|\begin{matrix} z \\ \bar{z} \end{matrix}\right|_{\substack{\text{VII} \\ A^{(1)} \\ A^{(2)}}} - \begin{bmatrix} \frac{1}{\mathcal{K}_{yF}} & \frac{1}{\mathcal{K}_{zF}} & 0 & 0 \\ 0 & 0 & \frac{1}{\mathcal{K}_{yF}} & \frac{1}{\mathcal{K}_{zF}} \end{bmatrix} \left|\begin{matrix} V \\ F \\ \hline V \\ F \end{matrix}\right|_{\substack{\text{VII} \\ A^{(1)} \\ A^{(2)}}} - (\ell_a - a) \begin{bmatrix} 1 \\ -1 \end{bmatrix} \left|\begin{matrix} \phi \\ \phi \end{matrix}\right|_{\substack{\text{VIII} \\ A^{(1)} \\ A^{(2)}}}$$

Eq. (20)

The last two matrix relations express the compatibility of the displacements y and z at points P1, P2 in terms of forces and moments at Stations $\text{VII}_{A^{(i)}}$ and deflections at Station $\text{VIII}_{A^{(i)}}$. Together with Eq. (14) they represent 10 of the 12 equations needed to eliminate the intermediate unknowns. The remaining 2 are easily written as follows

$$\left|\begin{matrix} M \\ M \end{matrix}\right|_{\substack{P1 \\ P2}} = \left|\begin{matrix} 0 \\ 0 \end{matrix}\right| = \begin{bmatrix} b & 1 & -a & 0 & 0 & 0 \\ 0 & 0 & 0 & b & 1 & -a \end{bmatrix} \left|\begin{matrix} V \\ M \\ F \\ \hline V \\ M \\ F \end{matrix}\right|_{\substack{\text{VII} \\ A^{(1)} \\ A^{(2)}}}$$

Eq. (21)

c. The Frequency Determinant

Now if Eqs. (14), (19), (20) and(21)are assembled into one matrix equation of 12 rows, there obtains the matrix equation shown below

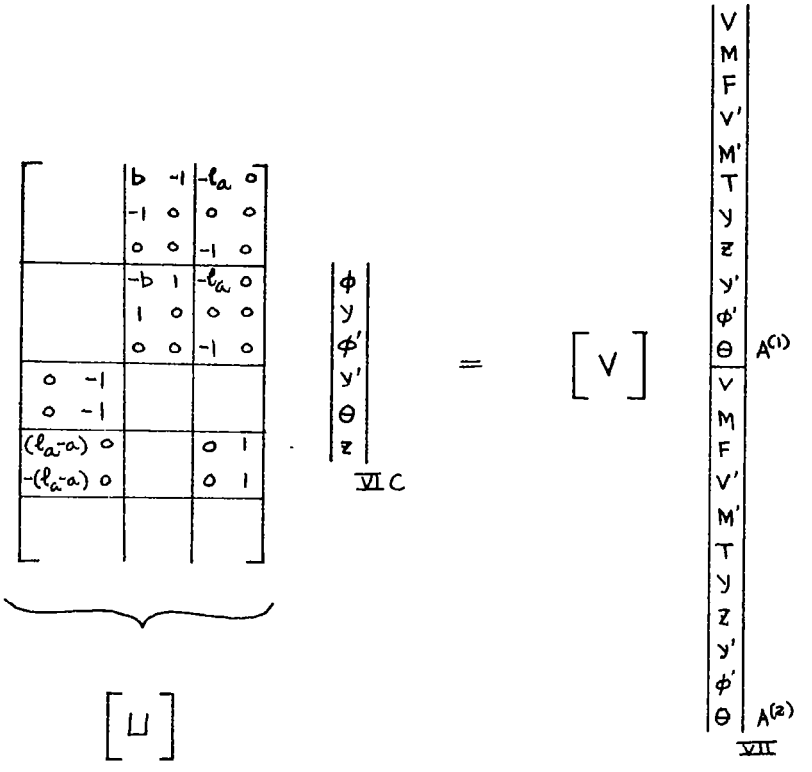

where the matrix [V] is as defined on the next page.

$$
[V] \triangleq \left[\begin{array}{ccc|c|cc|c|ccc|c|cc|c}
 & & & \left[\frac{1}{\mathcal{K}}\right]_{11} & & & \begin{smallmatrix}-1 & & \\ & -1 & \\ & & -1\end{smallmatrix} & & & & \left[\frac{1}{\mathcal{K}}\right]_{12} & & & \\
\hline
 & & & \left[\frac{1}{\mathcal{K}}\right]_{21} & & & & & & & \left[\frac{1}{\mathcal{K}}\right]_{22} & & & \begin{smallmatrix}-1 & & \\ & -1 & \\ & & -1\end{smallmatrix} \\
\hline
\left(\frac{1}{\mathcal{K}_{yv}}+\frac{1}{\mathcal{K}_{yv_{11}}}\right) & 0 & \frac{1}{\mathcal{K}_{yF}} & & 1 & 0 & & \frac{-1}{\mathcal{K}_{yv_{12}}} & 0 & 0 & & 0 & 0 & \\
\frac{1}{\mathcal{K}_{yv_{12}}} & 0 & 0 & & 0 & 0 & & -\left(\frac{1}{\mathcal{K}_{yv}}+\frac{1}{\mathcal{K}_{yv_{11}}}\right) & 0 & \frac{-1}{\mathcal{K}_{yF}} & & 1 & 0 & \\
\hline
\frac{-1}{\mathcal{K}_{yF}} & 0 & \frac{-1}{\mathcal{K}_{zF}} & & 0 & 1 & & 0 & 0 & 0 & & & & \\
0 & 0 & 0 & & 0 & 0 & & \frac{-1}{\mathcal{K}_{yF}} & 0 & \frac{-1}{\mathcal{K}_{zF}} & & & & \\
\hline
b & 1 & -a & & & & & 0 & 0 & 0 & & & & \\
0 & 0 & 0 & & & & & b & 1 & -a & & & &
\end{array}\right]
$$

Equations (12) and(13) are available to substitute into the right hand side of this equation and for the left-hand side it is merely necessary to again note (Fig. 3c) that the conditions at Station VI C are identical to those at Station IX . Hence, thru the use of Eqs. (12), (13), and (9) we may write

$$
[U]\left\{ [\nu_2] \begin{vmatrix} \phi \\ y \\ \phi' \\ y' \\ \theta \\ z \end{vmatrix}_{I} - \left[\sigma_2^{11}\right]_C \Big[[I] \,\Big|\, [I] \Big] \begin{vmatrix} V \\ V' \\ T \\ \hline V \\ V' \\ T \end{vmatrix}_{\substack{A^{(1)} \\ A^{(2)} \\ III}} \right\}
$$

$$
= [V] \left\{ \left[\begin{array}{c} \left[\sigma_1^1\right]_{A^{(1)}} \left[F_1^1\right] \\ \hline \left[\sigma_1^1\right]_{A^{(2)}} \left[F_2^1\right] \end{array}\right] \left[\sigma^2\right]_N \begin{vmatrix} \phi \\ y \\ \phi' \\ y' \\ \theta \\ z \end{vmatrix}_{I} + \left[\begin{array}{c} \left[\sigma_1^1\right]_{A^{(1)}} \left[F_1^2\right] \\ \hline \left[\sigma_1^1\right]_{A^{(2)}} \left[F_2^2\right] \end{array}\right] \begin{vmatrix} V \\ V' \\ T \\ \hline V \\ V' \\ T \end{vmatrix}_{\substack{A^{(1)} \\ A^{(2)} \\ III}} \right.
$$

$$
\left. + \left[\begin{array}{c|c} \left[\sigma_1^2\right]_{A^{(1)}} & \\ \hline & \left[\sigma_1^2\right]_{A^{(2)}} \end{array}\right] \begin{vmatrix} \phi \\ \phi' \\ z \\ \hline \phi \\ \phi' \\ z \end{vmatrix}_{\substack{A^{(1)} \\ A^{(2)} \\ V}} \right\}
$$

where

$[\sigma_2^{11}]_C$ = first three colums of $[\sigma_2^1]_C$

$[\sigma_1^j]_{A^{(i)}}$ = rows 1, 2, 11, 5, 6, 9, 4, 12, 7, 8, and 10 (in that order) of $[\sigma^j]_{A^{(i)}}$

This equation can now be rearranged as follows

$$[P] \begin{vmatrix} \Phi \\ y \\ \Phi' \\ y' \\ \theta \\ z \end{vmatrix}_I = [Q] \begin{vmatrix} V \\ V' \\ T \end{vmatrix} \text{III } A^{(1)} \begin{vmatrix} V \\ V' \\ T \end{vmatrix} \text{III } A^{(2)} \begin{vmatrix} \Phi \\ \Phi' \\ z \end{vmatrix} \text{V } A^{(1)} \begin{vmatrix} \Phi \\ \Phi' \\ z \end{vmatrix} \text{V } A^{(2)}$$

where

$$[P] \triangleq -[V] \begin{bmatrix} [\sigma_1^1]_{A^{(1)}}[F_1^1] \\ \hline [\sigma_1^1]_{A^{(2)}}[F_2^1] \end{bmatrix} [\sigma^2]_N + [U] [\nu_2]$$

and

$$[Q] \triangleq \left[[U] [\sigma_2^{11}]_C \left[[I] \middle| [I] \right] + \begin{bmatrix} [\sigma_1^1]_{A^{(1)}} [F_1^2] \\ \hline [\sigma_1^1]_{A^{(2)}} [F_2^2] \end{bmatrix} \middle| \begin{bmatrix} [\sigma_1^2]_{A^{(1)}} & \\ \hline & [\sigma_1^2]_{A^{(2)}} \end{bmatrix} \right]$$

By matrix inversion we may now write

$$\left|\begin{array}{c} V \\ V' \\ T \end{array}\right|_{III A^{(1)}} \quad \left|\begin{array}{c} V \\ V' \\ T \end{array}\right|_{III A^{(2)}} \quad \left|\begin{array}{c} \phi \\ \phi' \\ z \end{array}\right|_{V A^{(1)}} \quad \left|\begin{array}{c} \phi \\ \phi' \\ z \end{array}\right|_{V A^{(2)}} = [Q]^{-1} [P] \left|\begin{array}{c} \phi \\ y \\ \phi' \\ y' \\ \theta \\ z \end{array}\right|_{I} \qquad \text{Eq. (22)}$$

To complete the transfer from end to end of the Titan III, it is first necessary to use Eq. (12) and (13) again, this time in Eq. (18). The resulting equation is then substituted into Eq. (8) along with the first six rows of Eq.(22). A similar step is made by substituting the first six rows of Eq. (22), into Eq. (9). Finally Eqs. (8) and (9), modified in this way, are used in the right hand side of Eq. (3) to obtain, with the help of Eq. (4).

$$\left|\begin{array}{c} V \\ M \\ V' \\ M' \\ T \\ F \end{array}\right|_{X} = \left|\begin{array}{c} 0 \\ 0 \\ 0 \\ 0 \\ 0 \\ 0 \end{array}\right| = [\sigma]_T \left\{ [\nu] + [W] \left[\begin{array}{c} [\sigma_2^1]_{A^{(1)}} [F_1^1] \\ \hline [\sigma_2^1]_{A^{(2)}} [F_2^1] \end{array}\right] [\sigma^2]_N \right.$$

$$+ \left\{ [W] \left[\left[\begin{array}{c} [\sigma_2^1]_{A^{(1)}} [F_1^2] \\ \hline [\sigma_2^1]_{A^{(2)}} [F_2^2] \end{array}\right] [Q_1]^{-1} + \left[\begin{array}{c} [\sigma_2^2]_{A^{(1)}} \\ \hline [\sigma_2^2]_{A^{(2)}} \end{array}\right] [Q_2]^{-1} \right] \right.$$

$$\left. \left. - [\sigma^1]_C \left[[I] \,\middle|\, [I] \right] [Q_1]^{-1} \right\} [P] \right\} \left|\begin{array}{c} \phi \\ y \\ \phi' \\ y' \\ \theta \\ z \end{array}\right|_{I}$$

Eq. (23)

where

$$[Q_1]^{-1} = \text{first six rows of } [Q]^{-1}$$

$$[Q_2]^{-1} = \text{second six rows of } [Q]^{-1}$$

and

$$[W] \triangleq \left[\begin{array}{cccccc|cccccc}
1 & 0 & 0 & 0 & 0 & 0 & -1 & 0 & 0 & 0 & 0 & 0 \\
0 & 0 & 0 & 0 & 0 & -(\ell_\omega - a) & 0 & 0 & 0 & 0 & 0 & (\ell_\omega - a) \\
0 & 0 & 0 & 0 & 0 & 0 & 0 & 0 & 0 & 0 & 0 & 0 \\
0 & 0 & 0 & 0 & 0 & 0 & 0 & 0 & 0 & 0 & 0 & 0 \\
\hline
0 & 0 & 1 & 0 & 0 & 0 & 0 & 0 & -1 & 0 & 0 & 0 \\
0 & 0 & 0 & 1 & 0 & 0 & 0 & 0 & 0 & -1 & 0 & 0 \\
0 & 0 & 0 & 0 & 0 & 0 & 0 & 0 & 0 & 0 & 0 & 0 \\
0 & 0 & 0 & 0 & 0 & 0 & 0 & 0 & 0 & 0 & 0 & 0 \\
\hline
0 & 0 & (\ell_\omega - a) & 0 & 1 & 0 & 0 & 0 & (\ell_\omega - a) & 0 & 1 & 0 \\
0 & 0 & 0 & 0 & 0 & 0 & 0 & 0 & 0 & 0 & 0 & 0 \\
\hline
0 & 0 & 0 & 0 & 0 & 1 & 0 & 0 & 0 & 0 & 0 & 1 \\
0 & 0 & 0 & 0 & 0 & 0 & 0 & 0 & 0 & 0 & 0 & 0
\end{array}\right]$$

Equation (23) shows that for free vibration, a 6 x 6 determinant, which is a function of ω, must be zero. The procedure for obtaining natural frequencies, therefore, is to assume a series of trial values for ω, calculate the value of this 6 x 6 determinant, plot them vs. frequency, and interpolate for the values, ω_n, which make the determinant zero. This is repeated until the desired accuracy is obtained. These are, of course, the natural frequencies i.e. the eigen values for the vehicle.

d. Mode Shapes

After determining the natural frequencies as described in the preceding section, it is now possible to proceed to get the mode shape of vibration for any particular natural frequency. The procedure is as follows:

From the 6 x 6 matrix described at the end of Section 1c, the normalized "state vector" of the six displacements $\phi, y, \phi', y', \theta, z$ at Station I is obtained. The mode shape can, of course, only be determined to within an arbitrary factor since we are dealing with an eigen-value problem. It is convenient to normalize the "displacement vector"; specifically we will choose the pitch-displacement y or the yaw-displacement y' of the tip to be unity. The fact that V, M, V', M', T and F are all zero at Station I, enables us to write down all the twelve state quantities at Station I . Equations (1) and (2) provide means of obtaining the state vectors at each successive station until we reach Station II . Equation (22) yields the intermediate unknowns. These in conjunction with equations (5), (10), (11), and the fact that M, M', F are zero at $IV_{A^{(i)}}$ provide enough information to obtain the state vectors at IIIC and $IV_{A^{(i)}}$. Equations (1) and (2) are again used to traverse the lengths of the center body and cluster bodies yielding the state vectors at each mass station on them. Equations (6) and (18) can now be used to get the state vector at Station IX , where use of equations (1) and (2) enables the determination of the state vectors at each mass station of the tail section. At Station X, the vanishing of V, M, V', M', T, F provides a check on the accuracy of the numerical calculations.

The "mode shape" thus obtained gives information about the displacements $\phi, y, \phi', y', \theta$ and z at each mass station as well as about the forces and couples V, M, V', M', T and F in all sections of the vehicle.

2. Saturn I Lateral Bending

a. General

Saturn I can be assumed to have eight radial planes of symmetry, if the small effects of rocket engine mass and those of their support offsets are neglected (see Fig. 1a). Its center body can undergo bending motions in either of two distinct planes of symmetry, and neither will couple with center-body torsion, longitudinal motion, or bending in the other plane. In this case the clustered bodies carrying fuel will be identified by $A^{(i)}$ and those carrying LOX will be associated with the subscript $B^{(i)}$.

Figure 6a shows how Saturn I cluster-bodies are supported at the upper end by eight radial beams. This structure, called the"spider", lies in a plane perpendicular to the longitudinal axis. The aft cluster-body support is similar, but the attachment structures are beam-trusses in radial planes, and are called "outriggers." It was assumed that all spider-beam and outrigger-truss flexibility in a plane perpendicular to the longitudinal axis of the vehicle could be ignored based on three facts: (1) adjacent support points from one cluster body to another are very close (Fig. 6a), (2) the assembly forms a complete circle, and (3) there are radial members between all cluster-bodies and the center-body in the plane of the ends of the cluster-bodies. Accordingly, the model, shown in Fig. 6b, was used to represent the cluster-body attachment-structure flexibility. These "equivalent" beams are flexible for deflections

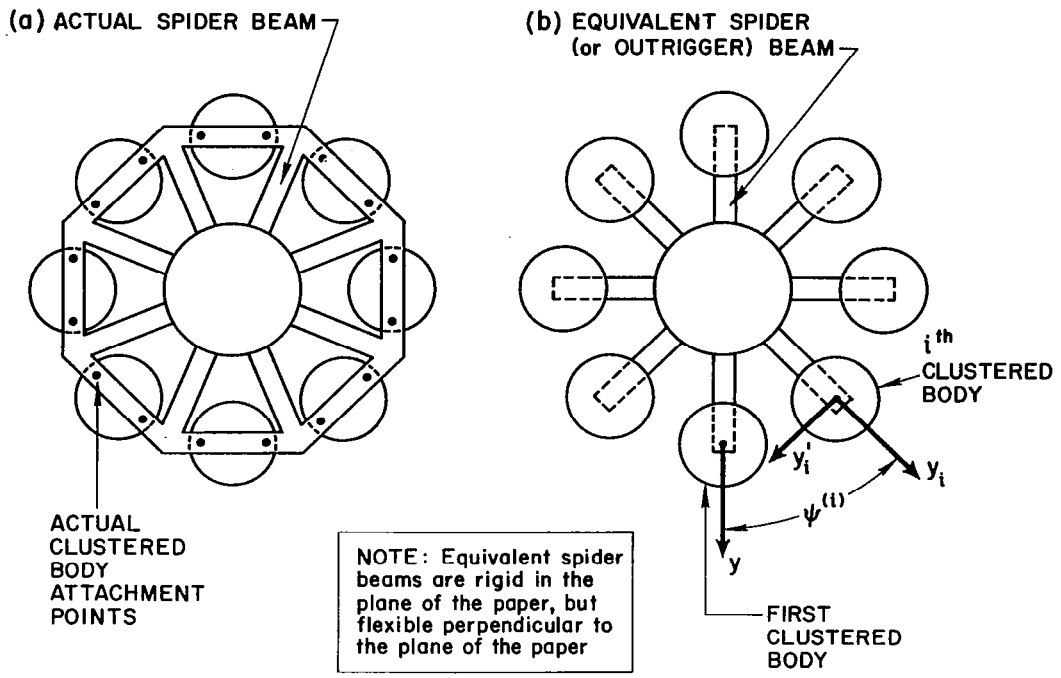

Figure 6. Cluster-Body Support Structure - **SATURN I**

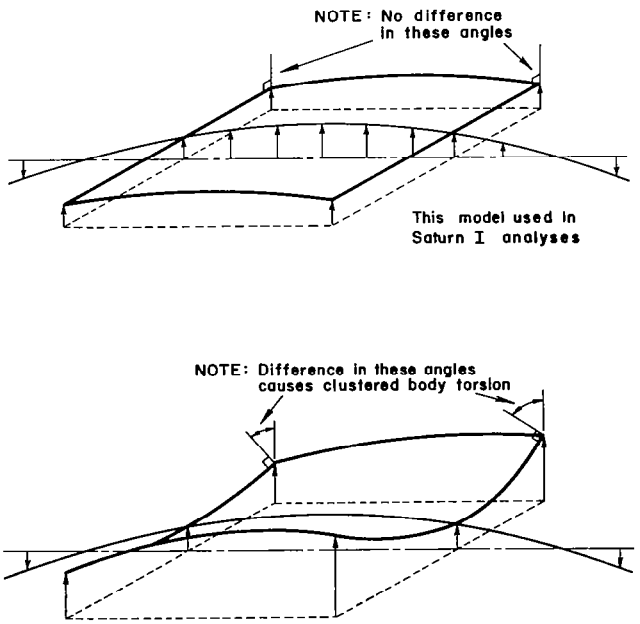

Figure 7. Effect of Support Flexibility on Cluster-Body Torsion

in a radial plane, and rigid for motion in a plane perpendicular to the longitudinal axis. Fig. 7 shows that if bending in the latter plane could occur, a difference in slope between outriggers and spiders would twist the cluster-bodies, even though only center-body bending is being considered. The assumption of rigidity in this plane, however, precludes cluster-body torsion for the case under consideration. Thus only two kinds of longitudinal transfers will be necessary in this analysis; namely, bending on center and clustered bodies and longitudinal motion on the clustered bodies.

b. Specializing the Longitudinal Transfers

Since this is a problem of bending in only one plane, Eqs. (1) and (2) reduce for the center-body to

$$\left|\mathcal{B}\right|_{i+1} = \left[E_b\right]_i \left|\mathcal{B}\right|_{i+\frac{1}{2}} \qquad \text{Eq. (1a)}$$

and

$$\left|\mathcal{B}\right|_{i+\frac{1}{2}} = \left[M_b\right]_i \left|\mathcal{B}\right|_i \qquad \text{Eq. (2a)}$$

Thus we may write in place of part of Eq. (3)

$$\left|\mathcal{B}\right|_{(\text{II},\text{VIC},\text{X})} = \left[\mu\right]_{(N,C,T)} \left|\mathcal{B}\right|_{(\text{I},\text{VC},\text{IX})} \qquad \text{Eq. (3a)}$$

where

$$\left[\mu\right] \triangleq \prod_{i=1}^{n} \left[E_b\right]_i \left[M_b\right]_i$$

Since bending on the clustered bodies still can occur in two planes and longitudinal motion can also take place, the equivalent transfers for these bodies merely reflect the lack of mass coupling, as follows:

$$\begin{vmatrix} \mathcal{B} \\ \mathcal{B}' \\ \mathcal{L} \end{vmatrix}_{i+1} = \begin{bmatrix} [E_b] & & \\ & [E_b] & \\ & & [E_\ell] \end{bmatrix}_i \begin{vmatrix} \mathcal{B} \\ \mathcal{B}' \\ \mathcal{L} \end{vmatrix}_{i+\frac{1}{2}} \qquad \text{Eq. } (1_b)$$

and

$$\begin{vmatrix} \mathcal{B} \\ \mathcal{B}' \\ \mathcal{L} \end{vmatrix}_{i+\frac{1}{2}} = \begin{bmatrix} [M_b] & & \\ & [M_b] & \\ & & [M_\ell] \end{bmatrix}_i \begin{vmatrix} \mathcal{B} \\ \mathcal{B}' \\ \mathcal{L} \end{vmatrix}_i \qquad \text{Eq. } (2_b)$$

So that

$$\begin{vmatrix} \mathcal{B} \\ \mathcal{B}' \\ \mathcal{L} \end{vmatrix}_{\text{VI}_{A^{(i)},B^{(i)}}} = \begin{bmatrix} [\mu] & & \\ & [\mu] & \\ & & [\lambda] \end{bmatrix}_{A,B} \begin{vmatrix} \mathcal{B} \\ \mathcal{B}' \\ \mathcal{L} \end{vmatrix}_{\underline{\text{V}}_{A^{(i)},B^{(i)}}} \qquad \text{Eq. } (3_b)$$

where

$$[\lambda] \triangleq \prod_{i=1}^{n} [E_\ell]_i \, [M_\ell]_i$$

It should be noted that for this case the number of masses, n , may be different not only from one section of the system to another, but also for longitudinal motion as compared to bending. And again, the quantities $[\mu]$ and $[\lambda]$ need only be obtained once for each kind of cluster-body, regardless of how many of such bodies there are, and despite the fact that two normal directions of bending are involved.

c. Cluster Attachments; The "Spider"

The attachment of the clustered bodies of the Saturn I to their supporting structure is complicated by the fact that there are two kinds of bodies. A summary of the end conditions is given in Table I.

As indicated earlier, the center-body can have transverse shears and bending moments in only one plane for the postulated motion, and may have no longitudinal forces. The spider beams, however, may individually experience transverse shears and bending moments in both radial and tangential directions, and longitudinal forces as well, so long as all forces and moments other than those in the plane of the center-body motion cancel among them.

Transfer from Station II to Station $IV_{A^{(i)},B^{(i)}}$ is pictured as taking place in four steps:

Step 1: rotation thru the angle Ψ (fig. 6b) from the plane of motion of the center-body to the azimuthal plane of the equivalent spider beam. Regarding forces, moments, and small angles as vectors, resolution from one axis system to another yields:

$$\begin{Bmatrix} \mathcal{B} \\ \mathcal{B}' \\ F \end{Bmatrix}_{\substack{\text{III spider} \\ \text{azimuthal} \\ \text{axis}}} = \begin{bmatrix} \cos\Psi \begin{bmatrix} 1 & & & \\ & 1 & & \\ & & 1 & \\ & & & 1 \end{bmatrix} & -\sin\Psi \begin{bmatrix} 1 & 0 \\ 0 & 1 \\ 0 & 0 \\ 0 & 0 \end{bmatrix} & \\ \sin\Psi \begin{bmatrix} 1 & & & \\ & 1 & & \\ & & 1 & \\ & & & 1 \end{bmatrix} & \cos\Psi \begin{bmatrix} 1 & 0 \\ 0 & 1 \\ 0 & 0 \\ 0 & 0 \end{bmatrix} & \\ & & 1 \end{bmatrix}_{[R]} \begin{Bmatrix} \mathcal{B} \\ V' \\ M' \\ F \end{Bmatrix}_{\substack{\text{III center} \\ \text{body} \\ \text{azimuthal} \\ \text{axis}}}$$

Note that, wherever possible, advantage is taken of the fact that quantities in the state vectors are zero.

Table I
Saturn I Cluster-Body End Conditions

	Fuel Tanks	LOX Tanks
"Spider"	1. Radial Bending Moment (M)=0 2. Tangential Bending Moment (M')=0 3. Longitudinal Force (F)=0	1. Radial Bending Moment (M)=0 2. Tangential Bending Moment (M') Carried 3. Longitudinal Force Carried
"Outrigger"	4. Radial Bending Moment (M)=0 5. Tangential Bending Moment (M') Carried 6. Longitudinal Force (F) Carried	4. Radial Bending Moment (M)=0 5. Tangential Bending Moment (M') Carried 6. Longitudinal Force (F) Carried

Note: Radial and tangential shears carried on all bodies at both ends.

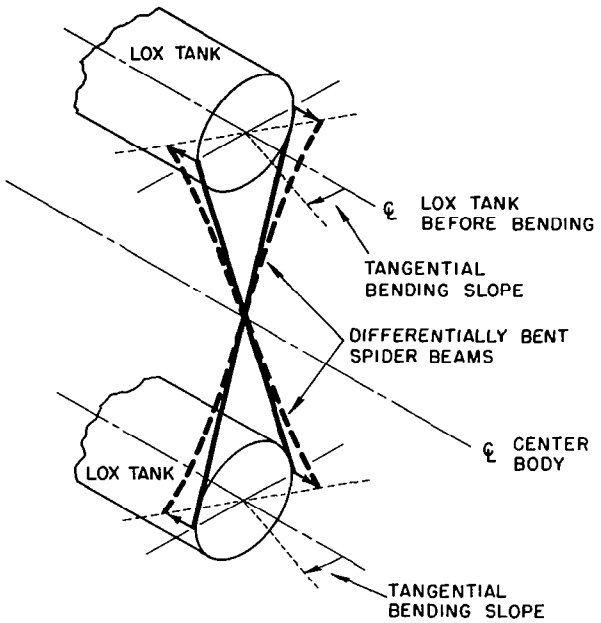

Figure 8. Support Flexibility for Tangential Moments due to Spider Beam Differential Bending - Saturn I

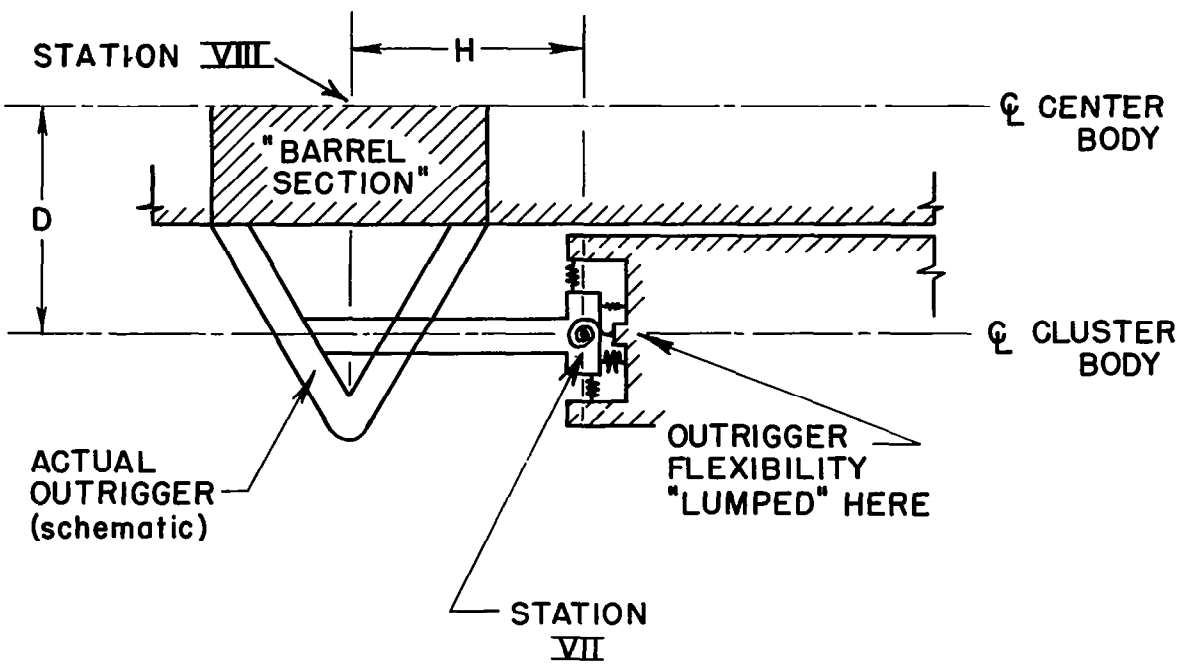

Figure 9. Mathematical Model for Outrigger Flexibility - SATURN I

Step 2: "turning the corner" from the longitudinal direction into the axis of the spider beam (i.e. into a radial direction). Again transforming coordinates, but noting that twisting of the equivalent spider beam can occur (See Fig. 8),

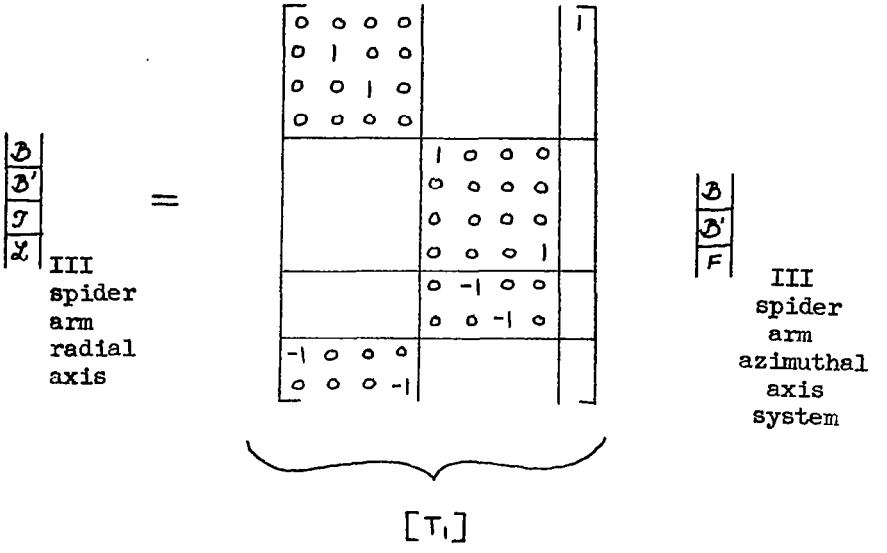

Step 3: traversing the length of the flexible spider beam. This is easily done by defining:

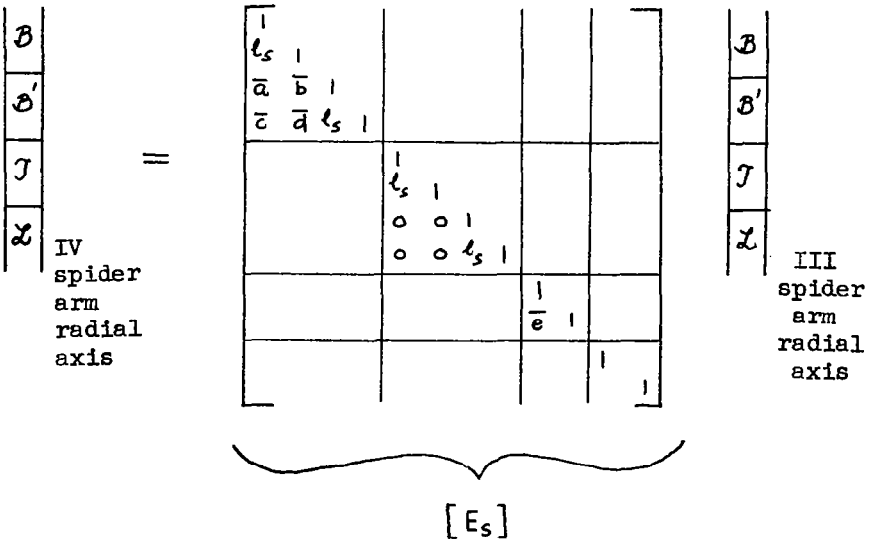

Here $\bar{a}, \bar{b}, \bar{c}, \bar{d}$ represent spider beam bending flexibility in the direction of the longitudinal axis of the vehicle, and $\bar{e}$ is its torsional flexibility. A derivation of these quantities is contained in Appendix B. The length from the center-body elastic axis to that of the clustered body is l_s.

Step 4: "turning the corner" back again, into the longitudinal axis system of the clustered body, clearly requires multiplication by a matrix, $[T_2]$, which is a 10 x 12 submatrix of the inverse of the 12 x 12 form of $[T_1]$

$$[T_2] \triangleq \begin{bmatrix} 1 & & & & & & & & & -1 & & \\ & 1 & & & & & & & & & -1 & \\ & & & & 1 & & & & -1 & & & \\ & & & & & & & 1 & & & & \\ & & & & & & 1 & & & & & \\ 1 & & & & & & & & & & & \\ & & 1 & & & & & & & & & \end{bmatrix}$$

The complete spider matrix is thus obtained by the product

$$[T_2]\ [E_s]\ [T_1]\ [R]$$

and the desired transfer is

$$\left|\begin{matrix}\mathcal{B}\\ \mathcal{B}'\\ \mathcal{L}\end{matrix}\right|_{\substack{\text{IV}\\ A^{(i)},B^{(i)}}} = [S^1]_{A^{(i)},B^{(i)}} \left|\begin{matrix}V\\ M\\ V'\\ M'\\ F\end{matrix}\right|_{\substack{\text{III}\\ A^{(i)},B^{(i)}}} + [S^2]_{A^{(i)},B^{(i)}} \left|\begin{matrix}\phi\\ y\end{matrix}\right|_{\substack{\text{III}\\ A^{(i)},B^{(i)}}}$$

Eq. (24)

where

$$[S^1] \triangleq \left[\begin{array}{cc|cc|c} \cos\Psi & \begin{bmatrix}1&0\\0&1\\0&\bar{b}\\0&0\end{bmatrix} & -\sin\Psi & \begin{bmatrix}1&0\\0&1\\0&\bar{b}\\0&0\end{bmatrix} & \begin{matrix}0\\\ell_s\\\bar{a}\\0\end{matrix} \\ \hline \sin\Psi & \begin{bmatrix}1&0\\0&1\\0&-\bar{e}\\0&0\end{bmatrix} & \cos\Psi & \begin{bmatrix}1&0\\0&1\\0&-\bar{e}\\0&0\end{bmatrix} & \\ \hline \begin{matrix}0\\0\end{matrix} & \begin{matrix}0\\-\bar{d}\cos\Psi\end{matrix} & \begin{matrix}0\\0\end{matrix} & \begin{matrix}0\\-\bar{d}\sin\Psi\end{matrix} & \begin{matrix}1\\\bar{c}\end{matrix} \end{array}\right]$$

$$[S^2] \triangleq \left[\begin{array}{cc} \cos\Psi & \begin{bmatrix}0&0\\0&0\\1&0\\0&1\end{bmatrix} \\ \hline \sin\Psi & \begin{bmatrix}0&0\\0&0\\1&0\\0&1\end{bmatrix} \\ \hline \cos\Psi & \begin{bmatrix}0&0\\\ell_s&0\end{bmatrix} \end{array}\right]$$

d. Cluster Attachments: The "Outrigger"

A procedure similar to that for the spider beams was followed in obtaining the transfer across the aft cluster-body attachment. The major difference is in arriving at a suitable elastic matrix. The outrigger structures are beam-trusses with joints whose dimensions are not negligible compared to the lengths of the members. For this reason, Turner's method (Reference 12) was used to compute influence coefficients for forces and moments in the plane of the truss, acting at the cluster-body attachment, with the center-body attachment fixed to "ground". The outrigger representation is shown in Fig. 9. The springs pictured schematically in this figure represent the following force-deflection relation

$$\begin{vmatrix} y \\ \phi \\ z \end{vmatrix}_O = \begin{bmatrix} \underline{a} & \underline{b} & \underline{c} \\ -\underline{d} & -\underline{e} & -\underline{f} \\ \underline{g} & \underline{h} & \underline{i} \end{bmatrix} \begin{vmatrix} V \\ M \\ F \end{vmatrix}_O$$

Making use of (a) these flexibility influence coefficients, (b) the transfer required to cross the rigid lengths D and H in Figure 9, and (c) a rotation-matrix which is the inverse of the matrix [R] filled out to 10 x 10 form, we obtain the outrigger transfer relation

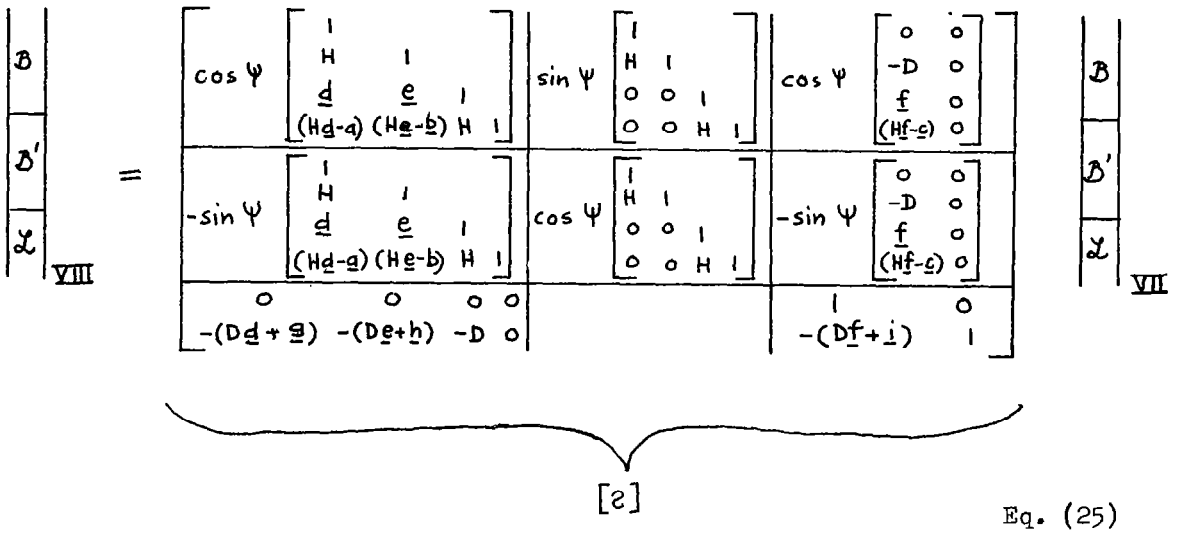

Eq. (25)

It should be noted that both the outrigger matrix [z] and the spider matrices [s$_i$] and [s$_j$] are dependent on the angle Ψ associated with a particular A or B cluster body. Thus these matrices must be identified by the indices $A^{(i)}$ or $B^{(i)}$; state (column)matrices associated with these transfers will, in general, also have to be so identified.

e. The Frequency Determinant

Consider bending motion along either of the principal axes shown in Figure 2. Symmetry allows the sum of all moments and forces which are applied to the center-body by the clustered bodies to be described in terms of quantities on the clustered bodies in only one quadrant.

The forces we are concerned about here are supplied at the cluster attachments and can be looked upon as consisting of inertia forces (and couples) of the masses on the cluster bodies and the intermediate unknowns $(V, M, V', M', T, F)_{III\ A^{(i)}, B^{(i)}}$.

Table II
Cluster-body Summation Coefficients and Azimuthal Constants - Saturn I

Total No. of Bodies	Total No. of Bodies	Body Index $(A^{(i)}, B^{(i)})$	Principal Axis No. 1			Principal Axis No. 2		
			$k_{A^{(i)},B^{(i)}}$	$\cos\psi^{(i)}$	$\sin\psi^{(i)}$	$k_{A^{(i)},B^{(i)}}$	$\cos\psi^{(i)}$	$\sin\psi^{(i)}$
2	0	$A^{(1)}$	2	1	0	2	0	-1
		$A^{(2)}$	0	-	-	0	-	-
3	0	$A^{(1)}$	1	1	0	1	0	-1
		$A^{(2)}$	2	$-1/2$	$\sqrt{3}/2$	2	$\sqrt{3}/2$	$1/2$
4	0	$A^{(1)}$	2	1	0	2	$1/\sqrt{2}$	$-1/\sqrt{2}$
		$A^{(2)}$	2	0	1	2	$1/\sqrt{2}$	$1/\sqrt{2}$
6	0	$A^{(1)}$	4	$\sqrt{3}/2$	$1/2$	4	$1/2$	$-\sqrt{3}/2$
		$A^{(2)}$	2	0	1	2	1	0
2	2	$A^{(1)}$	2	1	0	2	0	-1
		$A^{(2)}$	0	-	-	0	-	-
		$B^{(1)}$	2	0	1	2	1	0
		$B^{(2)}$	0	-	-	0	-	-
3	3	$A^{(1)}$	1	1	-	1	0	-1
		$A^{(2)}$	2	$-1/2$	$\sqrt{3}/2$	2	$\sqrt{3}/2$	$1/2$
		$B^{(1)}$	1	-1	0	1	0	1
		$B^{(2)}$	2	$1/2$	$\sqrt{3}/2$	2	$\sqrt{3}/2$	$-1/2$
4	4	$A^{(1)}$	2	1	0	4	$1/\sqrt{2}$	$1/\sqrt{2}$
		$A^{(2)}$	2	0	1	0	-	-
		$B^{(1)}$	4	$1/\sqrt{2}$	$1/\sqrt{2}$	2	1	0
		$B^{(2)}$	0	-	-	2	0	1

From a simple inspection, the intermediate unknowns on the two $A^{(1)}$ bodies will be equal and so would be those on the two $A^{(2)}$ bodies and those on the four B bodies. (This is so when bending along Principal Axis #1 is considered). In order to obtain a similar result for the inertia forces referred to the center body axis system, it is only necessary to (1) assume bending deflections ϕ and y along a principal axis, (2) resolve these displacements into ϕ, y, ϕ', y', z in the cluster body co-ordinate system, (3) assume forces and moments V, M, V', M' and F. in the co-ordinate system of each body to be proportional to displacements ϕ, y, ϕ', y', z and (4) retransform these forces and moments into the center body axis system.

Alternatively, a completely formal proof would consist of writing out the azimuthal rotation matrices $[R]_{A^{(i)},B^{(i)}}$ and outrigger matrices $[z]_{A^{(i)},B^{(i)}}$ for all eight bodies, lumping the cluster traverse matrices together with matrices $[T_2]$, $[E_s]$ and $[T_1]$ in the spider transfers for the three groups of bodies represented by the $A^{(1)}, A^{(2)}$ and B bodies respectively (See Fig. 2 and Table II) and using the displacement compatibility within these groups. This procedure establishes Table II.

For the case of the Saturn I, bending in the direction of Principal Axis #1, thus, the sum of transverse shear forces experienced at the center-body as reactions from the spider beams would be

$$2\, V_{III A^{(1)}} + 2\, V_{III A^{(2)}} + 4\, V_{III B^{(1)}}$$

Similarly the total bending moment for an arrangement with six cluster-bodies of the same kind, say A-bodies, bending along Principal Axis #2 would be

$$4\, M_{III A^{(2)}} + 2\, M_{III A^{(1)}}$$

Clearly the choice as to first cluster-body and principal axis direction is arbitrary; the angle $\psi_{(i)}$ must, however, be consistent. To preserve generality, the numerical coefficients which appear in the above equation will be called $k_{A^{(i)},B^{(i)}}$. They will be inputs to the problem, depending on the configuration being analyzed. For the first equation above, for example

$$k_{A^{(1)}} = 2$$

$$k_{A^{(2)}} = 2$$

$$k_{B^{(1)}} = 4$$

$$k_{B^{(2)}} = 0$$

Table II gives values of $k_{A^{(i)},B^{(i)}}$ and the sines and cosines of corresponding to Fig. 2. Note that for the Saturn I - axis #1 case we have reduced the problem to one of three cluster-bodies, $A^{(1)}, A^{(2)}$ and B.

It is now possible to express the transfer across the entire system using (a) Equ. (3a), (b) the as yet undetermined forces and moments carried in the spiders and outriggers, and (c) the summation of such forces and moments where the cluster-body structural attachments join the center-body. Thus

$$\left|\begin{matrix} V \\ M \end{matrix}\right|_X = \left|\begin{matrix} 0 \\ 0 \end{matrix}\right| =$$

$$= [\mu]_T \left\{ \left[\begin{matrix} [K] \\ [0] \end{matrix}\right] \left|\begin{matrix} V \\ M \end{matrix}\right|_{A^{(1)}} \left|\begin{matrix} V \\ M \end{matrix}\right|_{A^{(2)}} \left|\begin{matrix} V \\ M \end{matrix}\right|_{B}_{III} + \left([\mu^2]_C [\mu_2]_N + [\mu^1]_C [\mu_1]_N \right) \left|\begin{matrix} \phi \\ y \end{matrix}\right|_I - [\mu^1]_C [K] \left|\begin{matrix} V \\ M \end{matrix}\right|_{A^{(1)}} \left|\begin{matrix} V \\ M \end{matrix}\right|_{A^{(2)}} \left|\begin{matrix} V \\ M \end{matrix}\right|_{B}_{III} \right\}$$

where Eq. (26)

$[\mu^1]_C$ = first two colums of $[\mu]_C$

$[\mu^2]_C$ = second two columns of $[\mu]_C$

$[\mu_1]_N$ = first two rows of $[\mu]_N$

$[\mu_2]_N$ = second two rows of $[\mu]_N$

$$[K] = \left[k_{A^{(1)}} \begin{bmatrix} 1 & 0 \\ 0 & 1 \end{bmatrix} \middle| k_{A^{(2)}} \begin{bmatrix} 1 & 0 \\ 0 & 1 \end{bmatrix} \middle| k_B \begin{bmatrix} 1 & 0 \\ 0 & 1 \end{bmatrix} \right]$$

Note that the quantity inside the brace in this equation is the equivalent of Eqs. (8) and (9) specialized to the Saturn lateral bending case. The first step is to evaluate V and M at Station $\text{VIII}_{A^{(i)},B}$ in terms of V, M, V', M' and F at Station $\text{III}_{A^{(i)},B}$ and ϕ and y at Station I. If all the cluster-bodies were "built-in" at the attachment to the spider and outrigger, this would be a straight-forward matter. That is, we would simply use Eqs. (3a), (3b), (24) and (25) to write

$$\left|\begin{matrix}V\\M\end{matrix}\right|_{\substack{\text{VIII}\\A^{(i)},B^{(i)}}} = \left[\mathcal{Z}^{1}\right]_{A^{(i)},B^{(i)}} \begin{bmatrix}[\mu] & & \\ & [\mu] & \\ & & [\lambda]\end{bmatrix}_{A,B} \left\{ \left[S^{1}\right]_{A^{(i)},B^{(i)}} \left|\begin{matrix}V\\M\\V'\\M'\\F\end{matrix}\right|_{\substack{\text{III}\\A^{(i)},B^{(i)}}} + \left[S^{2}\right]_{A^{(i)},B^{(i)}} \left[\mu_2\right]_{C} \left|\begin{matrix}\phi\\y\end{matrix}\right|_{\text{I}} \right\}$$

where $\left[\mathcal{Z}^{1}\right]$ = first two rows of $[\mathcal{Z}]$

The variety of cluster-body end conditions encountered on Saturn I, and summarized in Table I, however, requires more detailed treatment. It is important to keep in mind that the fuel and LOX tanks are associated with indeces A and B. respectively.

Condition 1 in Table I implies that $\phi_{\text{IV}\,A^{(i)},B}$ can influence nothing "downstream", and that $\phi_{\text{V}\,A^{(i)},B}$ will constitute three more unknowns, since they are related to nothing "upstream". Similarly, Conditions 2 and 3 for the fuel tanks in Table I imply that $\phi_{\text{IV}\,A^{(i)}}$ and $z_{\text{IV}A^{(i)}}$ will be of no further influence in the transfer procedure, and that $\phi_{\text{V}\,A^{(i)}}$ and $z_{\text{V}A^{(i)}}$ will comprise four new unknowns. Old unknowns are therefore exchanged for new in the following steps.

Step 1: Conditions 1, 2, and 3 for the fuel tanks allow Eq. (24) to be specialized to

$$\left|\begin{matrix}M\\M'\\F\end{matrix}\right|_{\substack{\text{IV}\\A^{(i)}}} = \left|\begin{matrix}0\\0\\0\end{matrix}\right| = \begin{bmatrix}0 & \cos\psi & 0 & -\sin\psi & 0\\ 0 & \sin\psi & 0 & \cos\psi & 0\\ 0 & 0 & 0 & 0 & 1\end{bmatrix} \left|\begin{matrix}V\\M\\V'\\M'\\F\end{matrix}\right|_{\substack{\text{III}\\A^{(i)}}}$$

which leads to the conclusion that

$$\left|\begin{matrix} M \\ M' \\ F \end{matrix}\right|_{\substack{\text{III} \\ A^{(i)}}} = 0 \qquad \text{Eq. (27)}$$

Step 2: Condition 1 for the LOX tanks leads to the relation

$$F_{\text{III}B} = -M_{\text{III}B}\frac{\cos\psi_B}{\ell_s} + M'_{\text{III}B}\frac{\sin\psi_B}{\ell_s} \qquad \text{Eq. (28)}$$

Step 3: Condition 4 applied to Eq. (36) leads to the relation

$$\phi_{\text{V}(A^{(i)},B)} = -\frac{\mu_{21}}{\mu_{23}} V_{\text{V}(A^{(i)},B)} - \frac{\mu_{24}}{\mu_{23}} y_{\text{V}(A^{(i)},B)}$$

Where μ_{ij} is the element of $[\mu]$ in the i^{th} row, j^{th} column, and Condition 1 has also been used to advantage. It follows that

$$\left|\begin{matrix} V \\ y \end{matrix}\right|_{\substack{\text{VI} \\ A^{(i)},B}} = \underbrace{\begin{bmatrix} \mu_{11} - \mu_{13}\frac{\mu_{21}}{\mu_{23}} & \mu_{14} - \mu_{13}\frac{\mu_{24}}{\mu_{23}} \\ \mu_{41} - \mu_{43}\frac{\mu_{21}}{\mu_{23}} & \mu_{44} - \mu_{43}\frac{\mu_{24}}{\mu_{23}} \end{bmatrix}}_{[\bar{\mu}]_{A,B}} \left|\begin{matrix} V \\ y \end{matrix}\right|_{\substack{\text{V} \\ A^{(i)},B}} \qquad \text{Eq. (29)}$$

Using Eq. (28) and the remaining conditions at the outrigger in Table I, the transfer across the clustered bodies expressed by Eq. (36) is now replaced by

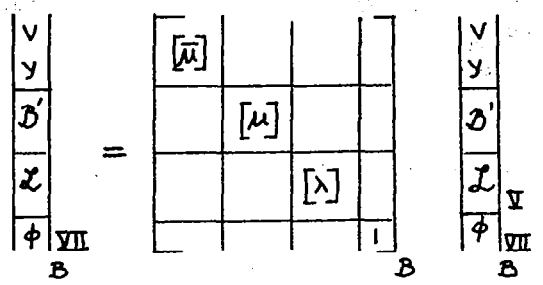

Eq. (30)

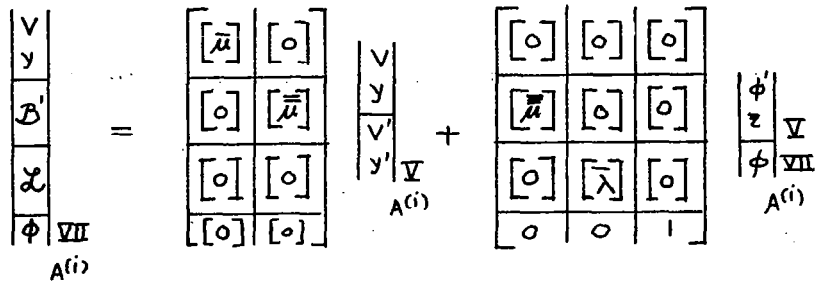

Eq. (31)

where:

$$[\bar{\bar{\mu}}]_A = \text{first and fourth columns of } [\mu]_A$$

$$[\bar{\bar{\mu}}]_A = \text{third column of } [\mu]_A$$

$$[\bar{\lambda}]_A = \text{second column of } [\lambda]_A$$

and the last row in each of these equations is an identity.

Substituting Eqs. (24) and (25) in Eqs. (30) and (31), V and M at Station $\text{VIII}_{A^{(i)},B}$ can be expressed in terms of quantities yet to be eliminated and ϕ and y at Station I, by the equations:

$$\left|\begin{matrix} V \\ M \end{matrix}\right|_{\text{VIII}\ A^{(i)}} =$$

$$= [z_2^1]_{A^{(i)}} \left\{ \underbrace{\begin{bmatrix} [\bar{\mu}] & & \\ & [\bar{\bar{\mu}}] & \\ & & \end{bmatrix}_A [s_2^1]_{A^{(i)}} \begin{bmatrix} [\bar{\bar{\mu}}] & & \\ & [\bar{\lambda}] & \\ & & 1 \end{bmatrix}_A}_{[\alpha]_{A^{(i)}}} \left|\begin{matrix} V \\ V' \\ \phi' \\ z \\ \phi \end{matrix}\right|_{\begin{matrix}\text{III}\\ \text{V}\\ \text{VII}\end{matrix}\ A^{(i)}} + \underbrace{\begin{bmatrix} [\bar{\mu}] & \\ & [\bar{\bar{\mu}}] \\ & \end{bmatrix}_A [s_2^2]_{A^{(i)}} [\mu_2]_N}_{[\beta]_{A^{(i)}}} \left|\begin{matrix} \phi \\ y \end{matrix}\right|_{\text{I}} \right\}$$

Eq. (32)

$$\left|\begin{matrix} V \\ M \end{matrix}\right|_{\text{VIII}\ B} = [z_2^1]_B \left\{ \underbrace{\begin{bmatrix} [\bar{\mu}] & & & \\ & [\mu] & & \\ & & [\lambda]_B & \\ & & & 1 \end{bmatrix} [s_2^1]_B}_{[\alpha]_B} \left|\begin{matrix} V \\ M \\ V' \\ M' \\ \phi \end{matrix}\right|_{\begin{matrix}\text{III}\\ \text{VII}\end{matrix}\ B} + \underbrace{\begin{bmatrix} [\bar{\mu}] & & \\ & [\mu] & \\ & & [\lambda] \\ & & \end{bmatrix} [s_2^2]_B [\mu_2]_N}_{[\beta]_B} \left|\begin{matrix} \phi \\ y \end{matrix}\right|_{\text{I}} \right\}$$

Eq. (33)

where:

$$\left[S_2^1\right]_{A^{(i)},B} = \begin{bmatrix} \cos\psi & -\sin\psi \\ 0 & 0 \\ \sin\psi & \cos\psi \\ 0 & 0 \end{bmatrix}_{A^{(i)},B}$$

$$\left[S_2^2\right]_{A^{(i)},B} = \begin{bmatrix} 0 & 0 \\ 0 & \cos\psi \\ 0 & 0 \\ 0 & \sin\psi \end{bmatrix}_{A^{(i)},B}$$

and $[z_2^i]_{A^{(i)},B}$ is formed from $[z]_{A^{(i)},B}$ by dropping the second column and moving column three to the last position.

These equations could now be inserted in the complete transfer, Eq. (26), and thus eliminate all the quantities at Station VIII. But, note, however, that fifteen intermediate unknowns would remain, namely V, V' at III, z at V; and ϕ at VII on $A^{(1)}$ and $A^{(2)}$; and V, M, V', M' at III and ϕ at VII on B. The fifteen simultaneous equations required to eliminate these unknowns are provided by the conditions that deflections at Station VIII must be compatible i.e.

$$\left|\begin{matrix} \phi \\ y \\ \phi' \\ y' \\ z \end{matrix}\right|_{\text{VIII}}_{A^{(i)},B} = \left|\begin{matrix} \phi \\ y \\ 0 \\ 0 \\ 0 \end{matrix}\right|_{\text{VIII}}_{C}$$

The left hand side of this compatibility equation is obtained by a process similar to that leading to Eqs. (31) and (32). The right hand side is available from Eqs. (36), (26), (28), (32), and (33). Thus

$$[z^2]_{A^{(i)}} \left\{ [\alpha]_{A^{(i)}} \left| \begin{array}{c} V \\ V' \\ \hline \phi' \\ \hline z \\ \hline \phi \end{array} \right|_{A^{(i)}} \begin{array}{l} \text{III} \\ \\ \text{V} \\ \text{VII} \end{array} + [\beta]_{A^{(i)}} \left| \begin{array}{c} \phi \\ y \end{array} \right|_{I} \right\}$$

$$= \left[\begin{array}{c} [\mu_2^2]_C [\mu_2]_N + [\mu_2']_C [\mu_1]_N \\ \hline [0] \end{array} \right] \left| \begin{array}{c} \phi \\ y \end{array} \right|_{I} - \left[\begin{array}{c} [\mu_2']_C \\ \hline [0] \end{array} \right] [K] \left| \begin{array}{c} V \\ 0 \\ \hline V \\ 0 \\ \hline V \\ M \end{array} \right| \begin{array}{l} A^{(1)} \\ A^{(2)} \\ \\ B \end{array} \quad \text{III}$$

and

$$[z^2]_B \left\{ [\alpha]_B \left| \begin{array}{c} V \\ M \\ \hline V' \\ M' \\ \hline \phi \end{array} \right|_{B} \begin{array}{l} \text{III} \\ \\ \text{VII} \end{array} \quad [\beta]_B \left| \begin{array}{c} \phi \\ y \end{array} \right|_{I} \right\}$$

$$= \left[\begin{array}{c} [\mu_2^2]_C [\mu_2]_N + [\mu_2']_C [\mu_1]_N \\ \hline [0] \end{array} \right] \left| \begin{array}{c} \phi \\ y \end{array} \right|_{I} - \left[\begin{array}{c} [\mu_2']_C \\ \hline [0] \end{array} \right] [K] \left| \begin{array}{c} V \\ 0 \\ \hline V \\ 0 \\ \hline V \\ M \end{array} \right| \begin{array}{l} A^{(1)} \\ A^{(2)} \\ \\ B \end{array} \quad \text{III}$$

where

$[\mu_2^2]_c$ = last two rows of $[\mu^2]_c$

$[\mu_2^1]_c$ = last two rows of $[\mu^1]_c$

$[z^2]$ is formed from the 3rd, 4th, 7th, 8th, and 10th rows of $[z]$ where the 2nd column is dropped, and column three moved to last position.

These three simultaneous matrix equations can now be combined into a single relation expressing the fifteen compatiblity equations. Thus,

$$[\bar{a}] \begin{array}{|c|l} V & \\ V' & \text{III} \\ \phi' & \\ z & \text{V} \\ \phi & \text{VII}_{A^{(1)}} \\ \hline V & \\ V' & \text{III} \\ \phi' & \\ z & \text{V} \\ \phi & \text{VII}_{A^{(2)}} \\ \hline V & \\ M & \\ V' & \\ M' & \text{III} \\ \phi & \text{VII}_B \end{array} = [\bar{P}] \left| \begin{array}{c} \phi \\ \hline y \end{array} \right|_I \qquad \text{Eq. (34)}$$

where

$$[\bar{a}] = \begin{array}{|c|c|c|} \hline \left[[z^2][\alpha] + [\eta]\right]_{A^{(1)}} & [\eta]_{A^{(2)}} & [\eta]_B \\ \hline [\eta]_{A^{(1)}} & \left[[z^2][\alpha] + [\eta]\right]_{A^{(2)}} & [\eta]_B \\ \hline [\eta]_{A^{(1)}} & [\eta]_{A^{(2)}} & \left[[z^2][\alpha] + [\eta]\right]_B \\ \hline \end{array}$$

$$[\bar{P}] = \begin{bmatrix} [\bar{v}] - [\mathcal{E}^2]_{A^{(1)}}[\beta]_{A^{(1)}} \\ [\bar{v}] - [\mathcal{E}^2]_{A^{(2)}}[\beta]_{A^{(2)}} \\ [\bar{v}] - [\mathcal{E}^2]_B [\beta]_B \end{bmatrix}$$

$$[\eta]_{(A^{(i)},B)} = \left[\begin{array}{c} [\mu_2^1]_C \\ \hline [0] \end{array}\right] \begin{bmatrix} k_{(A^{(i)},B)} & 0 & 0 & 0 & 0 \\ 0 & 0 & 0 & 0 & 0 \end{bmatrix}$$

$$[\bar{v}] = \left[\begin{array}{c} [\mu_2^2]_C [\mu_2]_N + [\mu_2^1]_C [\mu_1]_N \\ \hline [0] \end{array}\right]$$

A new matrix , $[\bar{K}]$, to be used in the next Equation, is defined as follows :

$$[\bar{K}] = \begin{bmatrix} k_{A^{(1)}} & 0 & 0 & 0 & 0 & k_{A^{(2)}} & 0 & 0 & 0 & 0 & k_B & 0 & 0 & 0 & 0 \\ 0 & 0 & 0 & 0 & 0 & 0 & 0 & 0 & 0 & 0 & 0 & k_B & 0 & 0 & 0 \end{bmatrix}$$

Now premultiplying Eq. (34) by $[\bar{a}]^{-1}$, substituting the appropriate rows of the resulting equation into Eqs. (32) and (33) and all of them into Eq.(26) we obtain the expression for the transfer across the complete vehicle.

$$\left|\begin{matrix} V \\ M \end{matrix}\right|_X = \left|\begin{matrix} 0 \\ 0 \end{matrix}\right| = [\mu]_T \left\{ [\mu^2]_C [\mu_2]_N + [\mu^1]_C [\mu_1]_N + \left[\begin{matrix} [K] \\ [0] \end{matrix}\right] \left[\begin{matrix} [\ell_2'][\beta] \\ [\ell_2'][\beta] \\ [\ell_2'][\beta] \end{matrix}\right] \begin{matrix} A^{(1)} \\ A^{(2)} \\ B \end{matrix} \right.$$

$$\left. + \left(\left[\begin{matrix} [K] \\ [0] \end{matrix}\right] \left[\begin{matrix} [\ell_2'][\alpha] & & \\ & [\ell_2'][\alpha] & \\ & & [\ell_2'][\alpha] \end{matrix}\right] \begin{matrix} A^{(1)} \\ A^{(2)} \\ B \end{matrix} - [\mu^1]_C [\bar{K}] \right) [\bar{Q}]^{-1} [\bar{P}] \right\} \left|\begin{matrix} \phi \\ y \end{matrix}\right|_I$$

$$\triangleq [\Delta] \left|\begin{matrix} \phi \\ y \end{matrix}\right|_I \qquad \text{Eq. (35)}$$

This shows that for the natural bending frequencies of the complete Saturn vehicle compared to Eq. (23) it is necessary to find the values of ω which make a 2 x 2 determinant equal to zero.

f. Mode Shapes

The procedure for obtaining the mode shapes is essentially similar to that used for getting the mode shapes of the fully coupled motion of Titan III described in Section I C(d) above. In this case, however, the procedure involved to obtain the"displacement vector" at Station I does not involve elaborate matrix operations since the final singular matrix in equation (35) is of a lower order, 2 x 2 instead of 6 x 6 in case of the fully coupled vibrations. Thus either one of the two equations comprising equation (35) allows solving for ϕ_I when $\omega = \omega_n$ and $y_I = 1$. Thus the state vector at Station I is completely defined (to within an arbitrary factor) and equations (1a) and (2a) with ω_n inserted provide a means for evaluating the state vectors at successive stations to the branching point at Station III. There, equation (34), premultiplying by $[\bar{Q}]^{-1}$ allows the

process to be continued, with the successive use of the spider matrix, equilibrium at Station III, more of Equation (1a) and (2a) plus (1b) and (2b) type of transfers and then the outrigger matrix. At Station VIII, compatibility of deflections provides a rigorous check of the calculation's accuracy to that point, a similar test occurs at Station X, whereV and M should be zero.

3. Saturn I Longitudinal Vibrations

a. General

Though the natural frequencies of longitudinal vibration of clustered launch vehicles of conventional design are likely to be considerably higher than those of transverse or torsional vibrations, a study of the former is of considerable interest. A major reason for this is the phenomenon of "pogo" oscillations which is really an instability involving the rocket engine thrust variation and structural properties of the vehicle as well as the liquid sloshing phenomenon.

The effect of coupled shell-liquid interaction is of considerable importance in case of the longitudinal oscillations. The present analysis does not take this interaction into account. However, many coupled shell-liquid oscillation analyses employ a generalized coordinate approach and the results of the present analysis may be found useful in these methods.

Due to the offset of the cluster centerline from the vehicle axis of symmetry, bending of the clustered bodies may be coupled to the longitudinal vibrations of the entire vehicle and provision must be made in the analysis for accounting for this bending.

The following sections indicate the analytical treatment of these longitudinal vibrations of Saturn I. A more detailed description will be found in Reference 16.

b. Considerations of Symmetry

In case of these longitudinal vibrations of the Saturn vehicle, it may be argued that all the four "A" bodies will behave identically as a group and so would the four "B" bodies. Pure longitudinal motion, however, is not the only type of natural motion of the vehicle. There can be harmonic oscillation with absolutely no motion of the center-body and higher stages of the vehicle. These modes are termed the "internally balanced modes" and are described in detail later in part D of this chapter.

If, as will be seen, it is possible to have cluster-body motion without any center-body motion, it will also be possible to have cluster-body radial bending with only pure extensite motion of the center-body. In fact the existance of non-zero values for the terms $\underline{c}$ and $\underline{f}$ on page 47 is evidence of a direct coupling between longitudinal motion and cluster-body radial bending.

While the same argument might be made for cluster tangential bending, it is more difficult to imagine a situation in which this kind of motion would exist as part of a longitudinal mode.

Furthermore, since there is complete polar symmetry, the azimuthal angle Ψ loses significance as does the difference between $A^{(1)}$ and $A^{(2)}$ and between $B^{(1)}$ and $B^{(2)}$. Thus, in this longitudinal analysis, we are dealing simply with longitudinal and radial bending quantities on un-numbered A and B cluster bodies.

c. Analysis

Since only longitudinal vibrations of the vehicle are being considered, the only quantities of interest on the nose section, center-body and tail section will be F and z. Thus

$$\left|\mathcal{L}\right|_{i+1} = \left[E_{\ell}\right]_i \left|\mathcal{L}\right|_{i+\frac{1}{2}} \qquad \text{Eq. (1c)}$$

$$\left|\mathcal{L}\right|_{i+\frac{1}{2}} = \left[M_{\ell}\right]_i \left|\mathcal{L}\right|_i \qquad \text{Eq. (2c)}$$

$$\left|\mathcal{L}\right|_{\text{II,VIc,X}} = \left[\lambda\right]_{\text{N,C,T}} \left|\mathcal{L}\right|_{\text{I,Vc,IX}} \qquad \text{Eq. (3c)}$$

As discussed above, the transfer matrices for the cluster-bodies can be simplified from the form in Eq. (3b) to

$$\left|\begin{matrix}\mathcal{B}\\ \mathcal{L}\end{matrix}\right|_{\text{A,B}}^{\text{VI}} = \left[\begin{array}{c|c} [\mu] & \\ \hline & [\lambda] \end{array}\right]_{\text{A,B}} \left|\begin{matrix}\mathcal{B}\\ \mathcal{L}\end{matrix}\right|_{\text{A,B}}^{\text{V}} \qquad \text{Eq. (3d)}$$

The matrices representing the transfer across the spider arms, involve only $[\bar{T}_1]$, $[\bar{E}_s]$ and $[\bar{T}_2]$ metrices, which differ from $[T_1]$, $[E_s]$ and $[T_2]$ (used for the transverse bending case) in that no tangential quantities need be carried and $[\bar{E}_s]$ uses $\bar{a},\bar{b},\bar{c},\bar{d}$ insead of $\bar{a},\bar{b},\bar{c},\bar{d},\bar{e}$ (see Appendix B).

$$[\bar{T}_1] \triangleq \left[\begin{array}{cccc|cc} 0 & 0 & 0 & 0 & 1 & 0 \\ 0 & 1 & 0 & 0 & 0 & 0 \\ 0 & 0 & 1 & 0 & 0 & 0 \\ 0 & 0 & 0 & 0 & 0 & 1 \\ \hline -1 & 0 & 0 & 0 & 0 & 0 \\ 0 & 0 & 0 & -1 & 0 & 0 \end{array}\right]$$

$$[\bar{T}_2] \triangleq \left[\begin{array}{cccc|cc} 0 & 0 & 0 & 0 & -1 & 0 \\ 0 & 1 & 0 & 0 & 0 & 0 \\ 0 & 0 & 1 & 0 & 0 & 0 \\ 0 & 0 & 0 & 0 & 0 & -1 \\ \hline 1 & 0 & 0 & 0 & 0 & 0 \\ 0 & 0 & 0 & 1 & 0 & 0 \end{array}\right]$$

The spider matrix for the longitudinal analysis will thus be denoted by $[\bar{S}]$, and is given by

$$[\bar{S}] = [\bar{T}_2]\,[\bar{E}_s]\,[\bar{T}_1]$$

satisfying the equation

$$\left|\begin{matrix}\mathcal{B} \\ \mathcal{L}\end{matrix}\right|_{\substack{\text{IV} \\ A,B}} = [\bar{S}] \left|\begin{matrix}\mathcal{B} \\ \mathcal{L}\end{matrix}\right|_{\substack{\text{III}^* \\ A,B}}$$

$\text{III}^*_{A,B}$ indicates the cluster-body azimuthal axis system at Station $\text{III}_{A,B}$.

The transfer matrices representing the outriggers will correspond to those used in the transverse analysis, but again eliminating the rotation matrix $[R]^{-1}$ referred to on page 48 and the tangential quantities. This relation is

$$\left|\begin{matrix}\mathcal{B}\\ \mathcal{L}\end{matrix}\right|_{\substack{\text{VIII}^*\\ A,B}} = \underbrace{\left[\begin{array}{cccc|cc} 1 & 0 & 0 & 0 & 0 & 0 \\ H & 1 & 0 & 0 & -D & 0 \\ \underline{d} & \underline{e} & 1 & 0 & \underline{f} & 0 \\ (H\underline{d}-\underline{a}) & (H\underline{e}-\underline{b}) & H & 1 & (H\underline{f}-\underline{c}) & 0 \\ \hline 0 & 0 & 0 & 0 & 1 & 0 \\ -(D\underline{d}+\underline{g}) & -(D\underline{e}-\underline{h}) & -D & 0 & -(D\underline{f}+\underline{i}) & 1 \end{array}\right]}_{[\bar{\mathcal{L}}]} \left|\begin{matrix}\mathcal{B}\\ \mathcal{L}\end{matrix}\right|_{\substack{\text{VII}\\ A,B}}$$

$\text{VIII}^*_{A,B}$ indicates the cluster-body azimuthal axis system at Station $\text{VIII}_{A,B}$.

Using (a) eq. (3c), (b) the as yet undetermined longitudinal forces carried in the spider arms and outriggers and (c) the summation of these forces at the cluster-body structural attachment to the centerbody, the transfer across the entire system can be written as

$$F_X = 0 = [\lambda^1]_T \left\{ [\theta] z_I + \left[\begin{matrix}[K]\\ [0]\end{matrix}\right] \left|\begin{matrix}F_A\\ F_B\end{matrix}\right|_{\text{VIII}} - [\lambda^1]_c [\bar{K}] \left|\begin{matrix}F_A\\ F_B\end{matrix}\right|_{\text{III}} \right\}$$

where $$[\bar{K}] \triangleq \left[\begin{array}{c|c} \left(k_{A(1)} + k_{A(2)}\right) & \left(k_{B(1)} + k_{B(2)}\right) \end{array}\right]$$

$$[\theta] \triangleq [\lambda^1]_c \lambda^1_N + [\lambda^2]_c \lambda^2_N$$

λ^1_N and λ^2_N are the first and second elements in column 2 of $[\lambda]_N$, respectively

$[\lambda^1]_c$ and $[\lambda^2]_c$ are columns 1 and 2 of $[\lambda]_c$ respectively

$[\lambda^1]_T$ = row 1 of $[\lambda]_T$

In order to be able to use equation (26a) to get the numerical equivalent of the frequency polynomial, we have to express the forces at $\text{III}_{A,B}$ and $\overline{\text{VIII}}_{A,B}$ in terms of z_I .

The spider matrix $[\bar{S}]$ in conjunction with Eq. (3c) can be used to write

$$\left|\begin{matrix}\beta \\ \alpha\end{matrix}\right|_{\text{IV}}_{A,B} = [\bar{S}^1] \left|\begin{matrix}V \\ M \\ F\end{matrix}\right|_{\text{III}^*}_{A,B} + [\bar{S}^2]\, \lambda_N^2\, z_I \qquad \text{Eq. (24a)}$$

where

$[\bar{S}^1] \triangleq$ columns 1, 2, and 5 of $[\bar{S}]$

$[\bar{S}^2] \triangleq$ column 6 of $[\bar{S}]$

Since the cluster boundary conditions are the same as in the earlier case of transverse bending vibrations, equations (27)thru (31) will hold in this case.

The six intermediate unknowns will be, in this case of longitudinal motion of the Saturn vehicle,

$$\left|\begin{matrix}V \\ z \\ \phi\end{matrix}\right|\begin{matrix}\text{III}^*_A \\ \text{V}_A \\ \text{VII}_A\end{matrix} \quad \text{and} \quad \left|\begin{matrix}V \\ M \\ \phi\end{matrix}\right|\begin{matrix}\text{III}^*_B \\ \text{VII}_B\end{matrix}$$

Using equations (24a),(29), (31), and noting from the outrigger matrix on page 48 that $F_{\text{VIII}\,A} = F_{\text{VII}\,A}$, we get

$$F_{\text{VIII}\,A} = \bar{\lambda}^1_A\, z_{\text{V}A} \qquad \text{Eq. (32a)}$$

Where $\bar{\lambda}^1_A$ is the first element of $[\bar{\lambda}]_A$.

Similarly, using equations (24a), (29), (30), and observing that

$$F_{VIII\,B} = F_{VII\,B} ,$$

we find that $$F_{VIII\,B} = [\lambda_1]_B \left|\begin{matrix} F \\ z \end{matrix}\right|_{V\,B}$$

where $[\lambda_1]_B$ = row 1 of $[\lambda]_B$

Noting from page 53 that

$$F_{III\,B} = -\frac{1}{\ell_s} M_{III^*B}$$

this becomes

$$F_{VIII\,B} = [\lambda_1]_B \left\{ [\bar{S}_1^1] \left|\begin{matrix} V \\ M \end{matrix}\right|_{\substack{III^* \\ B}} + [\bar{S}_1^2] \lambda_N^2 z_I \right\} \qquad \text{Eq. (33a)}$$

where $[\bar{S}_1^1]$ = columns 1, and 2 of $[\bar{S}_1]$

and $[\bar{S}_1^2]$ = column 3 of $[\bar{S}_1]$

$[\bar{S}_1]$ = rows 5 and 6 of $[\bar{S}_0]$ which is formed from $[\bar{S}]$ by adding $-\ell_s$ times column 5 to column 2 and dropping columns 3,4,and 5.

Thus, using (32a) and (33a) and noting that $F_{III\,A} = o$: Eq.(26a) simplifies to

$$F_X = o = [\lambda']_T \left\{ [\Theta] z_I - [\lambda']_C \left(k_{B^{(1)}} + k_{B^{(2)}}\right) F_{III\,B} \right.$$

$$\left. + \begin{bmatrix} \left(k_{A^{(1)}} + k_{A^{(2)}}\right) \\ o \end{bmatrix} \bar{\lambda}'_A z_{V\,A} + \begin{bmatrix} \left(k_{B^{(1)}} + k_{B^{(2)}}\right) \\ o \end{bmatrix} [\lambda_1]_B \left[[\bar{S}_1^1] \left|\begin{matrix} V \\ M \end{matrix}\right|_{\substack{III^* \\ B}} + [\bar{S}_1^2] \lambda_N^2 z_I \right] \right\}$$

Eq. (26b)

The six compatibility equations to be used to eliminate the six intermediate unknowns are

$$\left|\begin{matrix}\phi\\ y\\ z\end{matrix}\right|_{\substack{\text{VIII}\\ A,B}} = \left|\begin{matrix}0\\ 0\\ z\end{matrix}\right|_{\text{VIII C}}$$

The longitudinal displacement at Station VIIIC is

$$z_{\text{VIII C}} = \theta^2 z_I - (\lambda'_2)_C \left(K_{B(1)} + K_{B(2)}\right) F_{\text{III B}}$$

where

θ^2 ≜ 2nd element of $[\theta]$

$(\lambda'_2)_C$ ≜ 2nd element of $[\lambda']_C$

i.e.

$$z_{\text{VIII C}} = \theta^2 z_I + \underbrace{\frac{1}{\ell_s} (\lambda'_2)_C \left(k_{B(1)} + k_{B(2)}\right)}_{\epsilon_B} M_{\text{III}^*B}$$

Using Eqs. (28), (29), (30), (31) the following expressions are obtained for displacement at $\text{VIII}^*_{A,B}$

$$\left|\begin{matrix}\phi\\ y\\ z\end{matrix}\right|_{\text{VIII}^*A} = \underbrace{[\bar{z}'] \left[\begin{array}{c|c|c} [\bar{\mu}]_A\ [\bar{s}'_2] & & \\ \hline & [\bar{\lambda}]_A & \\ \hline & & 1 \end{array}\right] \left|\begin{matrix}V\\ z\\ \phi\end{matrix}\right|_{\substack{\text{III}^*\\ \text{V}\\ \text{VII}\\ A}}}_{[\bar{Q}_A]} + \underbrace{[\bar{z}'] \left[\begin{array}{c|c} [\bar{\mu}]_A\ [\bar{s}'_2] & \\ \hline [0] & \\ \hline 0 & \end{array}\right] \lambda^2_N z_I}_{[\bar{P}]_A}$$

and

$$\begin{vmatrix} \phi \\ y \\ z \end{vmatrix}_{VIII^*B} = \underbrace{[\bar{z}^1] \begin{bmatrix} [\bar{\mu}]_B\ [\bar{s}_3^1] & \\ [\lambda]_B\ [\bar{s}_1^1] & \\ & 1 \end{bmatrix}}_{[\bar{\alpha}]_B} \begin{vmatrix} V \\ M \\ \phi \end{vmatrix}_B^{III^*} + \underbrace{[\bar{z}^1] \begin{bmatrix} [\bar{\mu}]_B\ [\bar{s}_2^2] \\ [\lambda]_B\ [\bar{s}_1^2] \\ 0 \end{bmatrix} \lambda_N^2}_{[\bar{\beta}]_B} z_I$$

where

$[\bar{z}^1]$ = rows 3,4,6, of $[\bar{z}_9]$ which is formed from columns 1,4,5,6,3 of $[\bar{z}]$ in that order

$[\bar{s}_2]$ = rows 1 and 4 of $[\bar{s}]$

$[\bar{s}_2^1]$ = column 1 of $[\bar{s}_2]$

$[\bar{s}_2^2]$ = column 6 of $[\bar{s}_2]$

$[\bar{s}_3]$ = rows 1 and 4 of $[\bar{s}_0]$

$[\bar{s}_3^1]$ = columns 1 and 2 of $[\bar{s}_3]$

$[\bar{s}_3^2]$ = column 3 of $[\bar{s}_3]$

The compatibility relations can now be written in the following forms

$$[Q_A] \begin{vmatrix} V \\ z \\ \phi \end{vmatrix}_A^{III^*} = [P_A]\ z_I \qquad \text{Eq. (34a)}$$

and

$$[Q_B] \begin{vmatrix} V \\ M \\ \phi \end{vmatrix}_B^{III^*} = [P_B]\ z_I \qquad \text{Eq. (34b)}$$

where

$$[P_A] \triangleq \left|\begin{array}{c} 0 \\ 0 \\ \theta^2 - [\bar{\beta}]_A \end{array}\right|$$

$$[P_B] \triangleq \left|\begin{array}{c} 0 \\ 0 \\ \theta^2 - [\bar{\beta}]_B \end{array}\right|$$

$$[Q_B] \triangleq [\bar{\kappa}]_B - \left[\begin{array}{c|c|c} & & \\ & & \\ & \epsilon_B & \end{array}\right]$$

Premultiplying Eqs. (34a) and(34b) by $[Q_A]^{-1}$ and $[Q_B]^{-1}$ respectively, and substituting the results in Eq. (26b),

$$F_X = 0 = [\lambda']_T \Bigg\{ [\theta] + \left|\begin{array}{c} \left(k_{B^{(1)}} + k_{B^{(2)}}\right) \\ \hline 0 \end{array}\right| [\lambda_1]_B [\bar{S}_1^2] \lambda_N^2$$

$$+ \left|\begin{array}{c} \left(K_{A^{(1)}} + k_{A^{(2)}}\right) \\ \hline 0 \end{array}\right| [0 \;\; \bar{\lambda}'_A \;\; 0] [Q_A]^{-1} [P_A]$$

$$+ \left(k_{B^{(1)}} + k_{B^{(2)}}\right) \left\{ \left|\begin{array}{c} 1 \\ 0 \end{array}\right| \left[[\lambda_1]_B [\bar{S}_1] \,\middle|\, 0 \right] + \frac{1}{\ell_s} [\lambda']_c [0 \;\; 1 \;\; 0] \right\} [Q_B]^{-1} [P_B] \Bigg\} z_I$$

$$\triangleq \bar{\Delta} \; z_I$$

Eq. (35a)

The element $\overline{\Delta}$ in equation (35a) must be zero for free vibrations of the vehicle.

d. Mode Shapes

The procedure for obtaining the mode shapes will not involve obtaining the state vector at Station I, since the only displacement there is z_I . Assuming $z_I = 1$, the nose section can be traversed using equation (3c); equations (1c) and (2c) being used to obtain the state vector at each of the nose stations. At Station III, equation (3a) allows the process to be continued with the successive use of the spider matrices, equilibrium of Station III, more of equations (1c) and(2c), and then the oturigger matrix. At Station VIII, compatibility of deflections provides a check on the numerical work, a similar test occurs at Station X where F should vanish.

D. Internally Balanced Modes

The symmetry of the usual clustered configuration makes it possible for the clustered bodies to oscillate in groups so as to achieve equilibrium without motion of the center-body. The simplest of such modes is shown in Figure 10a; this is a sort of dilatational pattern and requires only two symmetrically arranged clustered bodies. In this motion, as well as the others described below, the cluster attachment flexibility enters, since the points of zero motion, in general, are at the center-body. The effect of the attachment structure will be in general, to couple longitudinal and radial motion. Figure 10b shows how this too can be balanced without center-body motion if there are at least four clustered bodies. The expressions from which the natural frequencies of these "internally balanced modes" can be calculated are different for fuel and LOX tanks, since their attachment fixities differ. Using Eq. (3b), and the component factors of the spider and outrigger matrices excepting the rotation matrices $[R]$ and $[R]^{-1}$, it can be shown that the expressions for the natural frequencies of these dilatational-longitudinal "internally balanced modes" are:

for fuel tanks, i.e. $A^{(i)}$ bodies,

$$\left(\lambda_{22} - \underline{i}\,\lambda_{12}\right)\left[\frac{\mu_{41} - \mu_{43}\,\frac{\mu_{21}}{\mu_{23}}}{\mu_{11} - \mu_{13}\,\frac{\mu_{21}}{\mu_{23}}} - \underline{a}\right] - \left(\lambda_{12}\,\underline{c}\,\underline{g}\right) = 0$$

Eq. (36)

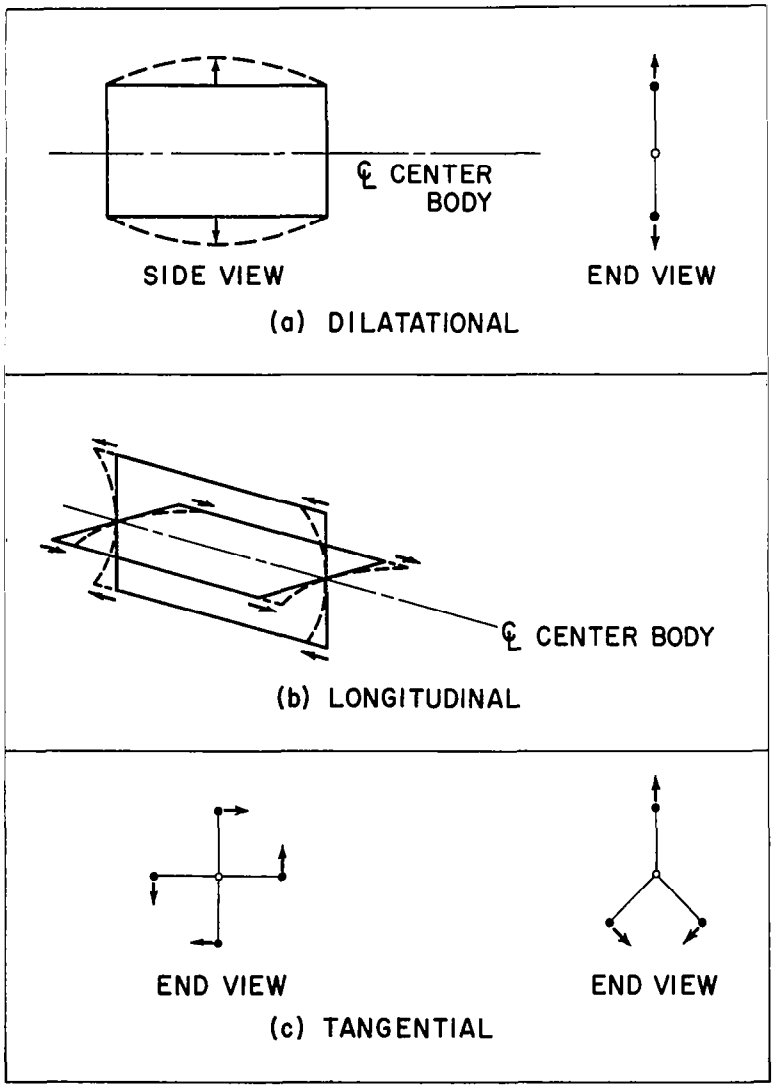

Figure 10 Schematics of Internally Balanced Modes

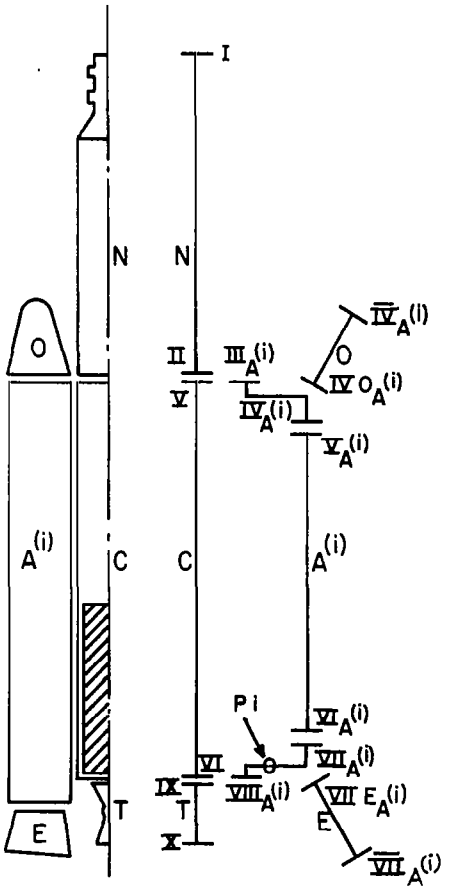

FIG. 11 REPRESENTATION OF OVERHUNG PORTIONS OF CLUSTERED BODIES

and for LOX tanks, i.e. $B^{(i)}$ bodies,

$$\left[\lambda_{21} + \lambda_{22}\left(\underline{c} - \underline{d}\,\ell_s\right)\right]\left[\frac{\mu_{41} - \mu_{43}\frac{\mu_{21}}{\mu_{23}}}{\mu_{11} - \mu_{13}\frac{\mu_{21}}{\mu_{23}}} - \underline{a}\right]$$

$$- \left[\lambda_{11} + \lambda_{12}\left(\underline{c} - \underline{d}\,\ell_s\right)\right]\left[\frac{\mu_{41} - \mu_{43}\frac{\mu_{21}}{\mu_{23}}}{\mu_{11} - \mu_{13}\frac{\mu_{21}}{\mu_{23}}}\,\underline{i} + \underline{c}\,\underline{\vartheta} - \underline{a}\,\underline{i}\right] = 0$$

Eq. (37)

Figure 10c shows a third such pattern, consisting of tangential motion which requires at least three clustered bodies. The appropriate characteristic expressions yielding the frequency of these modes are

for fuel tanks,

$$\mu_{31}\mu_{43} - \mu_{33}\mu_{41} = 0 \qquad \text{Eq. (38)}$$

and

for LOX tanks,

$$\mu_{31}\left(\mu_{42} - \bar{e}\,\mu_{43}\right) - \mu_{41}\left(\mu_{32} - \bar{e}\,\mu_{33}\right) = 0$$

Eq. (39)

E. Modifications to the Basic Longitudinal Transfers

The transfer matrices given in Section IB of this report can be used to properly represent almost all parts of a launch vehicle where shell deformations are not involved. There are special situations commonly encountered, however, which require additions to or modifications of these basic transfers for a realistic mathematical model. Three such cases are considered here.

1. Staging joints

Truss work joints, such as exist between the first and second stage of the Saturn I model, can be handled much like the outrigger structure, and also result in flexibilities concentrated in very short lengths. (See Figure 1a) Again, 'Turner's method (Reference 12) can be used for obtaining the influence coefficients of such structures; Appendix C derives a transfer matrix, denoted by the symbol $[J]$, which can simply be placed in series with the $[E_b]$, $[E_t]$, $[E_l]$ transfers with no other modification of the method.

2. Fuel Sloshing

Reference has been made earlier to the changes necessary to mass properties in order to properly approximate the dynamics of liquids carried by the launch vehicle. For the lateral motions, effective mass expressions were used. The theory adapted was that of a sloshing liquid in a rigid, cylindrical tank as given by Abramson, Chu, and Ransleben (Reference 13). They give the following expressions for

(a) side-force per unit lateral acceleration

$$M_L \left\{ 1 + \frac{2 \tanh\left(\xi_1 \frac{2h}{d}\right)}{\xi_1 \frac{2h}{d} \left(\xi_1^2 - 1\right)\left(\frac{\omega_1^2}{\omega^2} - 1\right)} \right\}$$

(b) side-force per unit angular acceleration

$$M_L h \left\{ \frac{1}{4\left(\frac{2h}{d}\right)^2} + \frac{\xi_1 \tanh\left(\xi_1 \frac{2h}{d}\right) + \frac{4}{\frac{2h}{d}\cosh\left(\xi_1 \frac{2h}{d}\right)} - \frac{2}{\frac{2h}{d}}}{\xi_1 \frac{2h}{d} \left(\xi_1^2 - 1\right)\left(\frac{\omega_1^2}{\omega^2} - 1\right)} \right\}$$

where M_L = mass of the liquid column of height h

ω_1 = first sloshing natural frequency = (rigid cylindrical tank) $\sqrt{\frac{2g}{d} \xi_1 \tanh\left(\xi_1 \frac{2h}{d}\right)}$

ξ_1 = first zero of the first derivative of the first order Bessel function of the first kind = 1.841

g = acceleration of gravity.

A brief examination of the dimensions involved in the case of the Saturn I shows that only the first mode of sloshing would have an appreciable effect on the bending modes of interest.

It seems commensurate with the accuracy of the overall calculation to make a simple adaptation of these expressions to the flexible tank situation actually encountered here. The difficulties in so doing are associated with the facts (a) that various lengths of the fluid column must be represented as concentrated masses, (b) that each such mass will be undergoing different and unprescribed amplitudes, and (c) that the farther a part of the column is from the free surface, the smaller will be the influence of the free surface.

For the case of the two dimensional waves in an infinitely deep liquid, bounded by plane vertical walls, Lamb (Reference 15) shows that the amplitude of oscillation in the first mode at a depth h_i is proportional to

$$\exp\left(-\pi \frac{h_i}{d}\right)$$

where d is the distance between the walls. Thus, it was considered reasonable to limit the liquid column which could be considered to be "sloshing" to a depth where only 5% of the surface wave motion occurs. Thus

$$h = -\frac{d}{\pi} \log_e 0.05$$

and d is now taken as the tank diameter. The amount of fluid undergoing sloshing between two stations on the tank, say $j-\frac{1}{2}$ to $j+\frac{1}{2}$ is proportional to

$$\int_{h_{j-\frac{1}{2}}}^{h_{j+\frac{1}{2}}} \exp\left(-\frac{\pi x}{d}\right) dx$$

This amount of fluid is a fraction of the total undergoing sloshing, and that fraction is expressible as

$$f_j = \frac{\int_{h_{j-\frac{1}{2}}}^{h_{j+\frac{1}{2}}} \exp\left(-\pi \frac{x}{d}\right)\, dx}{\int_0^h \exp\left(-\pi \frac{x}{d}\right)\, dx} = \frac{\exp\left(-\pi \frac{h_{j-\frac{1}{2}}}{d}\right) - \exp\left(-\pi \frac{h_{j+\frac{1}{2}}}{d}\right)}{0.95}$$

Thus, to account for sloshing in those sections of the tanks near a free surface the $[M_b]$ matrices must be written in the form

$$\left[M_{bf}\right]_j = \begin{bmatrix} 1 & 0 & \omega^2 U_{fj} & \omega^2 (m_{rj} + M_{fj}) \\ 0 & 1 & 0 & 0 \\ 0 & 0 & 1 & 0 \\ 0 & 0 & 0 & 1 \end{bmatrix}$$

where m_{rj} = solid contribution to mass at station j

$$M_{fj} = M_L \left\{ \frac{h_{j+\frac{1}{2}} - h_{j-\frac{1}{2}}}{h} + f_j \frac{2 \tanh\left(\xi_1 \frac{2h}{d}\right)}{\xi_1 \frac{2h}{d} \left(\xi_1^2 - 1\right)\left(\frac{\omega_1^2}{\omega^2} - 1\right)} \right\}$$

$$U_{fj} = M_L h f_j \left\{ \frac{1}{4\left(\frac{2h}{d}\right)^2} + \frac{\xi_1 \tanh\left(\xi_1 \frac{2h}{d}\right) + \frac{4}{\frac{2h}{d}\cosh\left(\xi_1 \frac{2h}{d}\right)} - \frac{2}{\frac{2h}{d}}}{\xi_1 \frac{2h}{d} \left(\xi_1^2 - 1\right)\left(\frac{\omega_1^2}{\omega^2} - 1\right)} \right\}$$

It has been noted earlier that an important fluid effect which is not accounted for in the longitudinal analysis presented here is the coupling between longitudinal fluid accelerations and the shell breathing resulting from "hoop stresses". It appears likely that an extension of the transfer matrix approach using classical shell theory could account for such effects.

3. Overhanging Structures

The Titan III has SRM engine nozzles and skirt structure aft of stations $\text{VII}_{A(i)}$ which contain considerable portions of the SRM bodies and which are likely to contribute appreciably to the modes of oscillation. Some accounting is therefore desirable that will represent this structure in the usual form; i.e. lumped masses and massless elastic elements.

Similar treatments could be used for the forward portions of the SRM's ahead of Station IV SRM. The revision to the mathematical model is shown in Figure 11.

The desired changes can conviently be included as follows: The continuity of deflections at Stations IV-V and at Stations VI-VII requires that

$$\left|\begin{matrix}\phi\\ y\\ \phi'\\ y'\\ \theta\\ z\end{matrix}\right|_{\text{IV}_{A(i)}} = \left|\begin{matrix}\phi\\ y\\ \phi'\\ y'\\ \theta\\ z\end{matrix}\right|_{\text{V}_{A(i)}} = \left|\begin{matrix}\phi\\ y\\ \phi'\\ y'\\ \theta\\ z\end{matrix}\right|_{\text{IV}O_{A(i)}}$$

and

$$\left|\begin{matrix}\phi\\ y\\ \phi'\\ y'\\ \theta\\ z\end{matrix}\right|_{\text{VI}_{A(i)}} = \left|\begin{matrix}\phi\\ y\\ \phi'\\ y'\\ \theta\\ z\end{matrix}\right|_{\text{VII}_{A(i)}} = \left|\begin{matrix}\phi\\ y\\ \phi'\\ y'\\ \theta\\ z\end{matrix}\right|_{\text{VII}E_{A(i)}}$$

Similarly the equilibrium of these joints requires

$$\left|\begin{matrix}V\\ M\\ V'\\ M'\\ T\\ F\end{matrix}\right|_{\text{V}_{A(i)}} = \left|\begin{matrix}V\\ M\\ V'\\ M'\\ T\\ F\end{matrix}\right|_{\text{IV}_{A(i)}} - \left|\begin{matrix}V\\ M\\ V'\\ M'\\ T\\ F\end{matrix}\right|_{\text{IV}O_{A(i)}} \qquad \text{Eq. (40)}$$

and

$$\begin{vmatrix} V \\ M \\ V' \\ M' \\ T \\ F \end{vmatrix}_{\overline{VII}_{A(i)}} = \begin{vmatrix} V \\ M \\ V' \\ M' \\ T \\ F \end{vmatrix}_{VI_{A(i)}} - \begin{vmatrix} V \\ M \\ V' \\ M' \\ T \\ F \end{vmatrix}_{VII\,E_{A(i)}} \qquad \text{Eq. (41)}$$

Since the engines and nose section extremities at $\overline{VII}_{A(i)}$ and $\overline{IV}_{A(i)}$ respectively, are free,

$$\begin{vmatrix} V \\ M \\ V' \\ M' \\ T \\ F \end{vmatrix}_{\overline{IV}_{A(i)}} = \begin{vmatrix} V \\ M \\ V' \\ M' \\ T \\ F \end{vmatrix}_{\overline{VII}_{A(i)}} = 0$$

The engines can be traversed using

$$\begin{vmatrix} V \\ M \\ V' \\ M' \\ T \\ F \end{vmatrix}_{\overline{VII}_{A(i)}} = [\sigma_1]_E \begin{vmatrix} V \\ M \\ \phi \\ y \\ V' \\ M' \\ \phi' \\ y' \\ T \\ \theta \\ F \\ z \end{vmatrix}_{VII\,E_{A(i)}} = \begin{vmatrix} 0 \\ 0 \\ 0 \\ 0 \\ 0 \\ 0 \end{vmatrix}$$

$[\sigma_1]_E$ is obtained by taking only the rows 1, 2, 5, 6, 9, 11 of the $[\sigma]_{E\ (12\times12)}$

This homogeneous set can be rewritten as

$$\begin{vmatrix} V \\ M \\ V' \\ M' \\ T \\ F \end{vmatrix}_{\text{VII}\,E_{A(i)}} = - \underbrace{\left[\sigma_1^1\right]_E^{-1} \left[\sigma_1^2\right]_E}_{[b_{ij}]} \begin{vmatrix} \phi \\ y \\ \phi' \\ y' \\ \theta \\ z \end{vmatrix}_{\text{VII}\,E_{A(i)}}$$

Eq. (42)

where $\left[\sigma_1^1\right]_E \triangleq$ columns 1, 2, 5, 6, 9, 11 of $\left[\sigma_1\right]_E$

$\left[\sigma_1^2\right]_E \triangleq$ columns 3, 4, 7, 8, 10, 12 of $\left[\sigma_1\right]_E$

Similarly for the front overhang between $\text{IV}O_{A(i)}$ and $\overline{\text{IV}}_{A(i)}$

$$\begin{vmatrix} V \\ M \\ V' \\ M' \\ T \\ F \end{vmatrix}_{\overline{\text{IV}}_{A(i)}} = \left[\sigma_1\right]_O \begin{vmatrix} V \\ M \\ \phi \\ y \\ V' \\ M' \\ \phi' \\ y' \\ T \\ \theta \\ F \\ z \end{vmatrix}_{\text{IV}\,O_{A(i)}} = \begin{vmatrix} 0 \\ 0 \\ 0 \\ 0 \\ 0 \\ 0 \end{vmatrix}$$

$\left[\sigma_1\right]_O$ is obtained by taking only the rows 1, 2, 5, 6, 9, 11 of $\underset{(12\times12)}{\left[\sigma\right]_O}$.

Note: Since we are moving from left to right in this transfer, the values of lengths of the elastic elements in the overhung nose section elastic matrices $[\mathcal{E}]_i$ will have to be negative.

Again rearranging gives

$$\left|\begin{matrix} V \\ M \\ V' \\ M' \\ T \\ F \end{matrix}\right|_{\text{IV } O_{A(i)}} = - \underbrace{\left[\sigma_1^1\right]_O^{-1} \left[\sigma_1^2\right]_O}_{\left[a_{ij}\right]} \left|\begin{matrix} \phi \\ y \\ \phi' \\ y' \\ \theta \\ z \end{matrix}\right|_{\text{IV } O_{A(i)}}$$

Eq. (43)

where

$\left[\sigma_1^1\right]_O$ = columns 1,2,5,6,9,11 of $\left[\sigma_1\right]_O$

$\left[\sigma_1^2\right]_O$ = columns 3,4,7,8,10,12 of $\left[\sigma_1\right]_O$

Equations (40, 41, 42, and 43) allow adding the forces and moments due to the overhung structures at their pointsof attachment. It is thus possible to modify Eq. (3) for the clustered-bodies and obtain the following equation for transfer from Station $\text{IV}_{A(i)}$ to $\text{VII}_{A(i)}$ including the effects of the overhung sections:

$$\left|\begin{matrix} \mathcal{B} \\ \mathcal{B}' \\ \mathcal{J} \\ \mathcal{L} \end{matrix}\right|_{\text{VII}_{A(i)}} = \underset{(12\times12)}{\left[E\right]_A} \underset{(12\times12)}{\left[\sigma\right]_A} \underset{(12\times9)}{\left[O\right]_A} \left|\begin{matrix} V \\ \phi \\ y \\ V' \\ \phi' \\ y' \\ T \\ \theta \\ z \end{matrix}\right|_{\text{IV}_{A(i)}}$$

Where $\left[O\right]_A$ and $\left[E\right]_A$ are defined on the next page.

$$[O]_A \triangleq \underset{(12\times 9)}{}$$

$$\left[\begin{array}{ccc|cc|cc} a_{11} & a_{12} & & a_{13} & a_{14} & a_{15} & a_{16} \\ a_{21} & a_{22} & & a_{23} & a_{24} & a_{25} & a_{26} \\ & & & & & & \\ a_{31} & a_{32} & & a_{33} & a_{34} & a_{35} & a_{36} \\ a_{41} & a_{42} & & a_{43} & a_{44} & a_{45} & a_{46} \\ & & & & & & \\ a_{51} & a_{52} & & a_{53} & a_{54} & a_{55} & a_{56} \\ & & & & & & \\ a_{61} & a_{62} & & a_{63} & a_{64} & a_{65} & a_{66} \end{array}\right]$$

$$[E]_A \triangleq \underset{(12\times 12)}{}$$

$$\left[\begin{array}{c|cc|cc|cc|cc} 1 & & & & & & & & \\ \hline & 1 & b_{11} & b_{12} & & b_{13} & b_{14} & b_{15} & b_{16} \\ & & b_{21} & b_{22} & & b_{23} & b_{24} & b_{25} & b_{26} \\ & & & & & & & & \\ \hline & & b_{31} & b_{32} & 1 & b_{33} & b_{34} & b_{35} & b_{36} \\ & & b_{41} & b_{42} & & b_{43} & b_{44} & b_{45} & b_{46} \\ & & & & & & & & \\ \hline & & b_{51} & b_{52} & & b_{53} & b_{54} & b_{55} & b_{56} \\ & & & & & & & & \\ \hline & & b_{61} & b_{62} & & b_{63} & b_{64} & b_{65} & b_{66} \end{array}\right]$$

II. NUMERICAL RESULTS AND COMPARISON WITH TEST

Table III shows the input breakdown for the NASA 1/5 Scale model of Saturn I at 48% fuel condition. Even after taking advantage of symmetry, a breakdown this fine results in a system with 114 degrees of freedom; the largest inverse required, however, is 15 x 15, and the largest frequency determinant 2 x 2.

Figure 12 is a plot of frequency determinant vs. trial frequency for this case. The abscissa is linear, but the ordinate is the signed log (to the base 10) of the determinantal values divided by 10 raised to a power. This power is determined for each plot as that which leaves the smallest value greater than unity after all values are so reduced. The natural frequencies are immediately obvious in this plot, as are the vertical asymptotes which indicate the existence of the internally balanced modes. Figure 13 shows the corresponding plots for the natural frequencies which involve no center-body motion. (i.e. for Eqs. (36) thru (39)).

A summary of calculated frequencies, including the effects of fuel slosh and 1g axial loads, is given in Tables V and VI. Comparison with test results using three different cable-harness suspensions (References 2 and 14) shows reasonably good agreement. None of the internally balanced modes listed in Table VII were obtained in the referenced tests, since shaking forces were always applied on the center-body there. Note that the rocket engine natural frequency is listed; although not all subsystems are sources of internally balanced modes, uncoupled engine modes can also be in equilibrium without center-body motion, since there are two similar sets of four identical engines.

Figures 14 thru 27 show modal deflections corresponding to the first six center-body bending modes of both the 48% full and 100% full conditions. The theoretical shapes are all normalized to unit deflection of Station 369, the first mass point in the analysis. The test points, however, are normalized to enhance the comparison; in a mode consisting mainly of cluster-body motion, for example, the maximum test deflection is made equal to the calculated value.

These calculations were repeated for Principal Axis #2 and neither frequencies nor deflection shapes showed significant differences.

A normal reaction to Fig. 14a, if unfamiliar with vibrations of branched beams, is that the shape is too complex for a fundamental mode; there is a tendency to feel that the cluster-body deflections should line up with the center-body, more like the test results. Some thought regarding the minimization of energy, however, will lead to the conclusion that, for branched systems, the motion of part of the system can have several nodes and reversals of curvature if such is necessary for equilibrium and minimizes the strain energy of the system.

Differences between theory and test for the fuel tank radial motion in Fig. 14a exists mainly because the first two zeros in Fig. 12 are very close to the fundamental uncoupled fuel tank mode listed in Table VII. Amplitudes near resonance are, of course, sensitive to small changes in frequency ratio and damping. The calculation neglects damping and so over-estimates the response of subsystems near resonance. The same comments apply to Fig. 15a; note here that merely changing from spring to link suspension systems in the Reference 14 test cause a phase change of 180° in the fuel tank radial motion. This also typifies behavior around resonance, and suggests that the spring-suspension mode at 14.7 cps really should be grouped with the fundamental mode. Note also that the effect of the staging joint between station 190 and 200 is noticeable even in these low modes, but might easily be "faired out" in drawing thru test points. Sloshing reduces the fuel-tank radial motion shown in Fig. 14a by a factor of 3 and increases that in Fig. 15a by the same amount.

The third test mode in Fig. 16a shows that the slope in tangential bending at the aft fuel tank attachment need not be equal to the center-body slope at that point. Thus, the rigidity assigned to this joint in the basic model is a poor assuption. The calculated center-body deflection in this area clearly shows the effect of being "forced" to follow the slope of the near-resonant (see Table X) fuel tank in tangential bending. This assumption could be easily relaxed by introducing a "concentrated spring" as the last station of the clustered bodies. Sloshing increases the first stage motion relative to second and third stages but the major effect is in improving frequency correlation (see Table V). Previous comments regarding cluster-body resonance and aft-attachment tangential bending slope all apply to a lesser extent to the comparison in Fig. 17. In this case, the flexibility of the second stage inner tank relative to the missile skin is becoming evident. Because of this, or perhaps the combination of this plus the outrigger tangential bending fixity, LOX-tank radial motion is apparently closer to resonance in the test results. In any event, the modal agreement is generally good. The effect of sloshing on this mode is rather small and tends to become still less with increasing modal number.

The fifth calculated natural mode (Fig. 18) has a family resemblance to the test data; that is, they are both "first antisymmetric" bending of the center-body. The $A^{(1)}$ radial motion is out of phase with respect to the translational motion at its end points, since it is being excited above its uncoupled natural frequency. The assumed rigidity of the outrigger for tangential bending slopes, however, forces the slope of the $A^{(2)}$ body at the aft end to be equal to that of the center-body, hence its more complicated shape.

Note that the calculated clustered LOX tank motion is in proper phase, but the tests show much less response than is predicted. Again from Table V the calculated system mode appears close to resonance with the uncoupled tangential mode of the clusted LOX tank. It is difficult to predict how the relative amplitudes would change if the tangential bending flexibility of the outrigger were included. If the response of the B-body were lowered, the balance of forces and moments would then require increased center-body motion, thus - in all likelihood - improving the center-body correlation as well.

Fig. 19 shows a comparison of calculated and test shapes for the sixth natural frequency. This shows quite good agreement everywhere except for the first-stage center-body. Again, one can speculate as to how corrections for second stage inner tank flexibility and outrigger tangential bending flexibility would affect these higher modes.

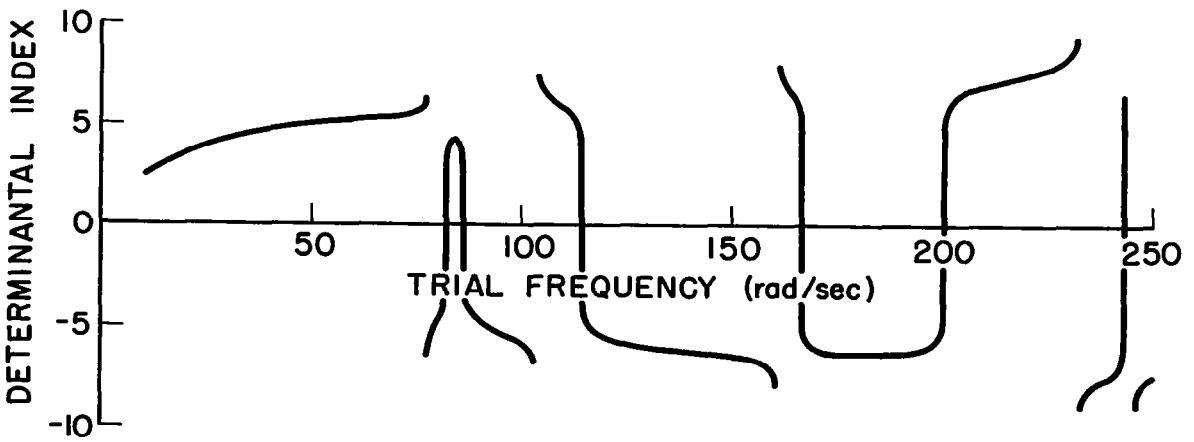

Figure 12. Frequency Determinant Index vs. Trial Frequency
Saturn I, 48% Full Condition

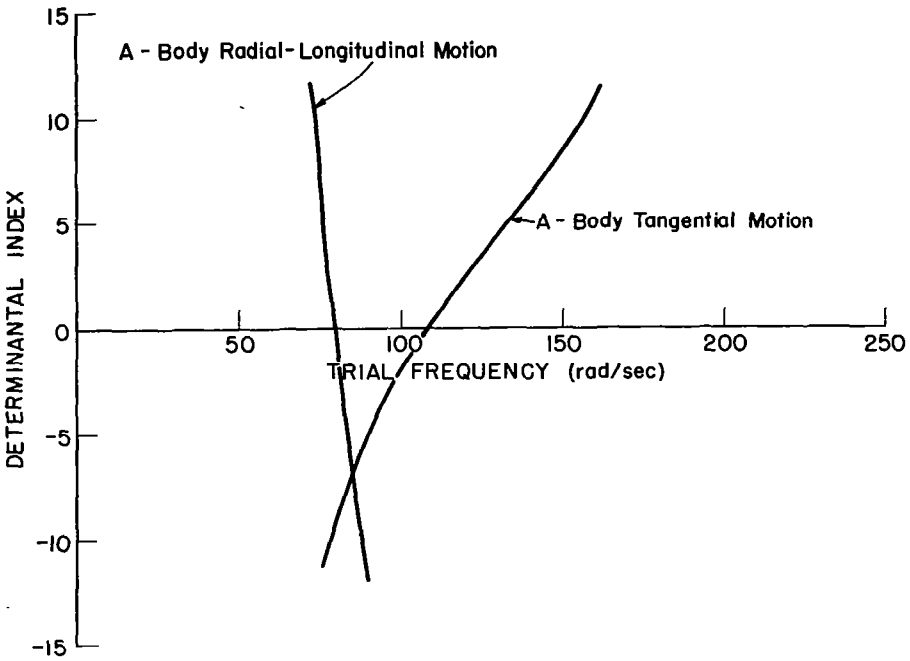

Figure 13a. Internally Balanced Modes: Frequency Determinant Index vs. Trial Frequency Saturn I, 48% Full A Body Motion

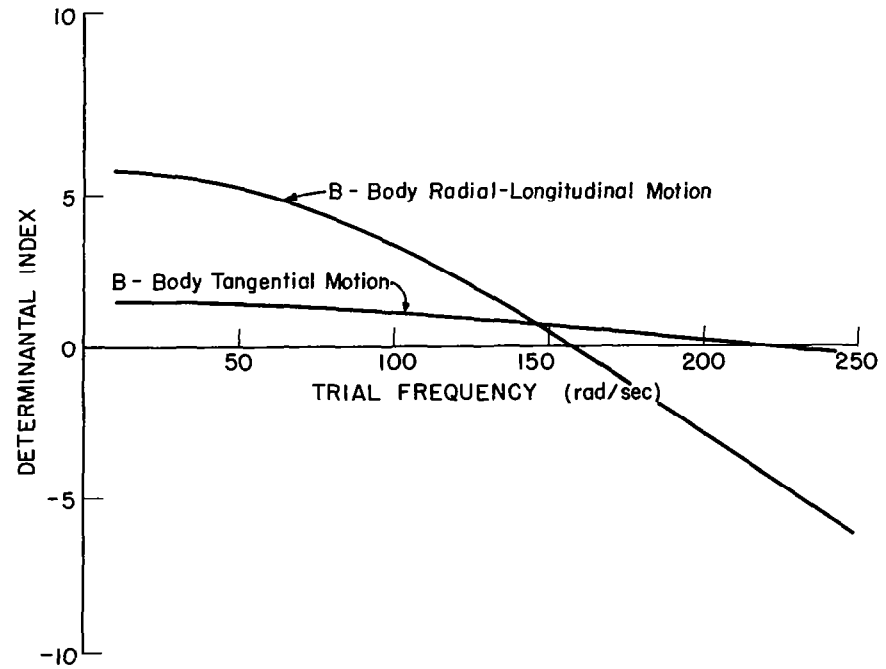

Figure 13b Internally Balanced Modes: Frequency Determinant Index vs. Trial Frequency Saturn I, 48% Full B Body Motion

Table III

1/5 Scale Saturn I , Breakdown for 48 % Full Condition

STATION DATA	LOC@	M	MW	MSTAR	L	EI*10**9	AE*10**6	GHT*10**6	A	I	SLOSH	SPARE
NOSE 1	379.7000	0.0184	0.0000	0.0000	19.9000	0.4000	13.1000	0.0000	0.0184	0.0000	0.0000	0.0000
2	359.4000	0.0317	0.0000	0.0000	15.6000	1.3000	21.5000	0.0000	0.0481	0.0000	0.0000	0.0000
3	343.8000	0.5025	0.0000	0.0000	8.3000	1.8000	24.1000	0.0000	0.5506	0.0000	0.0000	0.0000
4	335.5000	0.3425	0.0000	0.0000	9.3000	1.8000	24.1000	0.0000	0.8931	0.0000	0.0000	0.0000
5	362.2000	0.3425	0.0000	0.0000	9.3000	1.8000	24.1000	0.0000	1.2356	0.0000	0.0000	0.0000
6	316.9000	0.3425	0.0000	0.0000	9.3000	1.8000	24.1000	0.0000	1.5781	0.0000	0.0000	0.0000
7	307.6000	0.3425	0.0000	0.0000	10.6000	1.8000	13.9000	0.0000	1.9206	0.0000	0.0000	0.0000
8	297.0000	0.4800	0.0000	0.0000	11.5000	8.0000	8.8000	0.0000	2.4006	0.0000	0.0000	0.0000
9	285.5000	0.0187	0.0000	0.0000	13.5000	18.5000	44.6400	0.0000	2.4193	0.0000	0.0000	0.0000
10	272.0000	0.1651	0.0000	0.0000	9.1000	18.5000	44.6400	0.0000	2.5844	0.0000	0.0000	0.0000
11	262.9000	0.4270	0.0000	0.0000	12.2000	18.5000	44.6400	0.0000	3.0114	0.0000	0.0000	0.0000
12	250.7000	0.4270	0.0000	0.0000	12.2000	18.5000	44.6400	0.0000	3.4384	0.0000	0.0000	0.0000
13	238.5000	0.4270	0.0000	0.0000	12.2000	18.5000	44.6400	0.0000	3.8654	0.0000	0.0000	0.0000
14	226.3000	0.4270	0.0000	0.0000	12.2000	18.5000	44.6400	0.0000	4.2924	0.0000	0.0000	0.0000
15	214.1000	0.4270	0.0000	0.0000	18.2000	18.5000	44.6400	0.0000	4.7194	0.0000	0.0000	0.0000
16	195.9000	0.1513	0.0000	0.0000	0.0000	0.0000	0.0000	0.0000	4.8707	0.0000	0.0000	0.0000
JOINT	2.4250	0.1775	5.2250	0.0105	14.7500	4.6000	0.0000	9.4200	0.0006	33.3100	0.3161	-0.0088
CENTER 1	173.9000	0.0346	0.0000	0.0000	8.6000	3.5000	28.4000	5.3600	2.9570	0.0000	0.0000	0.0000
2	165.3000	0.0347	0.0000	0.0000	16.3000	1.6000	27.7000	5.3000	2.9917	0.0000	0.0000	0.0000
3	149.0000	0.0147	0.0000	0.0000	22.3000	1.5000	27.5500	5.2000	3.0064	0.0000	0.0000	0.0000
4	126.7000	0.0152	0.0000	0.0000	22.7000	1.5000	26.4000	4.9800	3.0216	0.0000	0.0000	0.0000
5	104.0000	0.0152	0.0000	0.0000	14.0000	1.5000	26.4000	4.9800	3.0368	0.0000	0.0000	0.0000
6	90.0000	0.1787	0.1750	0.0000	5.0000	1.8000	29.3000	5.5300	3.1968	0.0000	11.0000	0.0000
7	85.0000	0.1531	0.1491	0.0000	5.6000	1.8000	33.0000	6.2200	3.3441	0.0000	12.0000	0.0000
8	79.4000	0.2227	0.2169	0.0000	6.7000	1.8000	33.0000	6.2200	3.5574	0.0000	13.0000	0.0000
9	72.7000	0.2195	0.2138	0.0000	6.7000	1.8000	33.0000	6.2200	3.7707	0.0000	14.0000	0.0000
10	66.0000	0.2227	0.2169	0.0000	8.0000	1.8000	33.0000	6.2200	3.9840	0.0000	0.0000	0.0000
11	58.0000	0.3212	0.3045	0.0000	8.0000	2.6000	49.5000	9.3400	3.3052	0.0000	0.0000	0.0000
12	50.0000	0.1497	0.1148	1.3910	14.4000	4.0000	46.0000	8.6700	3.4549	0.0000	0.0000	0.0000
13	35.6000	0.2180	0.0000	0.0000	5.5000	4.7000	49.3000	9.3000	3.6729	0.0000	0.0000	0.0000
A BODY 1	173.9000	0.0000	0.0000	0.0000	7.9000	0.2160	8.8000	1.6660	0.0000	0.0000	0.0000	0.0000
2	166.0000	0.0138	0.0000	0.0000	19.0000	0.1600	5.9000	1.1130	0.0138	0.0000	0.0000	0.0000
3	147.0000	0.0025	0.0000	0.0000	19.2000	0.1185	5.0000	0.9430	0.0163	0.0000	0.0000	0.0000
4	127.8000	0.0067	0.0000	0.0000	22.7000	0.1185	5.0000	0.9430	0.0230	0.0000	0.0000	0.0000
5	105.1000	0.0034	0.0000	0.0000	15.1000	0.1292	5.2800	0.9970	0.0264	0.0000	0.0000	0.0000
6	90.0000	0.0727	0.0720	0.0000	9.4000	0.1400	5.7200	1.0800	0.0991	0.0000	21.0000	0.0000
7	80.6000	0.1993	0.1973	0.0000	13.6000	0.1400	5.7200	1.0800	0.2984	0.0000	22.0000	0.0000
8	67.0000	0.1993	0.1973	0.0000	11.0000	0.1400	5.9200	1.1200	0.4977	0.0000	0.0000	0.0000
9	56.0000	0.1208	0.1166	0.5895	11.0000	0.2160	13.7200	2.5900	0.6185	0.0000	0.0000	0.0000
10	45.0000	0.0121	0.0063	0.0000	7.1000	0.2160	29.1000	5.4900	0.6306	0.0000	0.0000	0.0000
B BODY 1	173.9000	0.0000	0.0000	0.0000	5.9500	0.4570	19.3000	3.6400	0.4871	0.0000	0.0000	0.0000
2	167.9500	0.0170	0.0000	0.0000	16.9500	0.2170	9.0500	1.7080	0.5041	0.0000	0.0000	0.0000
3	151.0000	0.0477	0.0000	0.0000	14.5000	0.2170	9.0500	1.7080	0.5518	0.0000	0.0000	0.0000
4	136.5000	0.0519	0.0000	0.0000	13.0000	0.2170	9.0500	1.7080	0.6037	0.0000	0.0000	0.0000
5	123.5000	0.0045	0.0000	0.0000	20.7000	0.2170	8.8600	1.6740	0.6082	0.0000	0.0000	0.0000
6	102.8000	0.0045	0.0000	0.0000	12.8000	0.2170	8.8600	1.6740	0.6127	0.0000	0.0000	0.0000
7	90.0000	0.0730	0.0720	0.0000	9.8000	0.2630	10.7000	2.0190	0.6857	0.0000	31.0000	0.0000
8	80.2000	0.2150	0.2106	0.0000	14.7000	0.2630	10.7000	2.0190	0.9007	0.0000	32.0000	0.0000
9	65.5000	0.2150	0.2106	0.0000	11.5000	0.2630	10.9500	2.0680	1.1157	0.0000	0.0000	0.0000
10	54.0000	0.1250	0.1108	0.6232	10.0000	0.4570	21.2000	4.0000	1.1329	0.0000	0.0000	0.0000
11	44.0000	0.0206	0.0192	0.0000	6.1000	0.4570	22.6000	4.2700	1.1579	0.0000	0.0000	0.0000
TAIL 1	-0.0000	0.0000	0.0000	0.0000	7.8000	4.7000	49.3000	9.3000	0.0000	0.0000	0.0000	0.0000

@ See Table IX for interpretation of column labels.

Table IV

1/5 Scale Saturn I , Breakdown for 100 % Full Condition

STATION DATA		LOC@	M	Mh	MSTAR	L	EI*10**9	AE*10**6	GHT*10**6	A	I	SLOSH	SPARE
NOSE	1	379.7000	0.0164	0.0000	0.0000	19.9000	0.4000	13.1000	0.0000	0.0164	0.0000	0.0000	0.0000
	2	359.4000	0.0317	0.0000	0.0000	15.6000	1.3000	21.5000	0.0000	0.0481	0.0000	0.0000	0.0000
	3	343.8000	0.5025	0.0000	0.0000	8.3000	1.8000	24.1000	0.0000	0.5506	0.0000	0.0000	0.0000
	4	335.5000	0.3425	0.0000	0.0000	9.3000	1.8000	24.1000	0.0000	0.8931	0.0000	0.0000	0.0000
	5	362.2000	0.3425	0.0000	0.0000	9.3000	1.8000	24.1000	0.0000	1.2356	0.0000	0.0000	0.0000
	6	316.9000	0.3425	0.0000	0.0000	9.3000	1.8000	24.1000	0.0000	1.5781	0.0000	0.0000	0.0000
	7	307.6000	0.3425	0.0000	0.0000	10.6000	1.8000	13.9000	0.0000	1.9206	0.0000	0.0000	0.0000
	8	297.0000	0.4800	0.0000	0.0000	11.5000	8.0000	8.8000	0.0000	2.4006	0.0000	0.0000	0.0000
	9	285.5000	0.0187	0.0000	0.0000	13.5000	18.5000	44.6400	0.0000	2.4193	0.0000	0.0000	0.0000
	10	272.0000	0.1651	0.0000	0.0000	9.1000	18.5000	44.6400	0.0000	2.5844	0.0000	0.0000	0.0000
	11	262.9000	0.4270	0.0000	0.0000	12.2000	18.5000	44.6400	0.0000	3.0114	0.0000	0.0000	0.0000
	12	250.7000	0.4270	0.0000	0.0000	12.2000	18.5000	44.6400	0.0000	3.4384	0.0000	0.0000	0.0000
	13	238.5000	0.4270	0.0000	0.0000	12.2000	18.5000	44.6400	0.0000	3.8654	0.0000	0.0000	0.0000
	14	226.3000	0.4270	0.0000	0.0000	12.2000	18.5000	44.6400	0.0000	4.2924	0.0000	0.0000	0.0000
	15	214.1000	0.4270	0.0000	0.0000	18.2000	18.5000	44.6400	0.0000	4.7194	0.0000	0.0000	0.0000
	16	195.9000	0.1513	0.0000	0.0000	0.0000	0.0000	0.0000	0.0000	4.8707	0.0000	0.0000	0.0000
JOINT		2.4250	0.1775	5.2250	0.0105	14.7500	4.6000	0.0000	9.4200	0.0006	33.3100	-0.3161	-0.0088
CENTER	1	173.9000	0.0346	0.0000	0.0000	8.6000	3.5000	28.4000	5.3600	2.9570	0.0000	0.0000	0.0000
	2	165.3000	0.0347	0.0000	0.0000	16.3000	1.6000	27.7000	5.3000	2.9917	0.0000	0.0000	0.0000
	3	149.0000	0.0147	0.0000	0.0000	13.8000	1.5000	27.5500	5.2000	3.0064	0.0000	0.0000	0.0000
	4	135.2000	0.1876	0.1838	0.0000	5.7000	1.5000	27.5500	5.2000	3.1876	0.0000	11.0000	0.0000
	5	129.5000	0.1876	0.1838	0.0000	5.6000	1.5000	26.4000	4.9800	3.3688	0.0000	12.0000	0.0000
	6	123.9000	0.1876	0.1838	0.0000	5.7000	1.5000	26.4000	4.9800	3.5500	0.0000	13.0000	0.0000
	7	118.2000	0.1876	0.1838	0.0000	5.7000	1.5000	26.4000	4.9800	3.7312	0.0000	14.0000	0.0000
	8	112.5000	0.1876	0.1838	0.0000	5.6000	1.5000	26.4000	4.9800	3.9124	0.0000	0.0000	0.0000
	9	106.9000	0.1876	0.1838	0.0000	5.7000	1.5000	26.4000	4.9800	4.0936	0.0000	0.0000	0.0000
	10	101.2000	0.1876	0.1838	0.0000	5.7000	1.5000	26.4000	4.9800	4.2748	0.0000	0.0000	0.0000
	11	95.5000	0.1876	0.1838	0.0000	5.5000	1.5000	26.4000	4.9800	4.4560	0.0000	0.0000	0.0000
	12	90.0000	0.1787	0.1750	0.0000	5.0000	1.8000	29.3000	5.5300	4.6160	0.0000	0.0000	0.0000
	13	85.0000	0.1531	0.1491	0.0000	5.6000	1.8000	33.0000	6.2200	4.7633	0.0000	0.0000	0.0000
	14	79.4000	0.2227	0.2169	0.0000	6.7000	1.8000	33.0000	6.2200	4.9766	0.0000	0.0000	0.0000
	15	72.7000	0.2195	0.2138	0.0000	6.7000	1.8000	33.0000	6.2200	5.1899	0.0000	0.0000	0.0000
	16	66.0000	0.2227	0.2169	0.0000	8.0000	1.8000	33.0000	6.2200	5.4032	0.0000	0.0000	0.0000
	17	58.0000	0.3212	0.3045	0.0000	8.0000	2.6000	49.5000	9.3400	5.7244	0.0000	0.0000	0.0000
	18	50.0000	0.1497	0.1148	2.8610	14.4500	4.0000	46.0000	8.6700	5.8741	0.0000	0.0000	0.0000
	19	35.5500	0.2180	0.0000	0.0000	5.4500	4.7000	49.3000	9.3000	6.0921	0.0000	0.0000	0.0000
A BODY	1	173.9000	0.0000	0.0000	0.0000	7.9000	0.2160	8.8000	1.6660	0.0000	0.0000	0.0000	0.0000
	2	166.0000	0.0138	0.0000	0.0000	12.9000	0.1600	5.9000	1.1130	0.0138	0.0000	0.0000	0.0000
	3	153.1000	0.0013	0.0000	0.0000	10.1000	0.1185	5.0000	0.9430	0.0151	0.0000	0.0000	0.0000
	4	143.0000	0.0012	0.0000	0.0000	9.5500	0.1185	5.0000	0.9430	0.0163	0.0000	0.0000	0.0000
	5	133.4500	0.1322	0.1311	0.0000	9.1000	0.1185	5.0000	0.9430	0.1485	0.0000	21.0000	0.0000
	6	124.3500	0.1322	0.1311	0.0000	9.1000	0.1185	5.0000	0.9430	0.2807	0.0000	22.0000	0.0000
	7	115.2500	0.1322	0.1311	0.0000	9.1000	0.1185	5.0000	0.9430	0.4129	0.0000	0.0000	0.0000
	8	106.1500	0.1322	0.1311	0.0000	9.1000	0.1292	5.2800	0.9970	0.5451	0.0000	0.0000	0.0000
	9	97.0500	0.1322	0.1311	0.0000	7.0500	0.1292	5.2800	0.9970	0.6773	0.0000	0.0000	0.0000
	10	90.0000	0.0727	0.0720	0.0000	9.4000	0.1400	5.7200	1.0800	0.7500	0.0000	0.0000	0.0000
	11	80.6000	0.1993	0.1973	0.0000	13.6000	0.1400	5.7200	1.0800	0.9493	0.0000	0.0000	0.0000
	12	67.0000	0.1993	0.1973	0.0000	11.0000	0.1400	5.9200	1.1200	1.1486	0.0000	0.0000	0.0000
	13	56.0000	0.1208	0.1166	1.2450	11.0000	0.2160	13.7200	2.5900	1.2694	0.0000	0.0000	0.0000
	14	45.0000	0.0121	0.0063	0.0000	7.1000	0.2160	29.1000	5.4900	1.2815	0.0000	0.0000	0.0000
B BODY	1	173.9000	0.0000	0.0000	0.0000	5.9000	0.4570	19.3000	3.6400	0.4871	0.0000	0.0000	0.0000
	2	168.0000	0.0170	0.0000	0.0000	9.9000	0.2170	9.0500	1.7080	0.5041	0.0000	0.0000	0.0000
	3	158.1000	0.0017	0.0000	0.0000	8.0500	0.2170	9.0500	1.7080	0.5058	0.0000	0.0000	0.0000
	4	150.0500	0.0018	0.0000	0.0000	8.0500	0.2170	9.0500	1.7080	0.5076	0.0000	0.0000	0.0000
	5	142.0000	0.0017	0.0000	0.0000	8.5500	0.2170	9.0500	1.7080	0.5093	0.0000	0.0000	0.0000
	6	133.4500	0.1330	0.1311	0.0000	9.1000	0.2170	9.0500	1.7080	0.6423	0.0000	31.0000	0.0000
	7	124.3500	0.1330	0.1311	0.0000	9.1000	0.2170	8.8600	1.6740	0.7753	0.0000	32.0000	0.0000
	8	115.2500	0.1330	0.1311	0.0000	9.1000	0.2170	8.8600	1.6740	0.9083	0.0000	0.0000	0.0000
	9	106.1500	0.1330	0.1311	0.0000	9.1000	0.2170	8.8600	1.6740	1.0413	0.0000	0.0000	0.0000
	10	97.0500	0.1330	0.1311	0.0000	7.0500	0.2170	8.8600	1.6740	1.1743	0.0000	0.0000	0.0000
	11	90.0000	0.0730	0.0720	0.0000	9.8000	0.2630	10.7000	2.0190	1.2473	0.0000	0.0000	0.0000
	12	80.2000	0.2150	0.2116	0.0000	14.7000	0.2630	10.7000	2.0190	1.4623	0.0000	0.0000	0.0000
	13	65.5000	0.2150	0.2106	0.0000	11.5000	0.2630	10.9500	2.0680	1.6773	0.0000	0.0000	0.0000
	14	54.0000	0.1250	0.1108	1.2797	10.0000	0.4570	21.2000	4.0000	1.8023	0.0000	0.0000	0.0000
	15	44.0000	0.0206	0.0192	0.0000	6.1000	0.4570	22.6000	4.2700	1.8195	0.0000	-0.0000	-0.0000
TAIL	1	-0.0000	0.0000	0.0000	0.0000	7.8000	4.7000	49.3000	9.3000	0.0000	0.0000	0.0000	0.0000

@ See Table IX for interpretation of column labels.

Table V: Summary of Bending of Saturn I
Calculated & Test Natural Frequencies (cps)
48% Full Condition, Principal Axis No. 1

Modal Number	1	2	3	4	5	6	7	8
Calculated ω_n (Free-Free) No slosh No axial Load	13.0	13.65	18.2	16.5	31.9	38.65	44.3	54.4
% Error (Nearest Exper.)	0	- 7.1	+12.5	+ 0.8	- 5.9	+ 0.4	+ 2.1	- 9.3
Calculated ω_n (Free-Free) With slosh lg axial Load	13.3	15.2	19.2	29.7	33.2	39.3	-	-
% Error (Nearest Exper.)	+ 2.2	- 1.9	- 7.7	+12.9	- 2.1	+ 1.0	-	-
Ref. 2 (2-cable suspension)	13.0	-	-	26.0	33.9	38.9	47.8	60.0
Ref. 14 (8-cable spring suspension)	13.6	14.7	20.8	25.5	34.7	-	-	-
Ref. 14 (8-cable link suspension)	14.1	15.5	20.8	26.3	35.0	38.5	43.4	-

Table VI: Summary of Bending of Saturn I
Calculated & Test Natural Frequencies (cps)
100% Full Condition, Principal Axis No. 1

Modal Number	1	2	3	4	5	6	7	8
Calculated ω_n (Free-Free) No slosh No axial load	8.6	10.7	11.5	15.0	21.83	28.9	34.9	37.7
% Error (Nearest Exper.)	- 5.4	0	- 0.9	-	+15.5	- 5.5	-	- 8.3
Calculated ω_n (Free-Free) With slosh lg axial Load	8.8	10.9	11.7	15.3	22.2	29.4	-	-
% Error (Nearest Exper.)	- 3.3	- 1.8	+ 0.9	-	+17.35	- 3.9	-	-
Ref. 2 (2-cable suspension)	9.1	10.5	-	-	18.4	30.6	-	-
Ref. 14 (8-cable spring suspension)	9.1	10.7	-	-	18.7	30.8	-	41.1
Ref. 14 (8-cable link suspension)	9.1	11.1	11.6	-	18.9	30.8	-	41.5

Table VII Saturn I - Summary of Internally Balanced Mode Frequencies (cps), 48% Full Condition			
Modal Number	No Sloshing No Axial Load	With Sloshing, 1g Axial Load	Kind of Motion
1	12.7	14.3	First Radial, Fuel Tank
2	17.3	18.0	First Tangential, Fuel Tank
3	25.2	29.3	First Radial, LOX* Tank
4	35.4	37.6	First Tangential, LOX* Tank
5	36.9	36.9	First Rocket Engine

*Clustered Body

Table VIII Saturn I - Summary of Internally Balanced Mode Frequencies (cps), 100% Full Condition		
Modal Number	No Sloshing, No Axial Load	Kind of Motion
1	8.7	First Radial,Fuel Tank
2	10.9	First Tangential,Fuel Tank
3	13.4	First Radial,LOX* Tank
4	19.4	First Tangential,LOX* Tank
5	34.1	Second Radial,Fuel Tank
6	37.0	First Rocket Engine Bending

*Clustered Body

Table IX
Interpretation of Column Labels Used in Tables III and IV

Label	Meaning for quantities on nose, center-body, cluster-body and tail	Meaning for quantities in JOINT matrix (See Appendix C)
LOC	= location in inches of the mass station measured forward from the end of the rocket engine	ℓ_s
M	m = mass of the tank plus the mass of the liquid assumed concentrated at a given station	M_s
MW	= mass of the liquid concentrated at a given station	ℓ_t
MSTAR	m^* = total liquid mass in a given clustered tank	$1/k_{F\phi}$
L	ℓ = length between successive mass points	ℓ_p
EI*10**9	EI = EI$\cdot 10^{-9}$ bending rigidity assumed constant between successive mass points	EI$\cdot 10^{-9}$
AE*10**6	AE = AE$\cdot 10^{-6}$ extensile-compressive rigidity constant between successive mass points	–
GHT*10**6	Ght = G$\cdot 10^{-6}$. effective web height and thickness	Ght$\cdot 10^{-6}$
A	A = Axial load in g's (i.e. to obtain force, multiply by 386.4 "/sec)	$1/k_{M\phi}$
I	I = mass moment of inertia in bending about an axis thru the center-body center line	I_s
SLOSH	= an indicator to tell program at what station to include slosh effects	$\left(\frac{\ell_T}{k_{F\phi}} - \frac{1}{k_{Fy}}\right)$
SPARE	Not used	$\left(\frac{\ell_T}{k_{M\phi}} - \frac{1}{k_{F\phi}}\right)$

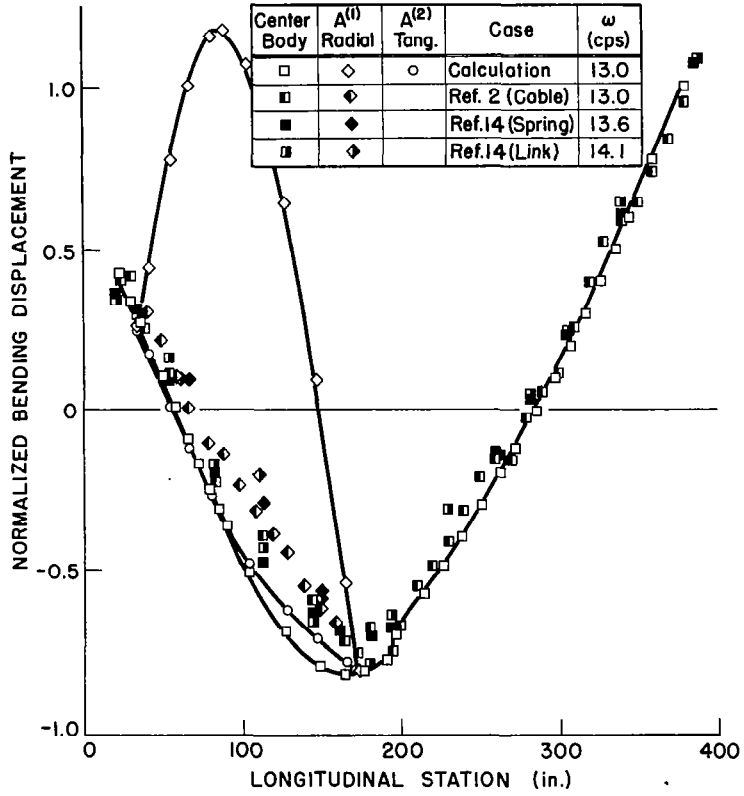

Figure 14a. 1st Natural Mode Shape - Saturn I, 48% full, motion of A bodies

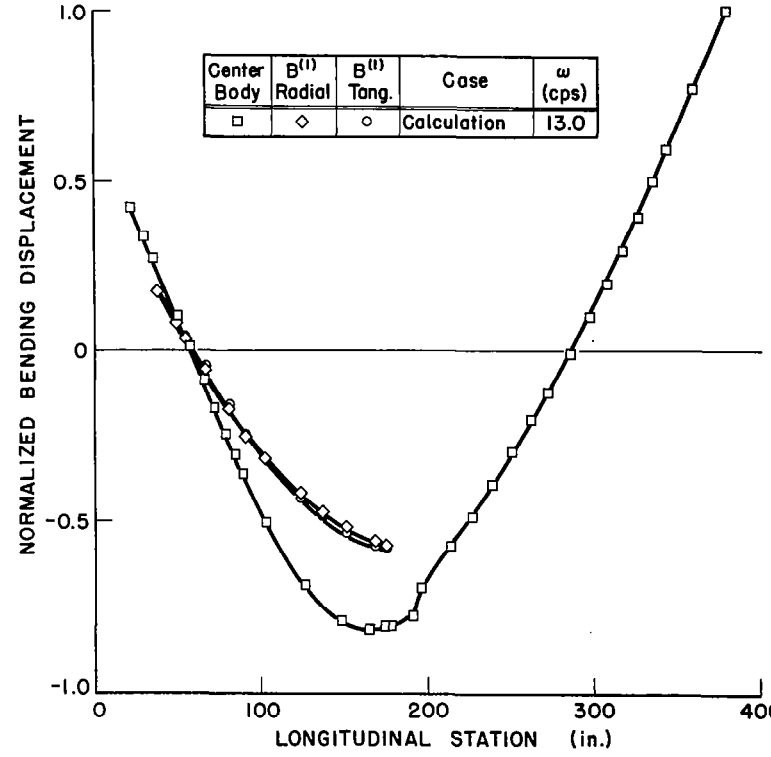

Figure 14b. 1st Natural Mode Shape - Saturn I, 48% full, motion of B bodies

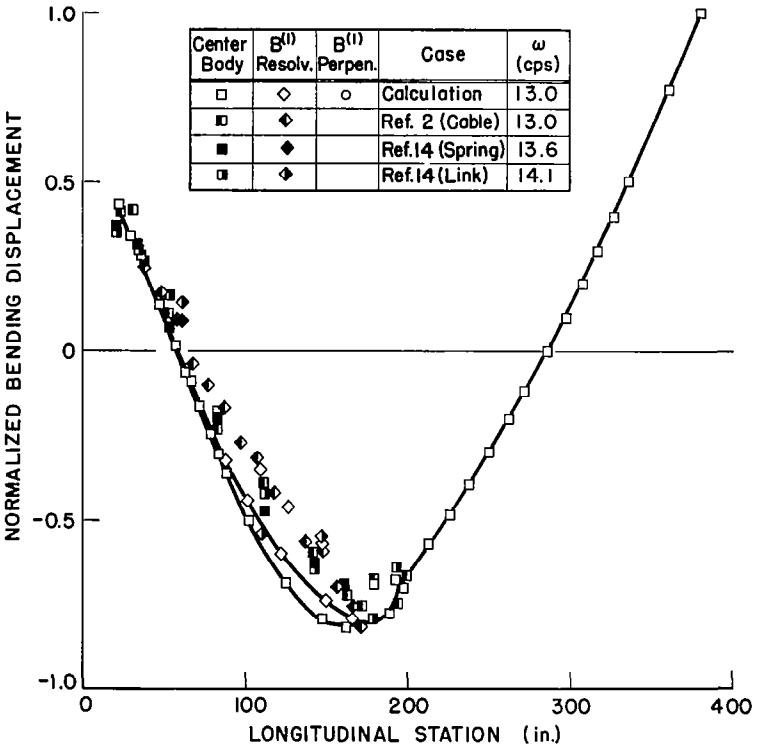

Figure 14c. 1st Natural Mode Shape – Saturn I, 48% full, motion of B bodies, resolved parallel and perpendicular to the vehicle bending plane

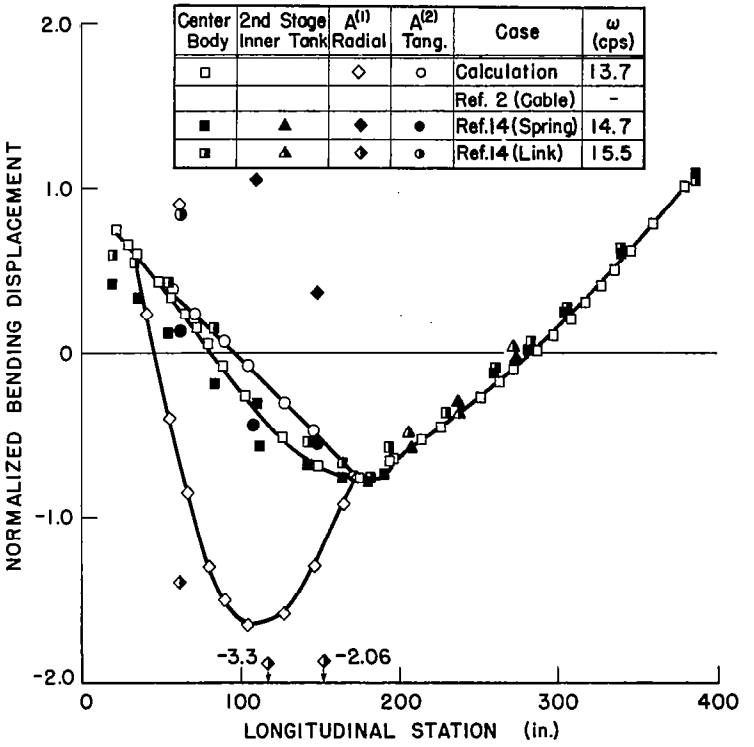

Figure 15a. 2nd Natural Mode Shape – Saturn I, 48% full, motion of A bodies

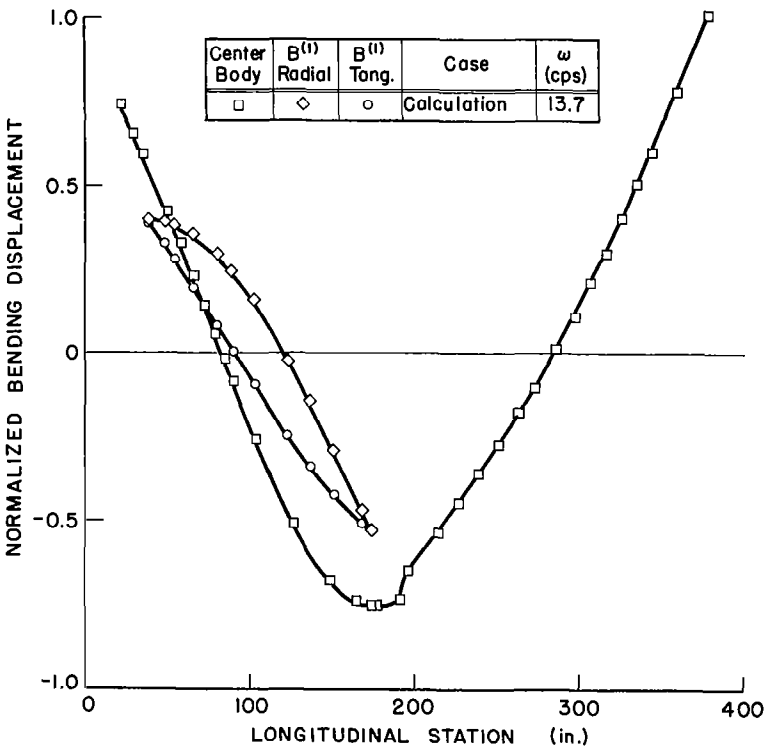

Figure 15b. 2nd Natural Mode Shape - Saturn I, 48% full, motion of B bodies

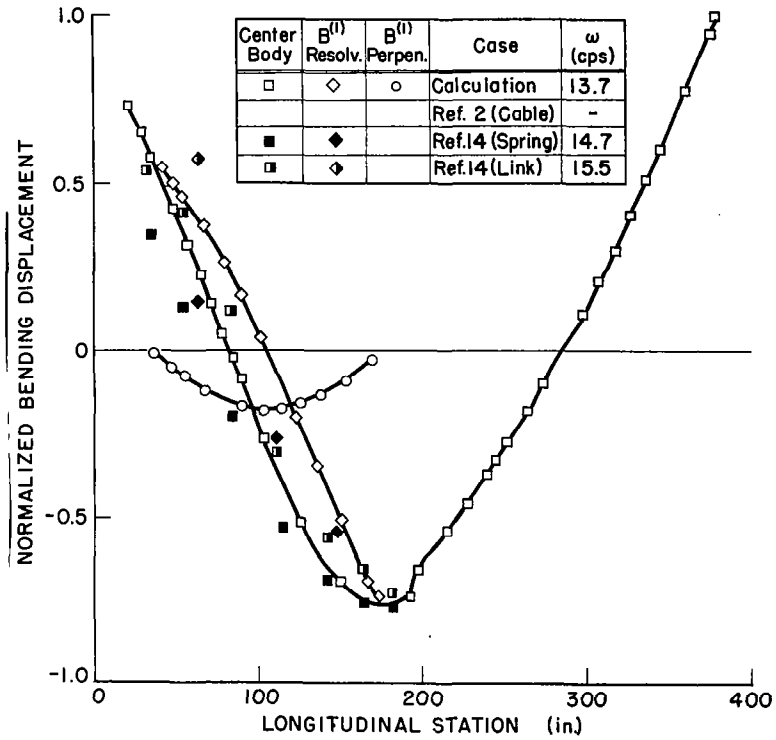

Figure 15c. 2nd Natural Mode Shape - Saturn I, 48% full, motion of B bodies, resolved parallel and perpendicular to the vehicle bending plane

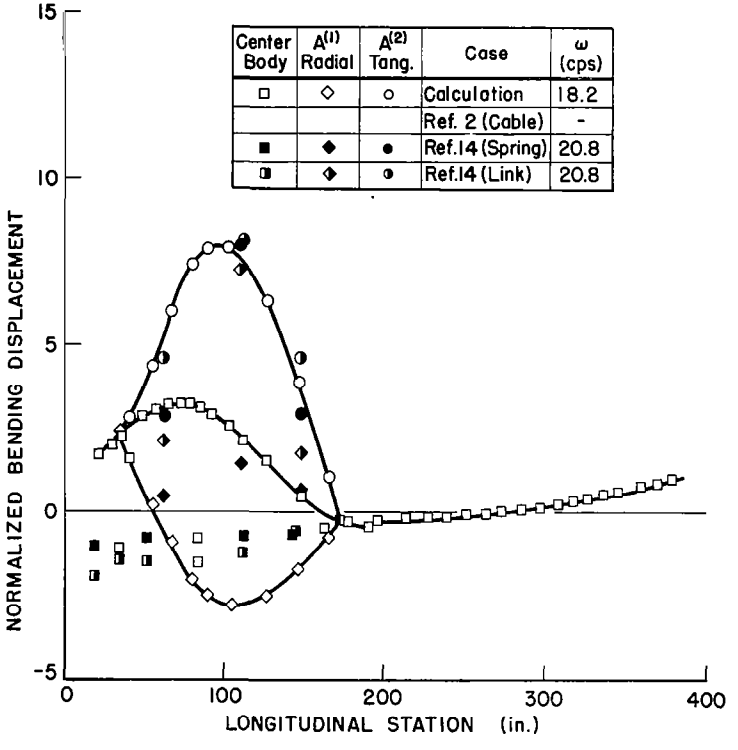

Figure 16a. 3rd Natural Mode Shape - Saturn I, 48% full, motion of A bodies

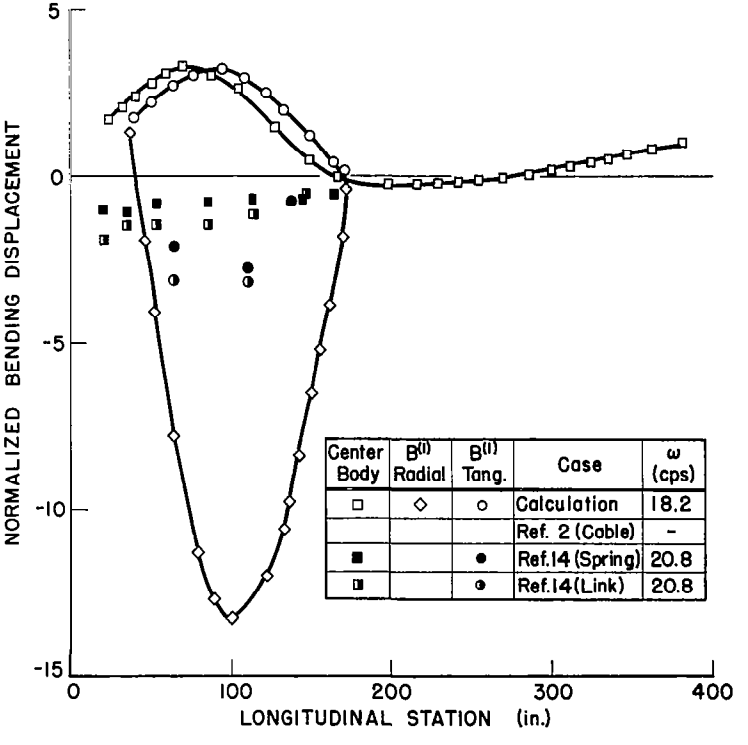

Figure 16b. 3rd Natural Mode Shape - Saturn I, 48% full, motion of B bodies

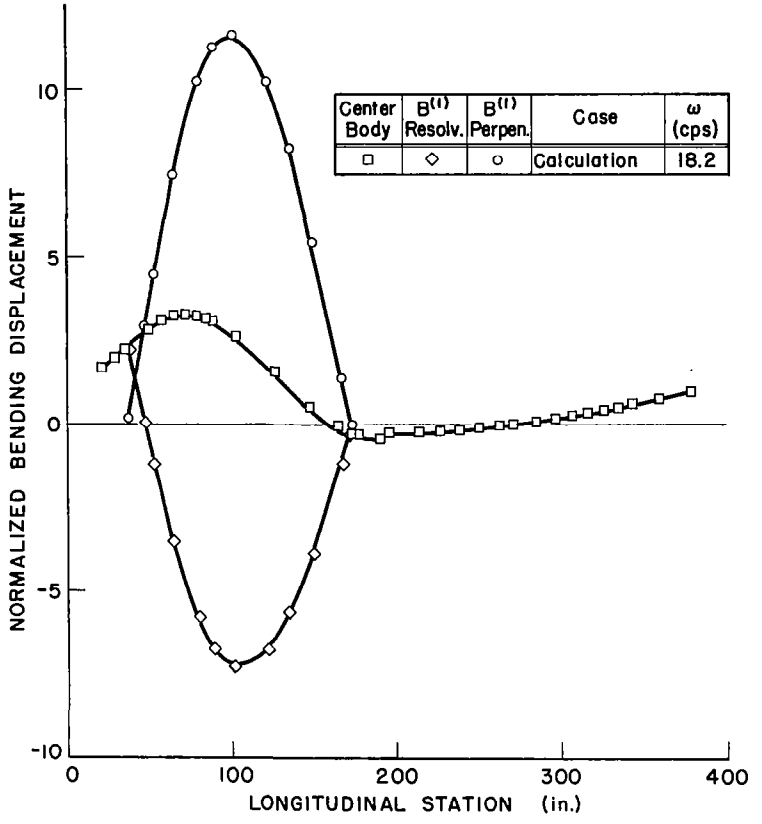

Figure 16c. 3rd Natural Mode Shape - Saturn I, 48% full, motion of B bodies, resolved parallel and perpendicular to the vehicle bending plane

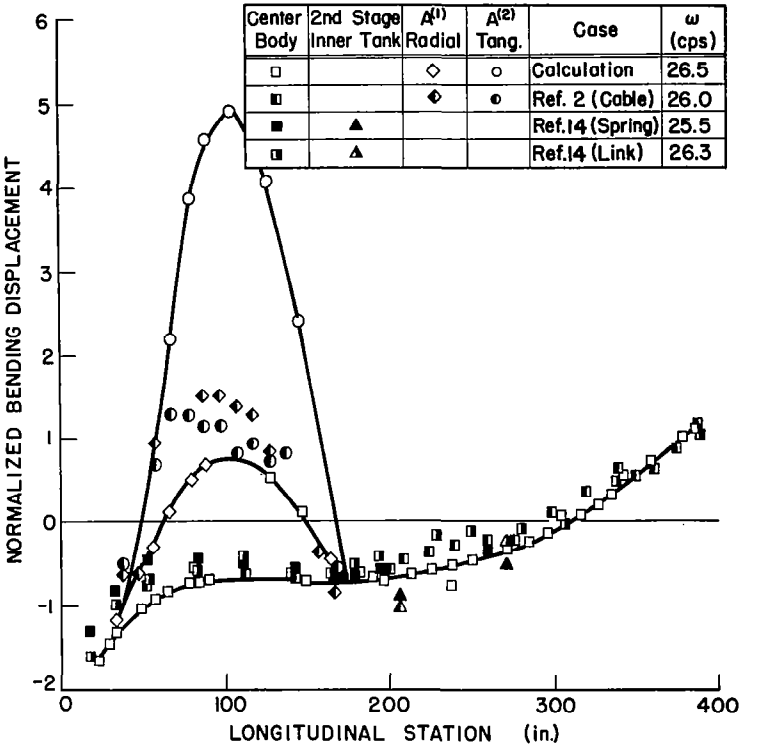

Figure 17a. 4th Natural Mode Shape - Saturn I, 48% full, motion of A bodies

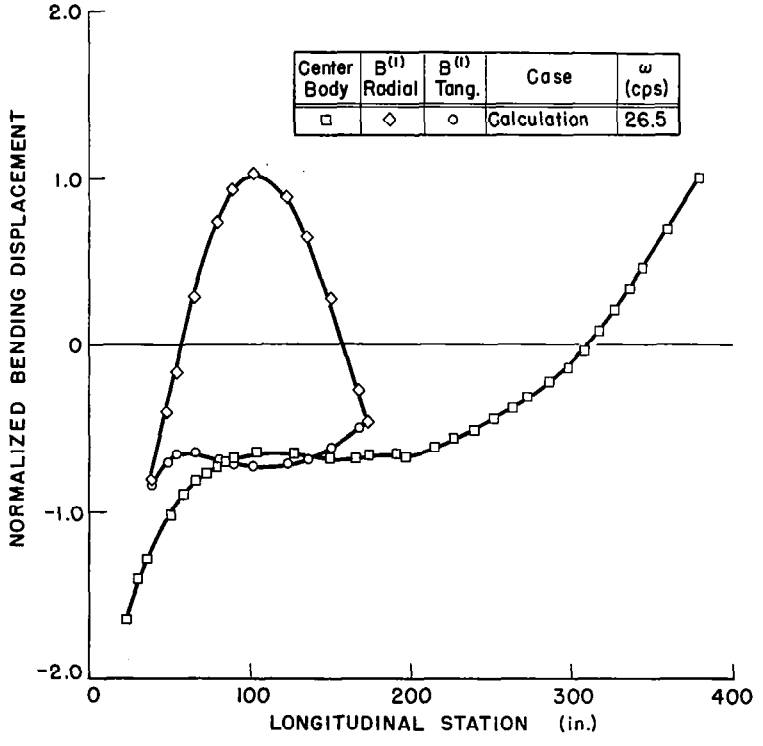

Figure 17b. 4th Natural Mode Shape - Saturn I, 48% full, motion of B bodies

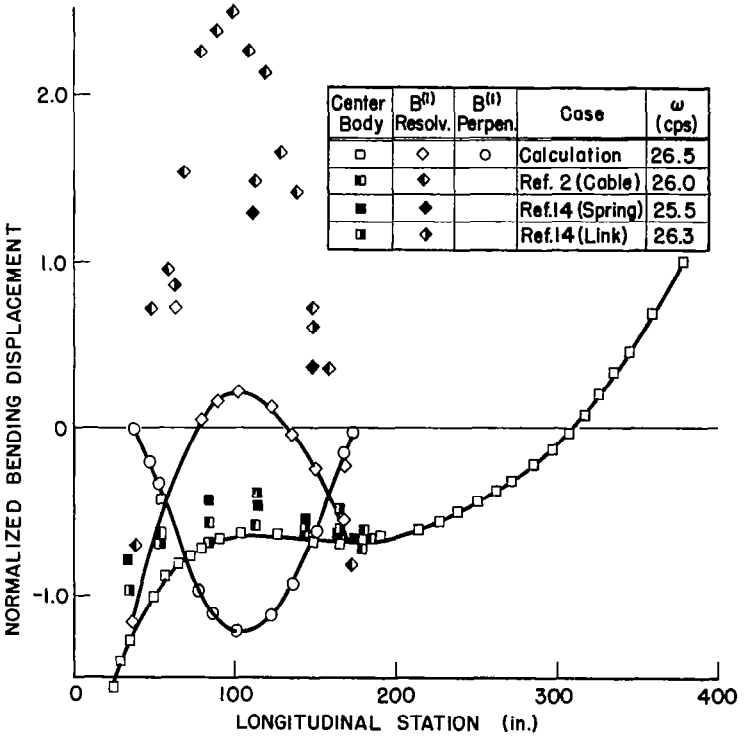

Figure 17c. 4th Natural Mode Shape - Saturn I, 48% full, motion of B bodies, resolved parallel and perpendicular to the vehicle bending plane

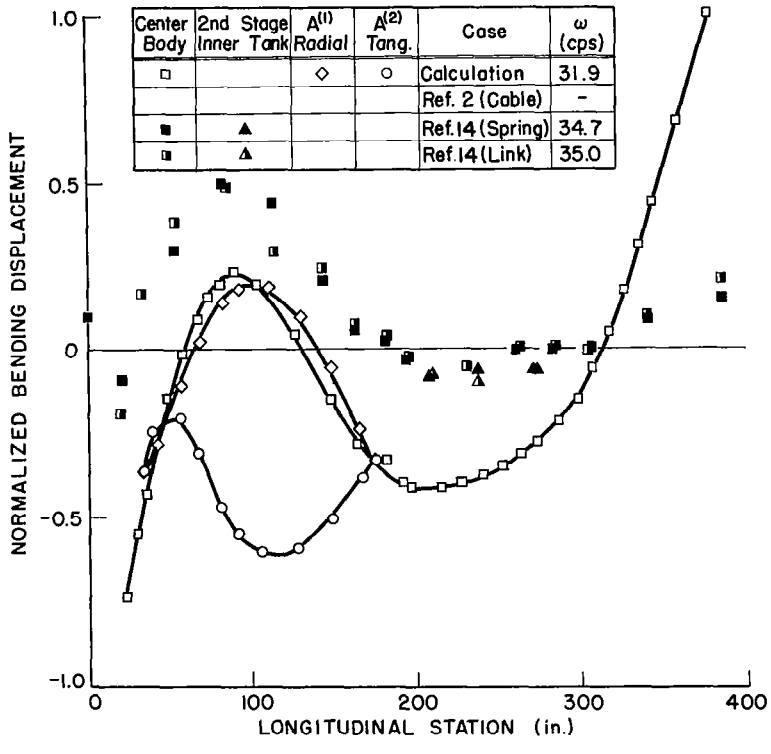

Figure 18a. 5th Natural Mode Shape - Saturn I, 48% full, motion of A bodies

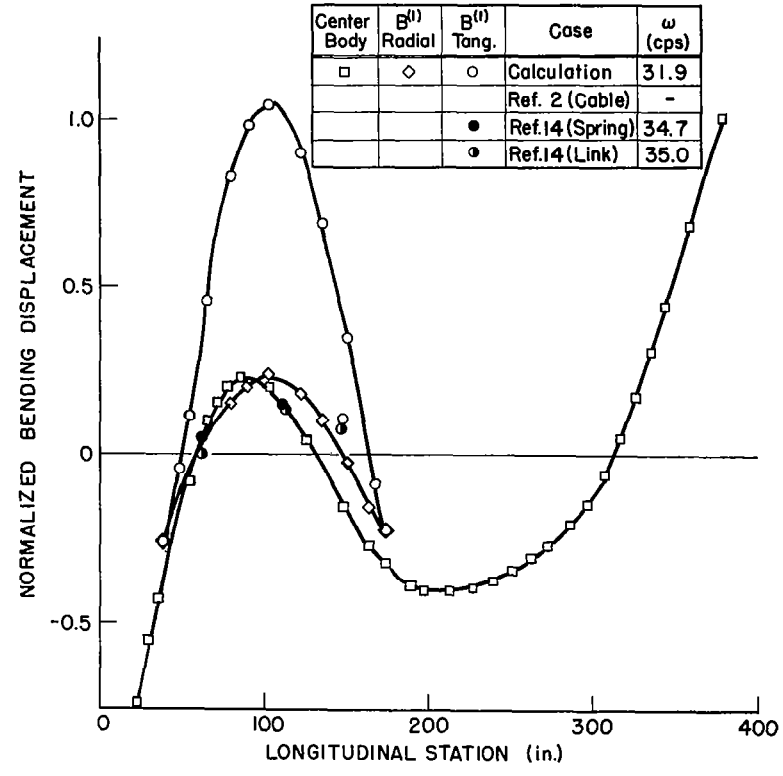

Figure 18b. 5th Natural Mode Shape - Saturn I, 48% full, motion of B bodies

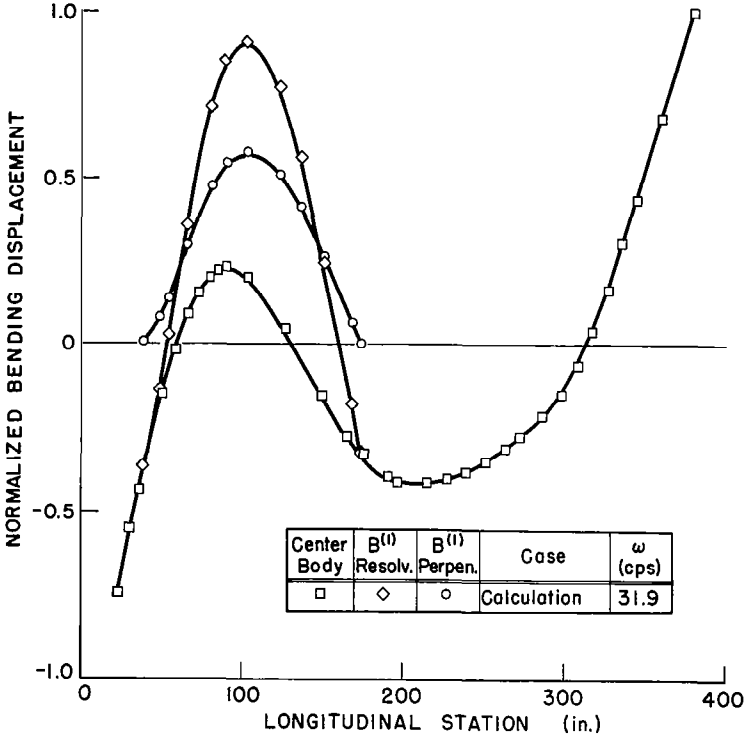

Figure 18c. 5th Natural Mode Shape - Saturn I, 48% full, motion of B bodies, resolved parallel and perpendicular to the vehicle bending plane

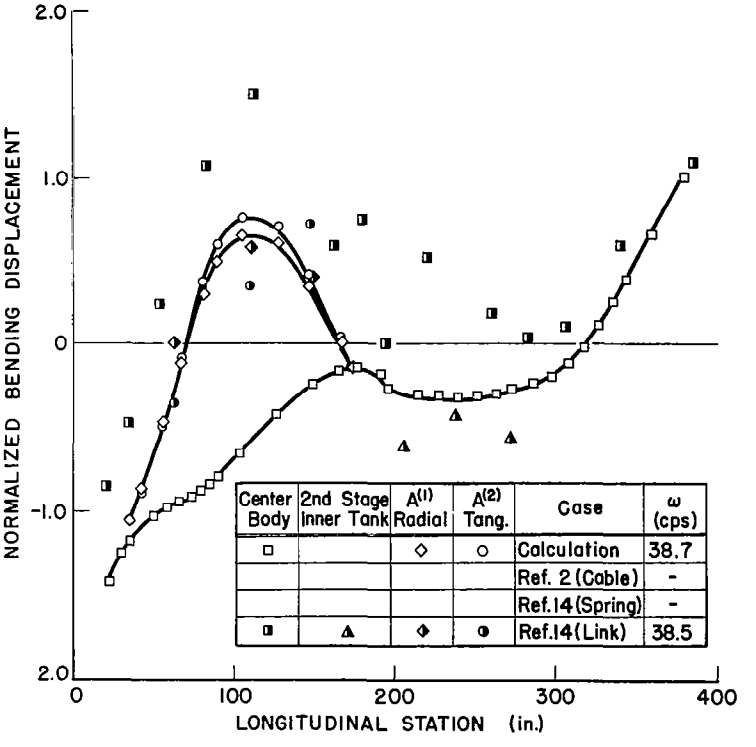

Figure 19a. 6th Natural Mode Shape - Saturn I, 48% full, motion of A bodies

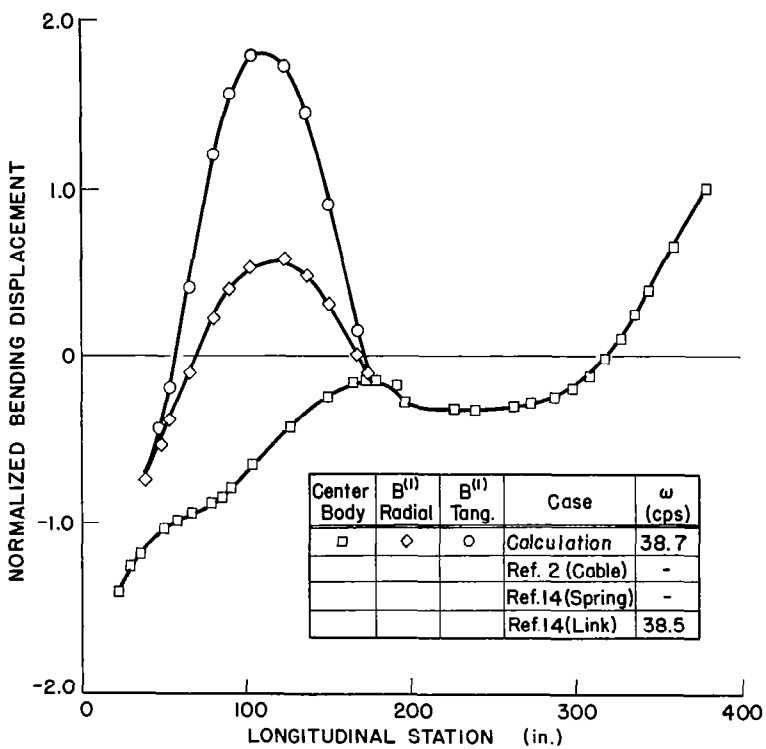

Figure 19b. 6th Natural Mode Shape - Saturn I, 48% full, motion of B bodies

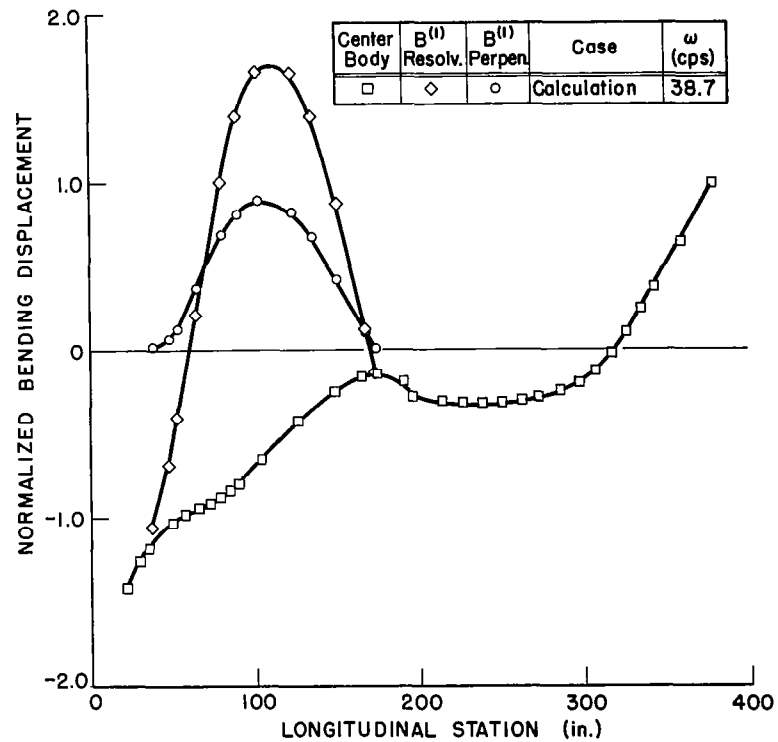

Figure 19c. 6th Natural Mode Shape - Saturn I, 48% full, motion of B bodies, resolved parallel and perpendicular to the vehicle bending plane

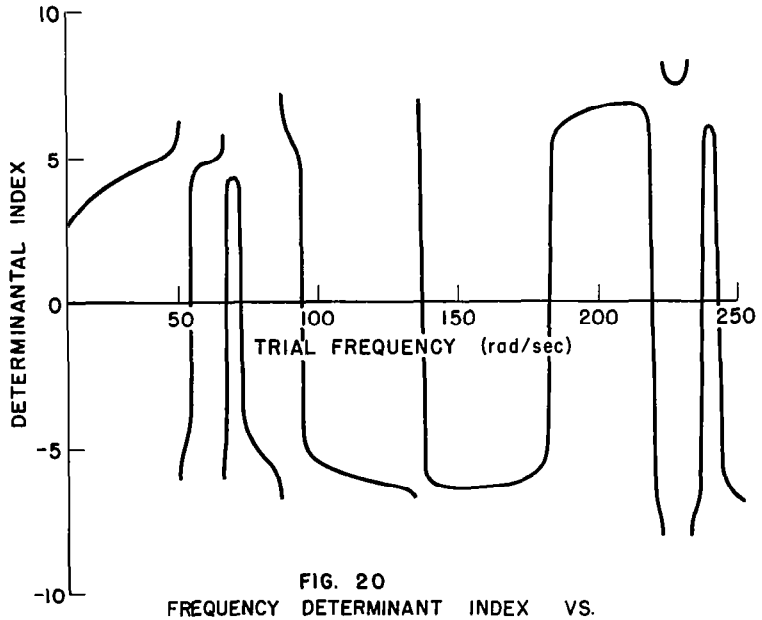

FIG. 20
FREQUENCY DETERMINANT INDEX VS.
TRIAL FREQUENCY - SATURN I, 100% FULL CONDITION

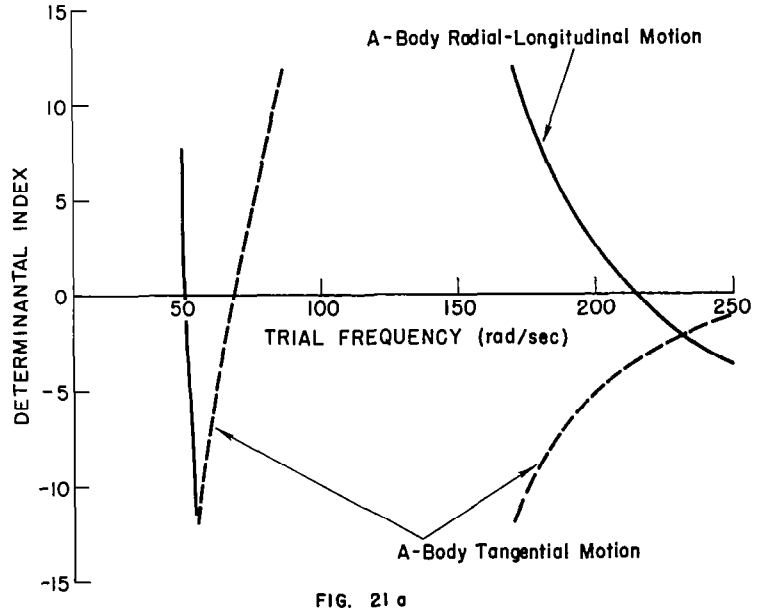

FIG. 21 a
INTERNALLY BALANCED MODES:
FREQUENCY DETERMINANT INDEX VS. TRIAL FREQUENCY
SATURN I, 100% FULL, A BODY MOTION

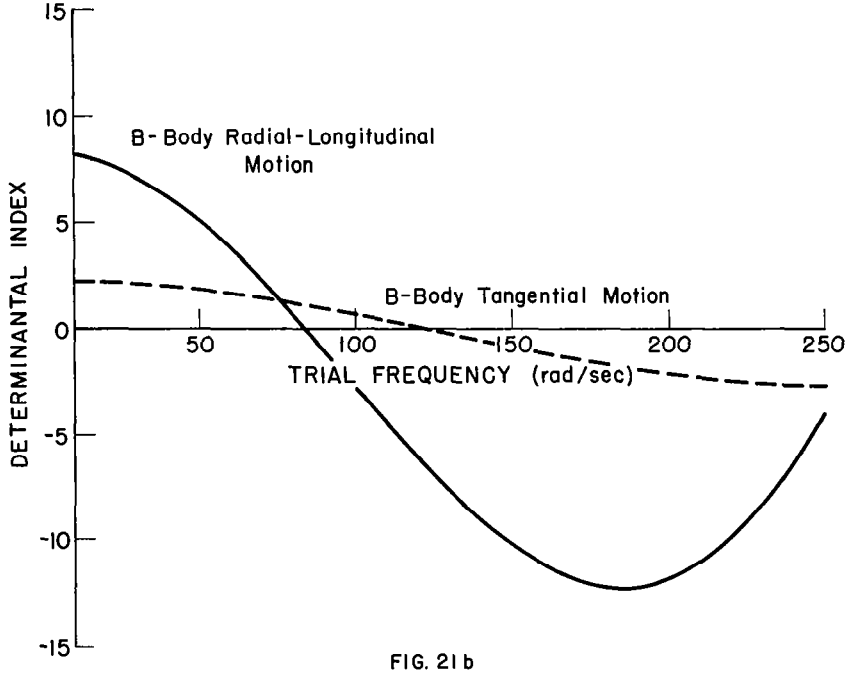

FIG. 21 b
INTERNALLY BALANCED MODES:
FREQUENCY DETERMINANT INDEX VS. TRIAL FREQUENCY
SATURN I, 100% FULL, B BODY MOTION

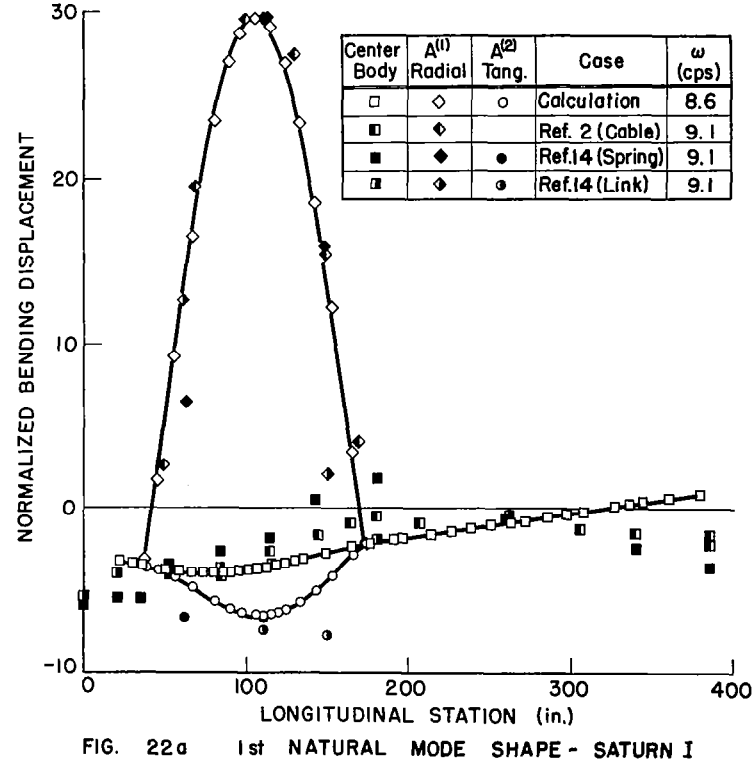

FIG. 22a 1st NATURAL MODE SHAPE - SATURN I
100% FULL, MOTION OF A BODIES

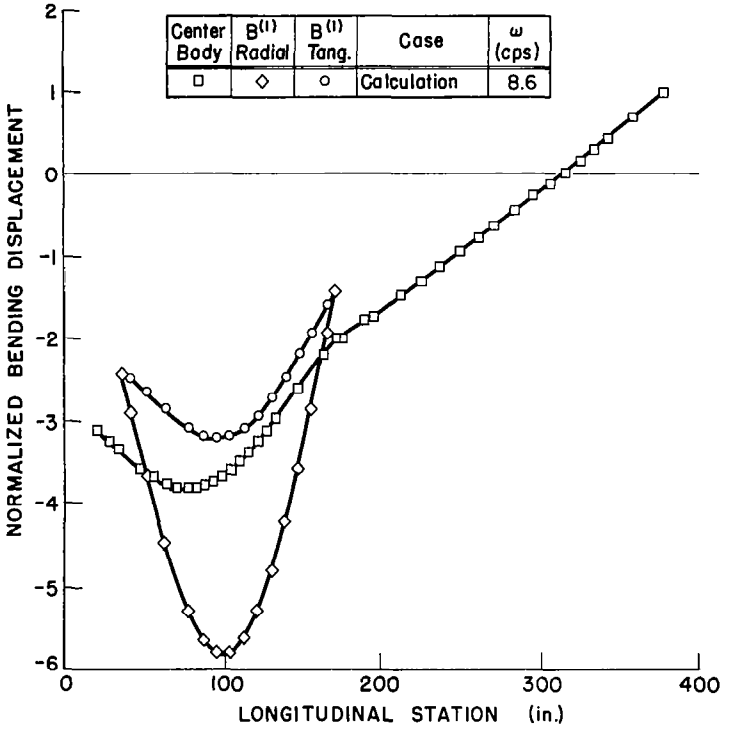

FIG. 22b 1st NATURAL MODE SHAPE - SATURN I 100% FULL, MOTION OF B BODIES

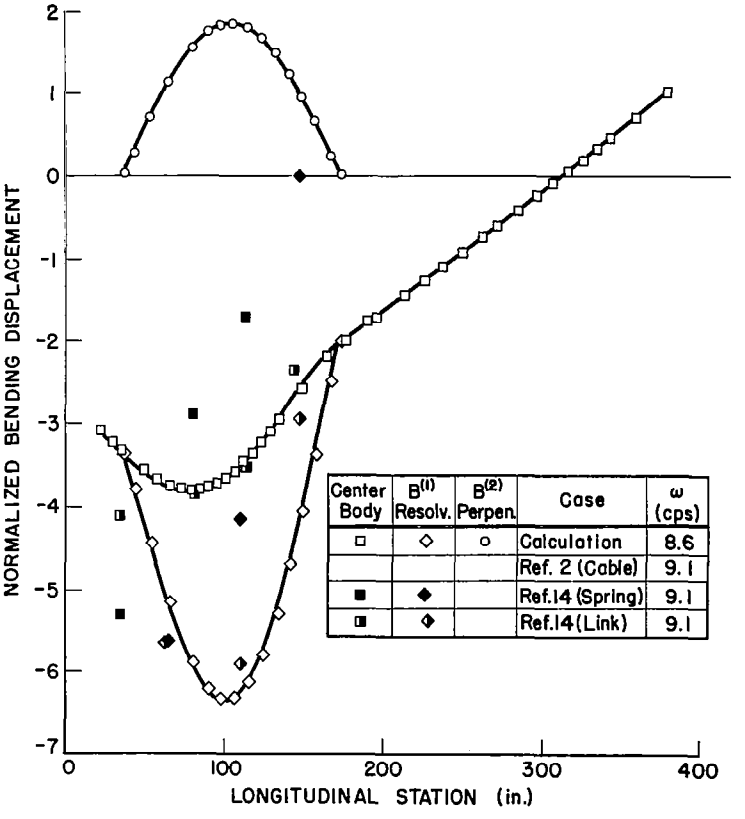

Figure 22c. 1st Natural Mode Shape - Saturn I, 100% full, motion of B bodies, resolved parallel and perpendicular to the vehicle bending plane

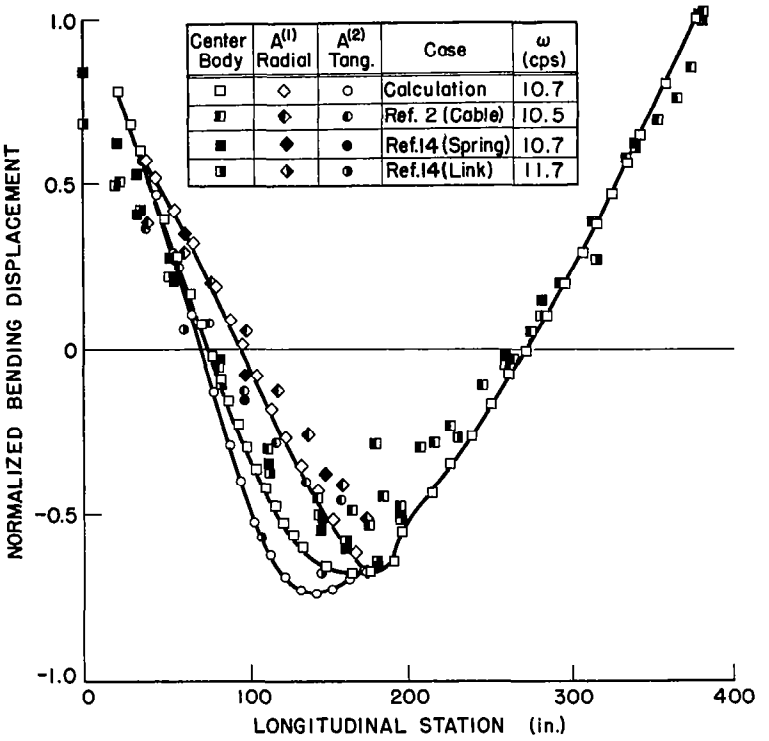

Figure 23a. 2nd Natural Mode Shape - Saturn I, 100% full motion of A bodies

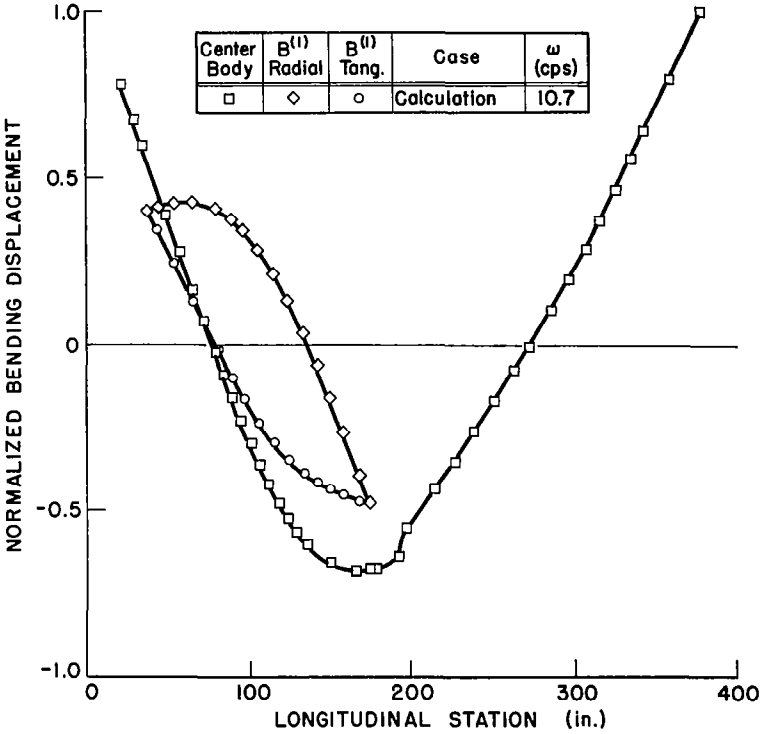

Figure 23b. 2nd Natural Mode Shape - Saturn I, 100% full motion of B bodies

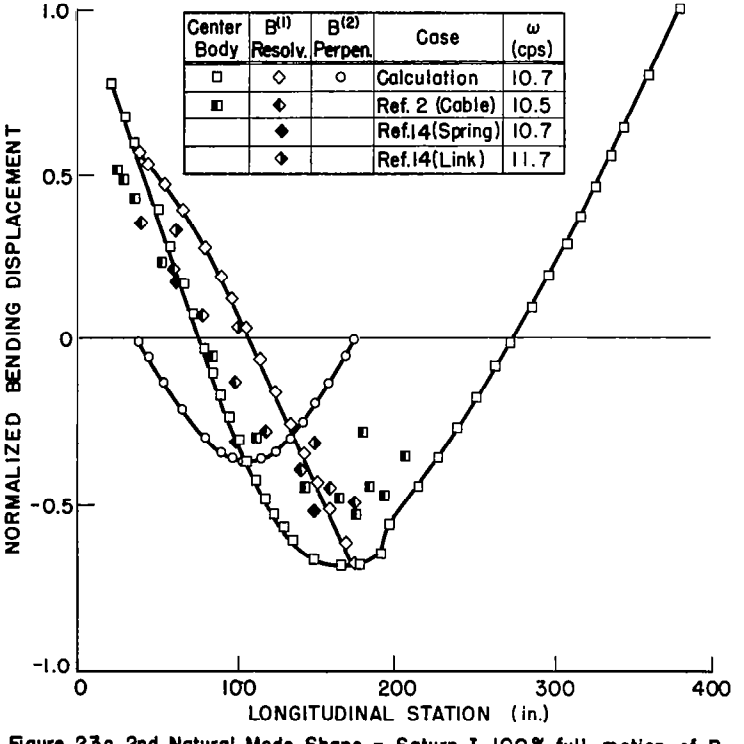

Figure 23c. 2nd Natural Mode Shape - Saturn I, 100% full, motion of B bodies, resolved parallel and perpendicular to the vehicle bending plane

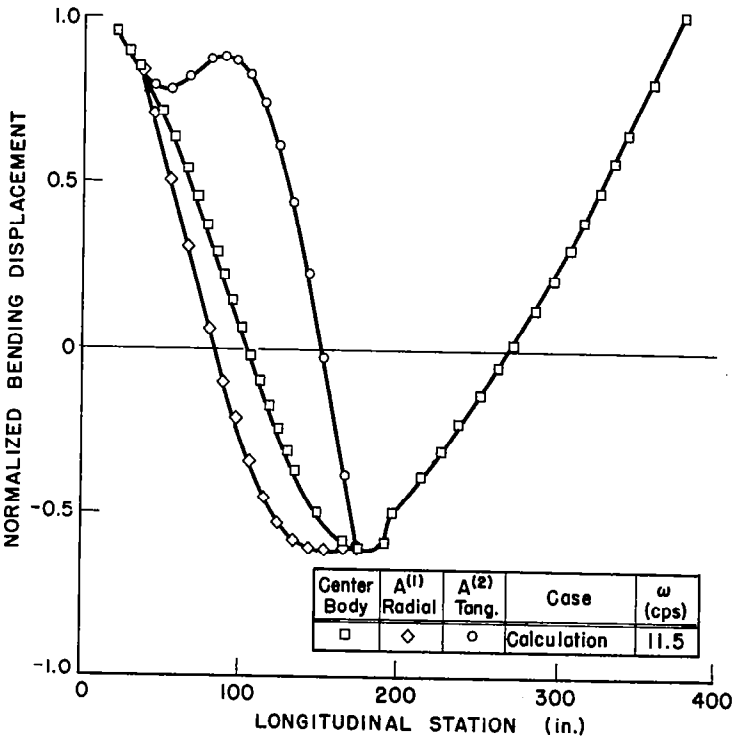

Figure 24a. 3rd Natural Mode Shape - Saturn I, 100% full motion of A bodies

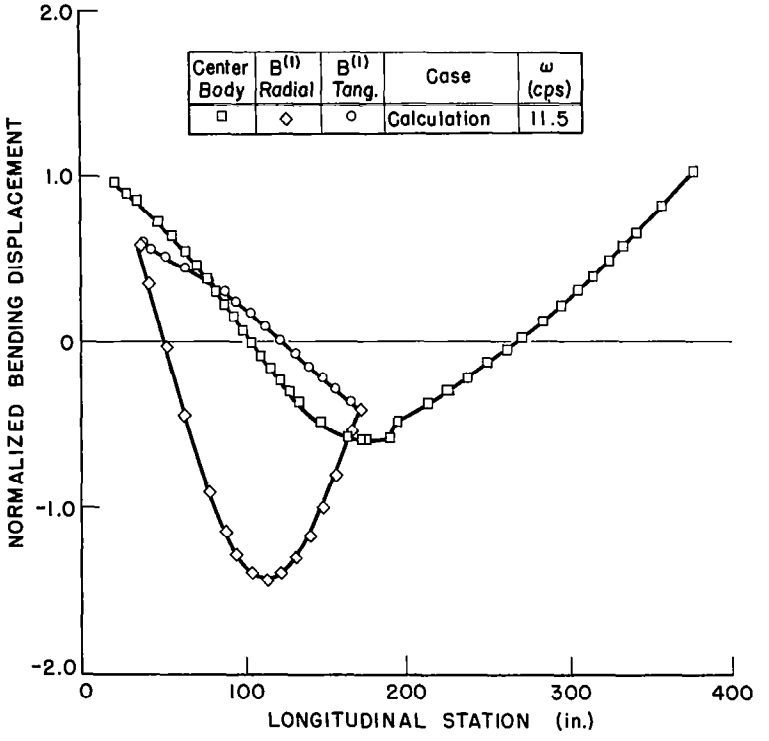

Figure 24b. 3rd Natural Mode Shape - Saturn I, 100% full motion of B bodies

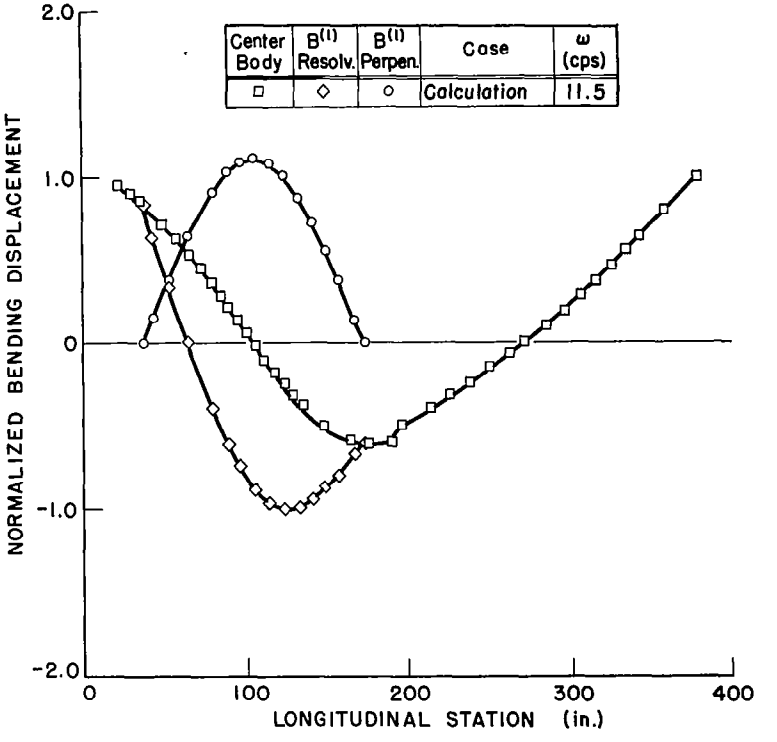

Figure 24c. 3rd Natural Mode Shape - Saturn I, 100% full, motion of B bodies, resolved parallel and perpendicular to the vehicle bending plane

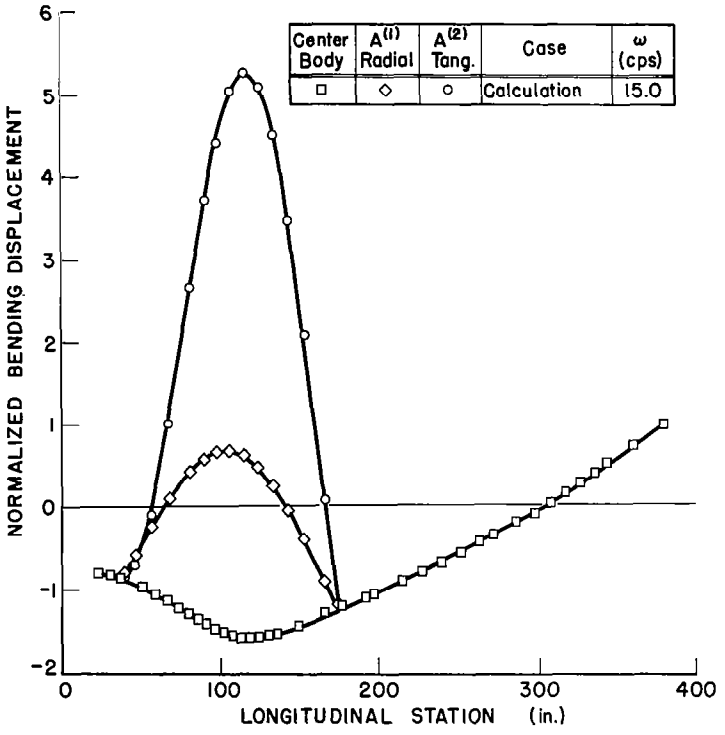

FIG. 25a 4th NATURAL MODE SHAPE
SATURN I 100% FULL MOTION OF A BODIES

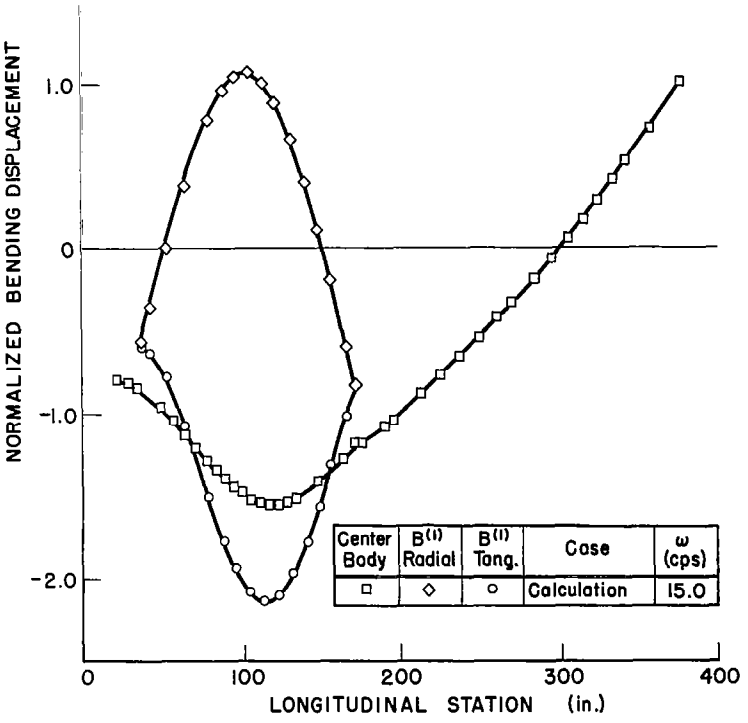

FIG. 25b 4th NATURAL MODE SHAPE
SATURN I 100% FULL MOTION OF B BODIES

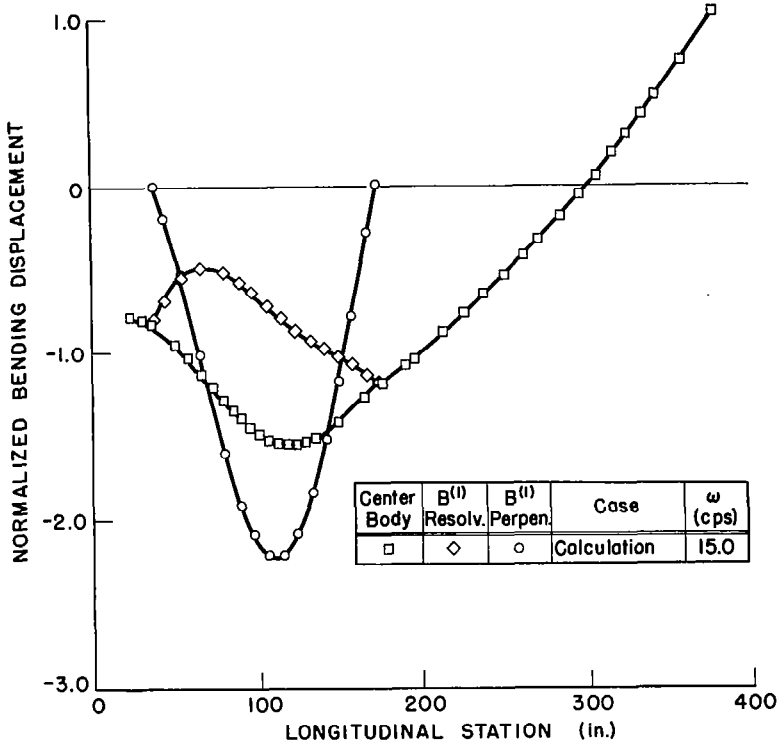

Figure 25c. 4th Natural Mode Shape – Saturn I, 100% full motion of B bodies, resolved parallel and perpendicular to the vehicle bending plane

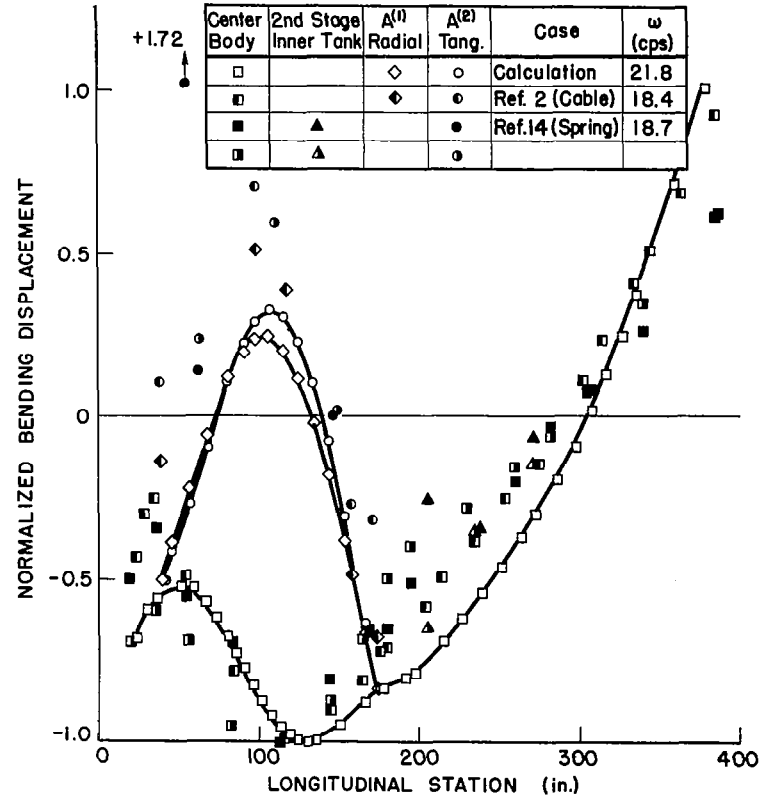

Figure 26a. 5th Natural Mode Shape – Saturn I, 100% full motion of A bodies

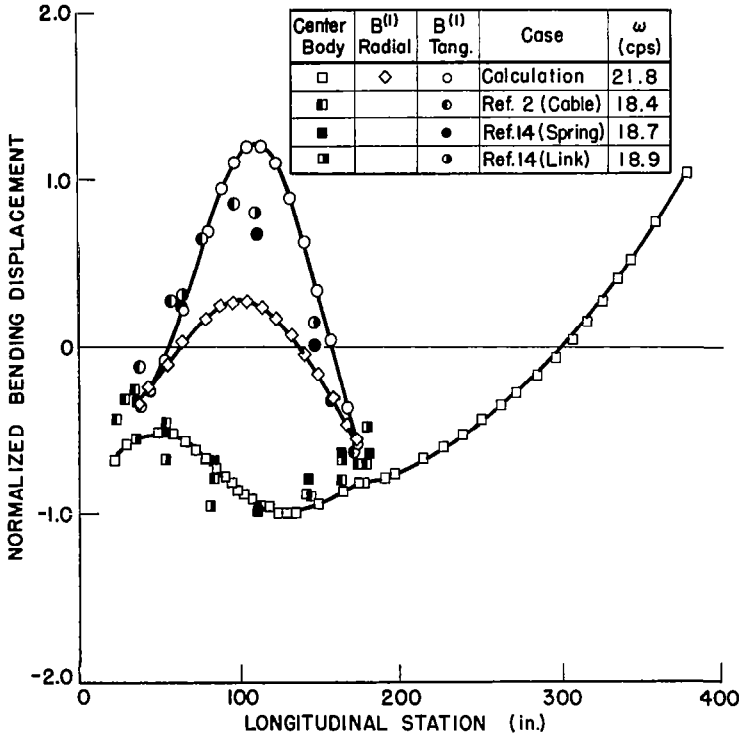

Figure 26 b. 5th Natural Mode Shape – Saturn I, 100% full motion of B bodies

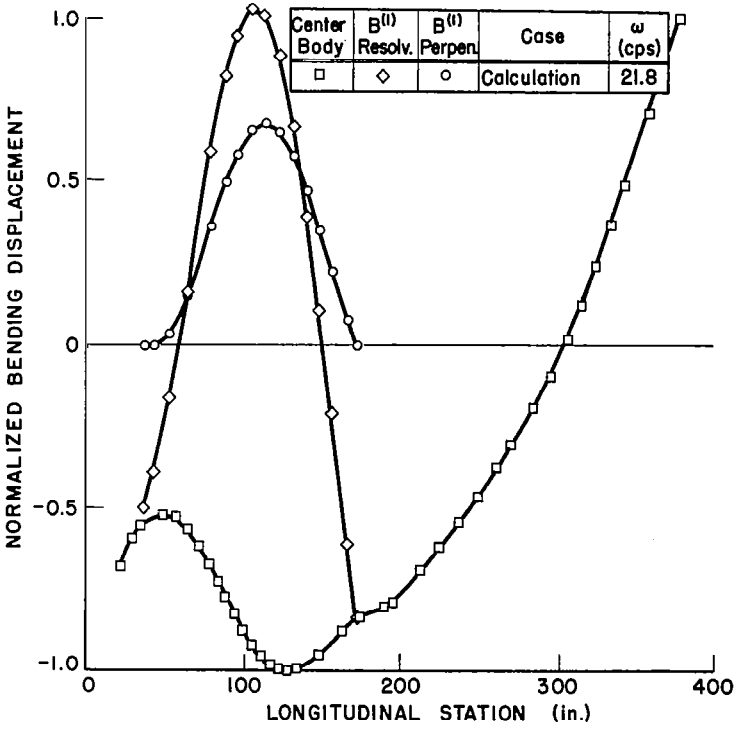

FIG.26c 5th NATURAL MODE SHAPE
SATURN I 100% FULL MOTION OF B BODIES

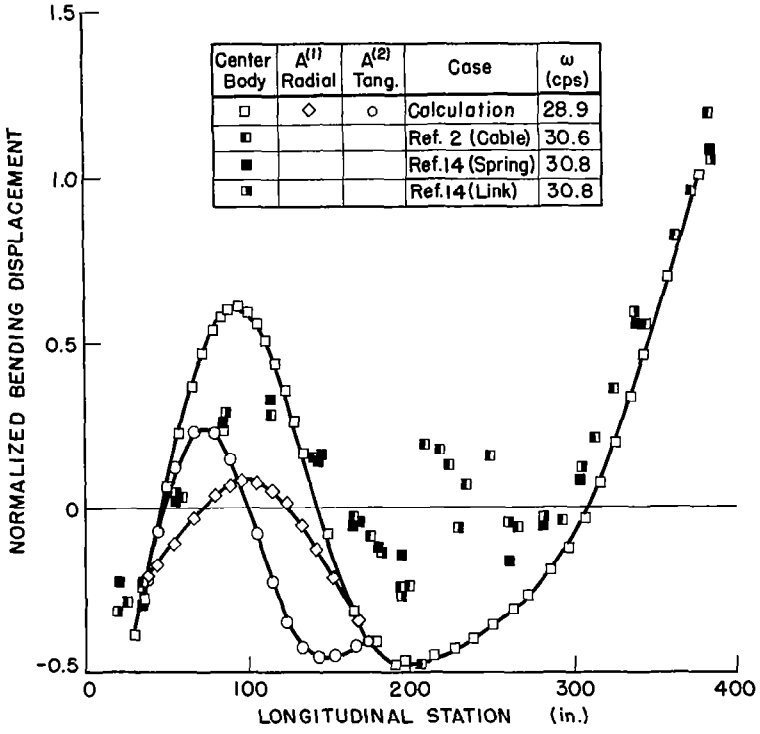

Figure 27a. 6th Natural Mode Shape - Saturn I, 100% full motion of A bodies

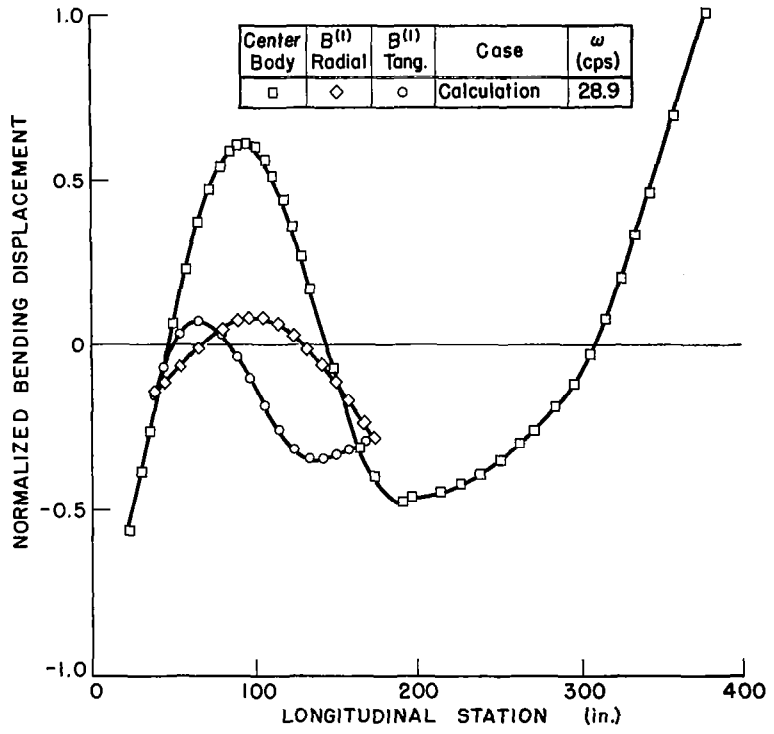

Figure 27b. 6th Natural Mode Shape – Saturn I, 100% full motion of B bodies

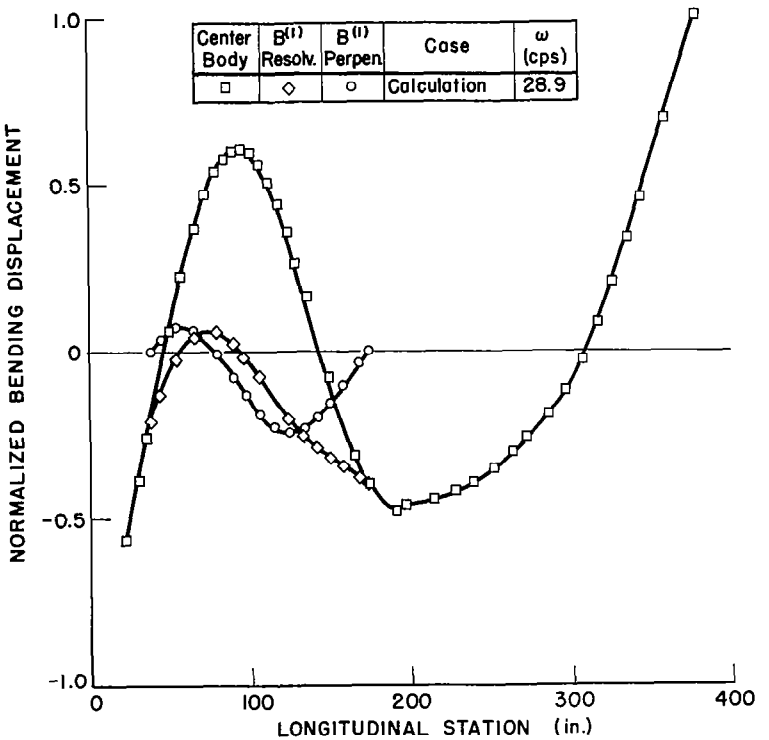

FIG.27c 6th NATURAL MODE SHAPE
SATURN I 100% FULL MOTION OF B BODIES

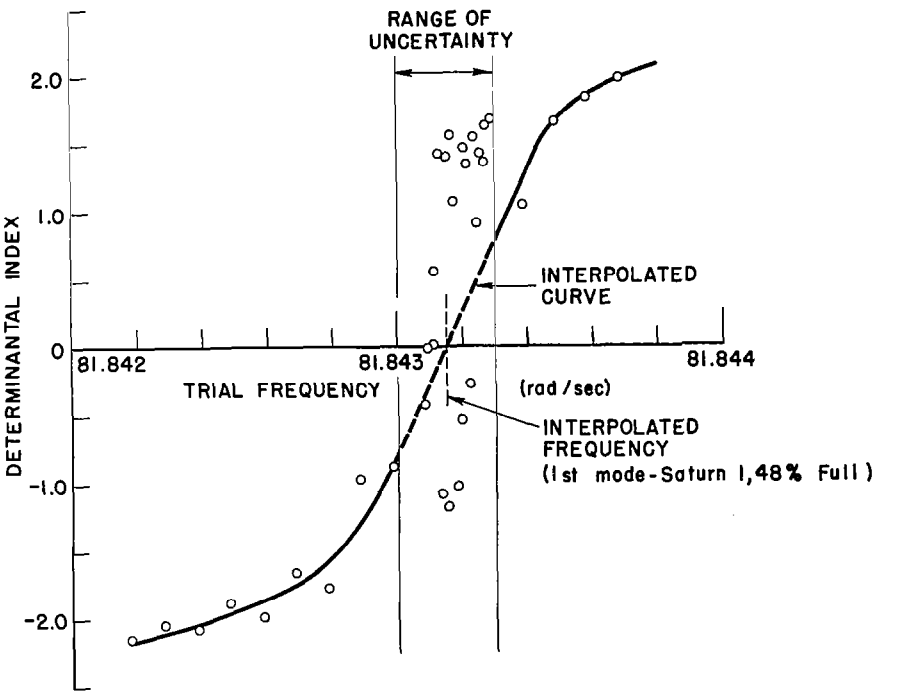

Fig. 28 TYPICAL BEHAVIOR OF FREQUENCIES ON FREQUENCY RESPONSE CURVE FOR SATURN I, 100% FULL TEST RESULTS

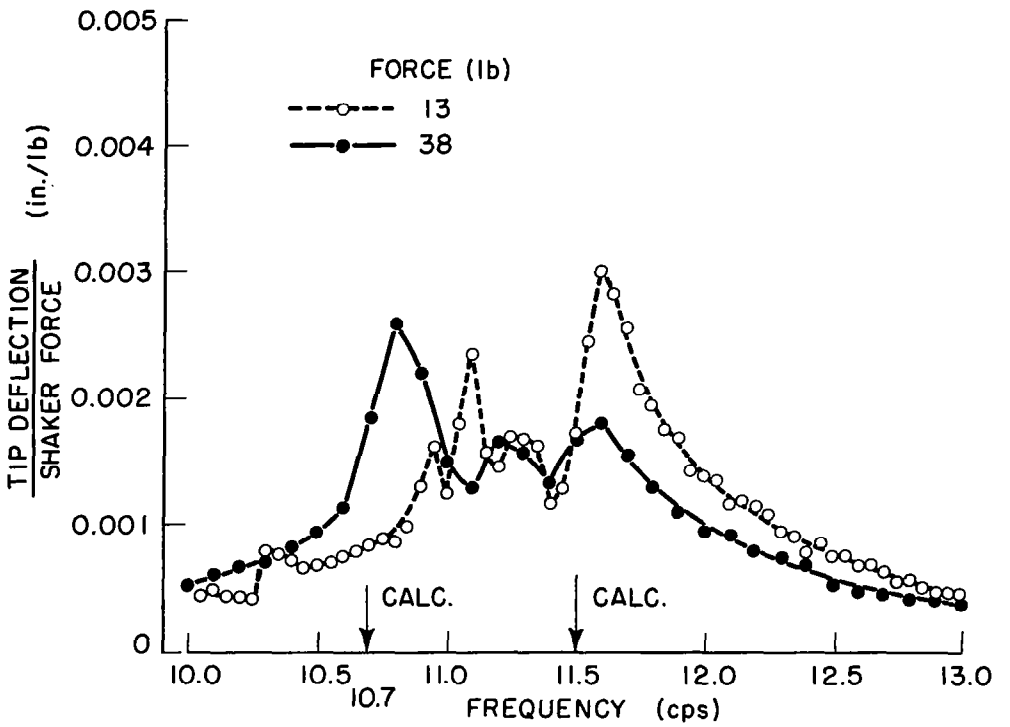

FIG. 29

COMPARISON: CALCULATED FREQUENCIES ON FREQUENCY RESPONCE CURVE FOR SATURN I, 100% FULL TEST RESULTS

III. CONCLUSIONS

A Matrix-Holzer formulation of vibration problems for branched systems has been shown to have certain conceptual and operational advantages*. A fully coupled analysis of the Titan IIIC launch vehicle programmed and allowing for the longitudinal, torsional and bi-planar bending motion of up to ten mass stations each, on the upper stages, first-stage center-body and first stage cluster bodies, respectively, can be handled within the capacity of an IBM 7074 computer. Application of the method to the prediction of the uncoupled lateral bending of the Saturn I clustered launch vehicle configuration resulted in reasonably good agreement for the first eight natural frequencies and six mode shapes, when compared with shake test results. The effects of staging joints and fuel sloshing were shown to be appreciable for the lowest modes, those due to 1g longitudinal loads were not. An assumption regarding fixity of cluster-body support points for tangential bending slope was indicated as a source of significant mode shape difference, in spite of the fact that adjacent tanks were supported by points very close to one another. There was no appreciable bending mode shape or frequency difference for the Saturn I configuration between the two distinct planes of symmetry.

The results of the study emphasize that (1) fundamental modes of clustered vehicles can have more complex curvature and node points than experience with unbranched beams would suggest and (2) internally balanced modes can exist in branched systems which will probably not be found in tests where only the center-body is excited.

---

*Just prior to completing this project, a similar approach carried out under the auspices of MSFC, Huntsville by R.F. Glaser and E.E. Beam, was called to the first author's attention. From the abstract available, the analyses seem to parallel one another.

IV. APPENDICES

Appendix A - Derivation of the Elastic Matrix

The approach taken here is to account for shear deflections and axial loands as though there is no interaction between the two.

Beam theory, accounting for deflections due to uniformly distributed shear in the web, gives the following expressions for the bending deflection and slope at the top of a uniform cantilever beam of length ℓ under a tip load V, and tip moment M (but no axial load).

$$y = \frac{M\ell^2}{2EI} + \frac{V\ell^3}{3EI}(1+\eta)$$

$$\phi = -\left[\frac{M\ell}{EI} + \frac{V\ell^2}{2EI}\right]$$

where:

$$\eta = 3\frac{E}{G}\frac{I}{ht\ell^2}$$

h = height of the web

t = thickness of the web

From Figure A-1:

$$\phi_{i+1} - \frac{V_i\ell_i^2}{2EI} - \frac{M_i\ell_i}{EI} = \phi_i$$

or,

$$\phi_{i+1} = \frac{V_i\ell_i^2}{2EI} + \frac{M_i\ell_i}{EI} + \phi_i$$

and

$$y_{i+1} = y_i + \phi_{i+1}\ell_i - \frac{M_i\ell_i^2}{2EI} - \frac{V_i\ell_i^3}{3EI}(1+\eta_i)$$

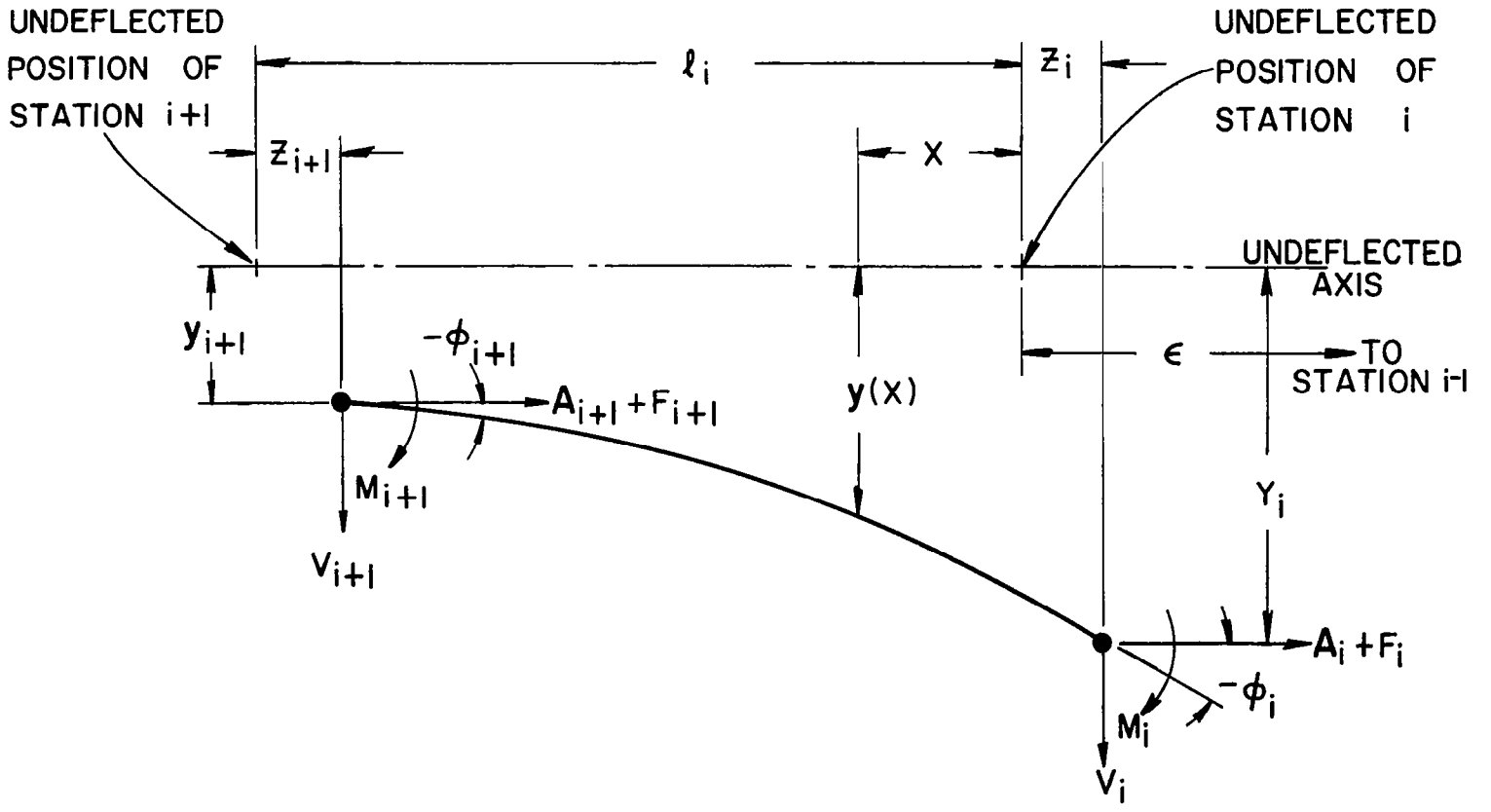

FIG. A-1 UNCOUPLED BENDING AND EXTENSILE MOTION REPRESENTATION

So that substituting the new expression for ϕ_{i+1} ,

$$y_{i+1} = \frac{V_i \ell_i^3}{3EI}\left(\frac{1}{2} - \eta_i\right) + \frac{M_i \ell_i^2}{2EI} + \phi_i \ell_i + y_i$$

Now to account for axial load effects, consider a deflected elastic beam element with constant properties under tension. The governing differential equation for this beam segment, neglecting shear deflections and second order terms, is

$$\frac{d^2y}{dx^2} = \frac{M(x)}{EI} = \frac{M_i + V_i x - A_i\left[y_i - y(x)\right]}{EI}$$

Where it is understood that $x=o$ at station i and $x=\ell$ at station $i+1$.

Rewriting the equation,

$$\frac{d^2y(x)}{dx^2} - \frac{A_i}{EI}y(x) = \frac{M_i - A_i y_i}{EI} + \frac{V_i}{EI}x$$

it is clear that the general solution is of the form

$$y(x) = A \sinh kx + B \cosh kx + Cx + D$$

Substituting this into the differential equation, and expressing (A, B, C, D) in terms of the quantities (V_i, M_i, ϕ_i, y_i) at $x = o$ we get

$$y(\ell) = y_{i+1} = V_i\left[\frac{\sinh k\ell}{kA_i} - \frac{\ell}{A_i}\right] + M_i\left[\frac{\cosh k\ell}{A_i} - \frac{1}{A_i}\right] + \phi_i \frac{\sinh k\ell}{k} + y_i$$

and $$\left(\frac{dy}{dx}\right)_{x=\ell} = \phi_{i+1} = V_i\left[\frac{\cosh k\ell}{A_i} - \frac{1}{A_i}\right] + M_i \frac{K \sinh k\ell}{A_i} + \phi_i$$

where

$$k = \sqrt{\frac{A_i}{E_i}}$$

Finally, applying station $i+1$ boundary conditions to the original expression for moment in the first equation given in this Appendix, and substituting for y_{i+1} from the above,

$$M_{i+1} = V_i \frac{\sinh k\ell}{k} + M_i \cosh k\ell + \phi_i \frac{A_i}{k} \sinh k\ell$$

Thus, from these expressions for M_{i+1}, ϕ_{i+1}, and y_{i+1}, one can write the elastic matrix for a uniform beam under axial tension load, A_i :

$$\begin{vmatrix} V \\ M \\ \phi \\ y \end{vmatrix}_{i+1} = \begin{bmatrix} 1 & 0 & 0 & 0 \\ \frac{\sinh k\ell}{k} & \cosh k\ell & \frac{A_i}{k} \sinh k\ell & 0 \\ \frac{1}{A_i}(\cosh k\ell - 1) & \frac{k}{A_i} \sinh k\ell & 1 & 0 \\ \frac{1}{A_i}\left(\frac{\sinh k\ell}{k} - \ell\right) & \frac{1}{A_i}(\cosh k\ell - 1) & \frac{\sinh k\ell}{k} & 1 \end{bmatrix}_i \begin{vmatrix} V \\ M \\ \phi \\ y \end{vmatrix}_{i+\frac{1}{2}}$$

Consider the series expansions

$$\sinh k\ell = k\ell + \frac{(k\ell)^3}{3!} + \frac{(k\ell)^5}{5!} + \cdots\cdots$$

$$\cosh k\ell = 1 + \frac{(k\ell)^2}{2!} + \frac{(k\ell)^4}{4!} + \cdots\cdots$$

Thus,

$$\frac{\sinh k\ell}{k} = \ell\left[1 + \frac{\ell^2}{3!}\frac{A_i}{EI} + \cdots\cdots\right]$$

and

$$\frac{(\cosh k\ell - 1)}{A_i} = \frac{\ell^2}{2EI} + \frac{\ell^4}{4!}\frac{A_i}{(EI)^2} + \cdots\cdots$$

which allows the elastic matrix to be simplified,

if $\frac{\ell^2 A_i}{EI} << 1$, to

$$\begin{bmatrix} 1 & 0 & 0 & 0 \\ \ell & 1 & \ell A & 0 \\ \frac{\ell^2}{2EI} & \frac{\ell}{EI} & 1 & 0 \\ \frac{\ell^3}{3EI} & \frac{\ell^2}{2EI} & \ell & 1 \end{bmatrix}_i$$

The bending elastic matrix $[E_b]$ to be used in this analysis will be, accounting for shear deflections,

$$\begin{bmatrix} 1 & 0 & 0 & 0 \\ \ell & 1 & \ell A & 0 \\ \frac{\ell^2}{2EI} & \frac{\ell}{EI} & & 0 \\ \frac{\ell^3}{3EI}\left(\frac{1}{2}-\eta\right) & \frac{\ell^2}{2EI} & \ell & 1 \end{bmatrix}_i$$

where

$$\eta_i = \left[\frac{3EI}{Ght\ell^2}\right]_i$$

Again assuming no interaction of the large steady axial load with infinitesimal extensile motion, we may, of course, write (again from Figure A-1):

$$\begin{vmatrix} F \\ z \end{vmatrix}_{i+1} = \begin{bmatrix} 1 & 0 \\ -\frac{\ell}{AE} & 1 \end{bmatrix}_i \begin{vmatrix} F \\ z \end{vmatrix}_{i+\frac{1}{2}}$$

which can be written symbolically as

$$\left|\mathcal{Z}\right|_{i+1} = \left[E_\ell\right]_i \left|\mathcal{Z}\right|_{i+\frac{1}{2}}$$

In like manner, the elastic matrix $[E_t]$. For torsion is found to have the form,

$$\begin{bmatrix} 1 & 0 \\ -\frac{\ell}{GJ} & 1 \end{bmatrix}_i$$

which is to be used in the transfer equation,

$$\left|\mathcal{T}\right|_{i+1} = \left[E_t\right]_i \left|\mathcal{T}\right|_{i+\frac{1}{2}}$$

It is to be emphasized that $V_i, M_i, \phi_i, y_i, T_i, \theta_i, F_i$ and z_i are all small quantities of the first order, while A_i is assumed to be large and constant.

For compression loads, that is when A_i is negative, the approximate form of the elastic matrix may be used directly. The exact form, however, would involve an imaginary value of k . This would simply have the effect of changing all the hyperbolic functions to trigonometric functions.

Appendix B - Derivation of Spider Beam Flexibility Terms: Saturn I

1. Lateral Bending. For lateral bending, the out-of-plane deflection of the spider beams will be antisymmetric. Thus, half of the beam, pinned at the center, may be considered, as shown in Figure B-1. The relationships between the lengths ℓ_1, ℓ_2 and ℓ_3 are shown in Figure B-2. Considering the bending expressions for a beam in antisymmetric bending(for unit shear and moment at the tip):

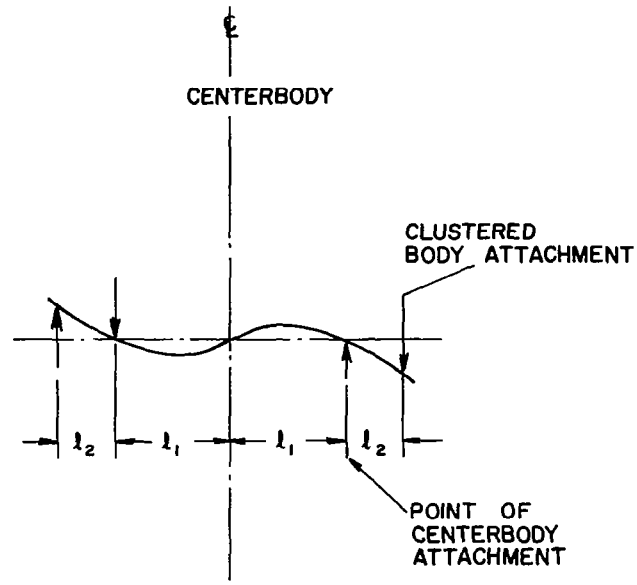

FIG. B-1 ACTUAL SPIDER BEAM BENDING IN VEHICLE TRANSVERSE BENDING - SATURN I

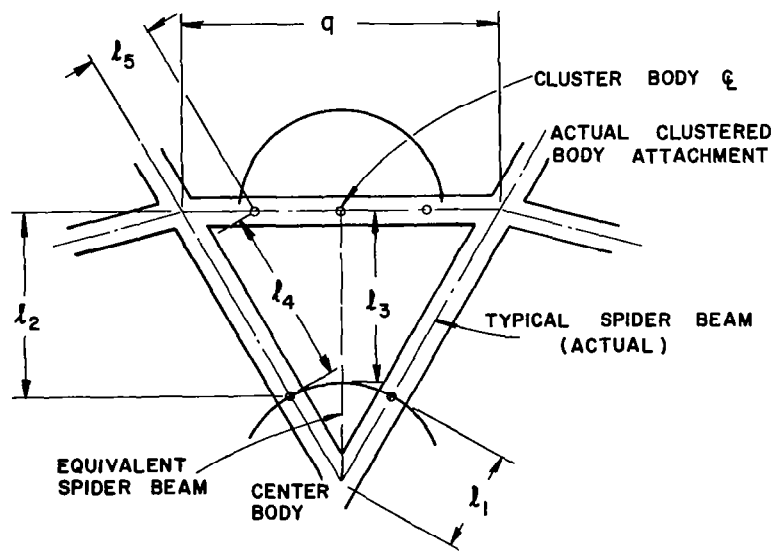

FIG. B-2 DETAILS OF SPIDER
SATURN I

$$y_V = \frac{1}{3}\frac{\ell_2^2 \ell_1}{EI} + \frac{1}{3}\frac{\ell_2^3}{EI}$$

$$y_M = \frac{1}{3}\frac{\ell_1 \ell_2}{EI} + \frac{1}{2}\frac{\ell_2^2}{EI}$$

$$\phi_V = \frac{1}{3}\frac{\ell_1 \ell_2}{EI} + \frac{1}{2}\frac{\ell_2^2}{EI}$$

$$\phi_M = \frac{1}{3}\frac{\ell_1}{EI} + \frac{\ell_2}{EI}$$

or

$$y_{n+1} = y_n + \phi_n(\ell_1+\ell_2) - V_n\left[(\ell_1+\ell_2)\frac{\ell_2^2}{3EI} - (\ell_1+\ell_2)\left(\frac{\ell_1}{3}+\frac{\ell_2}{2}\right)\frac{\ell_2}{EI}\right]$$

$$+ M_n\left(\frac{\ell_1}{3}+\frac{\ell_2}{2}\right)\frac{\ell_2}{EI}$$

Thus we can write the transfer equation

$$\begin{vmatrix} V \\ M \\ \phi \\ y \end{vmatrix}_{\text{Outb'd.}} = \begin{bmatrix} 1 & 0 & 0 & 0 \\ \ell_s & 1 & 0 & 0 \\ \bar{a} & \bar{b} & 1 & 0 \\ \bar{c} & \bar{d} & \ell_s & 1 \end{bmatrix} \begin{vmatrix} V \\ M \\ \phi \\ y \end{vmatrix}_{\text{Inb'd.}}$$

Where it is clear that for the lateral bending case, we must write:

$$\ell_s = \ell_1 + \ell_2$$

$$\bar{a} = \frac{\ell_2}{EI}\left(\frac{\ell_1}{3}+\frac{\ell_2}{2}\right)$$

$$\bar{b} = \frac{1}{EI}\left(\frac{\ell_1}{3}+\ell_2\right)$$

$$\bar{c} = \frac{\ell_2}{EI}\left(\frac{\ell_1+\ell_2}{3}\right)\left(\ell_1+\frac{\ell_2}{2}\right)$$

$$\bar{d} = \frac{1}{EI}\left(\frac{\ell_1^2}{3}+\ell_1\ell_2+\frac{\ell_2^2}{2}\right)$$

EI is the bending rigidity of the spider arms for bending in the direction along the vehicle longitudinal axis and the lengths are defined in Figure B-2.

Note that this is actually too stiff by the amount of the flexibility of spider beam arms in torsion. This term will only affect deflections due to shear (i.e., longitudinal loads) not moments, and can be considered to be a simple spring in series with a spider arm which has a clustered body attachment point on its torsion axis.

This spring rate is given by

$$\frac{GJ}{\ell_2 \ell_5^2}$$

and would modify only the term $\bar{c}$ to the value

$$\bar{c} = \frac{\ell_2 (\ell_1 + \ell_2)\left(\ell_1 + \frac{\ell_2}{2}\right)}{3EI} - \frac{\ell_2 \ell_5^2}{GJ}$$

To obtain the torsion flexibility term, $\bar{e}$, examine the deflection at the tip of the antisymmetrically bending spider beam under a unit load. Call this

$$y_V = \frac{1}{3EI}\left(\ell_1 \ell_2^2 + \ell_2^3\right)$$

If we define the distance between the support points for a single cluster tank as q, then a unit out-of-plane load in opposite directions on these two support points causes a couple of magnitude q, and an angular deflection equal to

$$\frac{2 y_V}{q} = \frac{2}{3} \frac{1}{qEI}\left(\ell_1 \ell_2^2 + \ell_2^3\right)$$

Thus, the angular deflection at the tip of an equivalent spider beam under a unit moment is

$$\frac{2}{3} \frac{1}{q^2 EI}\left(\ell_1 \ell_2^2 + \ell_2^3\right)$$

and, referring to the equation,

$$\bar{e} \triangleq -\frac{2}{3} \frac{1}{q^2 EI}\left(\ell_1 \ell_2^2 + \ell_2^3\right)$$

Here again the expression has assumed that the clustered body attachment is on the torsion axis of the spider arms. To account for the offset, it is necessary to consider the additional tangential bending slope at the clustered body, due to torsion of the spider arms. For a unit shear force at each attachment point the additional angle is

$$\frac{2\,\frac{\ell_2 \ell_5^2}{GJ}}{q}$$

Thus, the total tangential bending slope per unit tangential bending moment would be

$$\frac{2}{q^2}\left[\frac{1}{3EI}\left(\ell_1\ell_2^2+\ell_2^3\right)+\frac{\ell_2\ell_5^2}{GJ}\right]$$

and

$$\bar{e} = -\frac{2}{q^2}\left[\frac{\ell_1\ell_2^2+\ell_2^3}{3EI}+\frac{\ell_2\ell_5^2}{GJ}\right]$$

2. Longitudinal Motion. For the case of longitudinal vibrations, the spider arm bending will be symmetric, as shown in Figure B-3. In the same manner as for transverse bending, it is possible to arrive at "equivalent"spider beam flexibility members for longitudinal moses. These are:

$$\ell_s = \ell_1 + \ell_3$$

$$\bar{\bar{a}} = \frac{\ell_2}{EI}\left(\ell_1+\frac{\ell_2}{2}\right)$$

$$\bar{\bar{b}} = \frac{1}{EI}\left(\ell_1+\ell_2\right)$$

$$\bar{\bar{c}} = \frac{1}{EI}\left[\frac{\ell_2^3}{6}+\ell_1\ell_2\left(\ell_1+\frac{\ell_2}{2}\right)\right]-\frac{\ell_2\ell_5^2}{GJ}$$

$$\bar{\bar{d}} = \frac{1}{EI}\left[\frac{\ell_2^2}{2}+\ell_1\left(\ell_1+\ell_2\right)\right]$$

Here the term $\bar{e}$ will not enter.

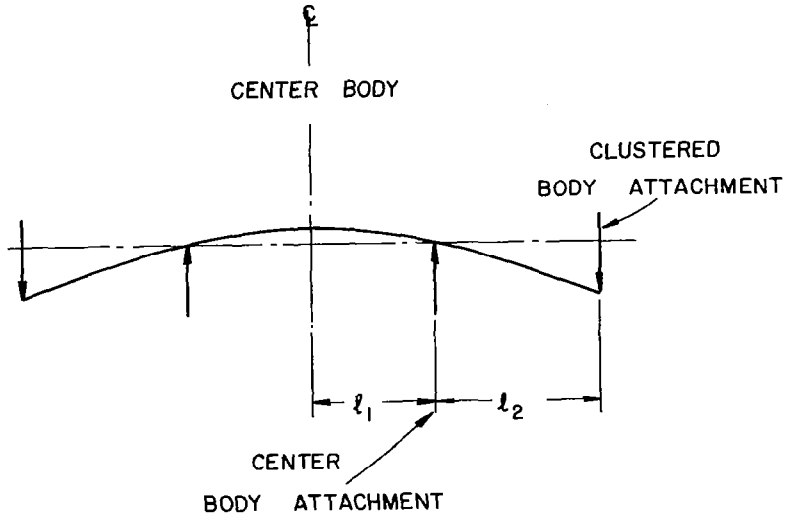

FIG. B-3 ACTUAL SPINDER BEAM BENDING IN VEHICLE LONGITUDINAL VIBRATIONS SATURN I

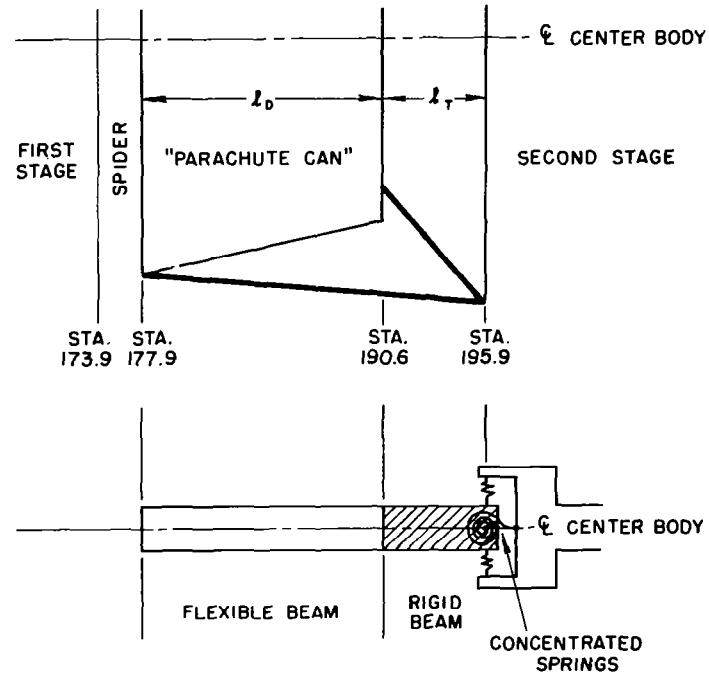

FIG. C-1 Saturn I Staging Joint Schematic and Mathematical Model

Appendix C - Derivation of Staging Joint Matrix: Saturn I

The joint could be represented as a concentrated spring at the top of the staging joint truss, with the distance between the top of the first stage and the bottom of the second stage considered as rigid. Instead, the effect of such flexibilities as the "parachute can" which exists in the Saturn I is represented as shown in the lower half of Figure C-1.

The matrix representing the change in deflection across the concentrated spring and rigid beam is arrived at as follows:

We express differences in the slopes and deflections from STA.195.86 to STA 190.635 as in the Appendix A derivation, calling them stations i and $i+1$, respectively:

$$-\phi_i - (-\phi_{i+1}) = \frac{V_i}{k_{F\phi}} + \frac{M_i}{k_{M\phi}}$$

$$\text{or} \qquad \phi_{i+1} = \phi_i + \frac{V_i}{k_{F\phi}} + \frac{M_i}{k_{M\phi}}$$

$$\text{and} \qquad y_i - y_{i+1} = \frac{V_i}{k_{Fy}} + \frac{M_i}{k_{My}} + (-\phi_{i+1})\,\ell_T$$

$$\text{or} \qquad y_{i+1} = y_i + \phi_{i+1}\,\ell_T - \frac{V_i}{k_{Fy}} - \frac{M_i}{k_{My}}$$

$$= y_i + \phi_i\,\ell_T + V_i\left(\frac{\ell_T}{k_{F\phi}} - \frac{1}{k_{Fy}}\right) + M_i\left(\frac{\ell_T}{k_{M\phi}} - \frac{1}{k_{My}}\right)$$

The transfer of bending quantities across the staging joint (i.e., from station 195.86 to station 173.868), then, is given by

$$\begin{bmatrix} 1 & 0 & 0 & \bar{\omega}^2 M_s \\ \ell_s & 1 & -\bar{\omega}^2 I_s & 0 \\ 0 & 0 & 1 & 0 \\ 0 & 0 & \ell_s & 1 \end{bmatrix} \begin{bmatrix} 1 & 0 & 0 & 0 \\ \ell_D & 1 & \ell_D A & 0 \\ \frac{\ell_D^2}{2EI} & \frac{\ell_D}{EI} & 1 & 0 \\ \frac{\ell_D^3}{3EI}\left(\frac{1}{2}-\eta\right) & \frac{\ell_D^2}{2EI} & \ell_D & 1 \end{bmatrix} \underbrace{\begin{bmatrix} 1 & 0 & 0 & 0 \\ \ell_T & 1 & 0 & 0 \\ \frac{1}{k_{F\phi}} & \frac{1}{k_{M\phi}} & 1 & 0 \\ \left(\frac{\ell_T}{k_{F\phi}} - \frac{1}{k_{Fy}}\right) & \left(\frac{\ell_T}{k_{M\phi}} - \frac{1}{k_{F\phi}}\right) & \ell_T & 1 \end{bmatrix}}_{[J_b]}$$

Note that the mass characteristics ℓ_s, M_s and I_s of the spider, assumed to be rigid, have been lumped with the staging joint. Properties in the elastic matrix are those of the "parachute can."

Similarly, for longitudinal motions, we can write:

$$\begin{bmatrix} 1 & \bar{\omega}^2 M_s \\ 0 & 1 \end{bmatrix} \begin{bmatrix} 1 & 0 \\ -\frac{\ell_D}{AE} & 1 \end{bmatrix} \underbrace{\begin{bmatrix} 1 & 0 \\ -\frac{1}{k_{Fz}} & 1 \end{bmatrix}}_{[\bar{F}]}$$

where

$\frac{1}{k_{Fz}}$ = longitudinal deflection across the joint truss for a unit longitudinal force = $.0617 \times 10^{-5}$

BIBLIOGRAPHY

1. Runyan, H.L. and Leonard, R.W., "Research, Design Considerations and Technological Problems of Structures for Launch Vehicles", NASA SP-11, Vol. 2 (1962).

2. Mixson, J.S., Catherine, J.J., Arman, A., "Investigation of the Lateral Vibration Characteristics of a 1/5 Scale Model of a Saturn SA-1," NASA TN D-1593 (1963).

3. Hung, F.C.S. and Stone, D.J., "Prediction of Stiffness and Vibration Characteristics of Trusses, Multi-Stage Cylinders, and Clustered Cylinders", ASD-TR 61-645 (1961).

4. Lianis, G. and Fontenot, L.L., "Analysis of Vibrations of Clustered Boosters", AIAA J. 1, 607-616 (1963).

5. Bisplinghoff, R.L., Ashley, H., and Halfman, R.L., "Aeroelasticity", (Addison-Wesley Publishing Co., Inc., Cambridge, Mass., 1955), 1st Ed. Chap. 4, p. 164-168

6. Storey, R.E., "Dynamic Analysis of Clustered Boosters with Application to Titan III", AIAA Preprint No. 63-208 (1963).

7. Milner, J.L., "Three Dimensional Multiple Beam Analysis of a Saturn I Vehicle", NASA TMX 53098 (1964).

8. Keith, J.S. et al., "Methods in Structural Dynamics for Thin Shell Clustered Launch Vehicles", FDL-TDR-64-105 (1965).

9. Targoff, W.P., "The Associated Matrices of Coupled Bending Torsion", J. Aerospace Sci. 14, 579-582, (1947).

10. Thompson, W.T., "Matrix Solution for the Vibration of Nonuniform Beams", J. Applied Mech., 337-339 (1950).

11. Pestel, E.C. and Leckie, F.A., "Matrix Methods in Elastomechanics", (McGraw-Hill Book Company, 1963), Chap. 3, p. 55-59; Chap. 6.

12. Turner, M.J. et al., "Stiffness and Deflection Analyses of Complex Structures", J. Aerospace Sci. 23, 805-823 (1956).

13. Abramson, H.N., Wen-Hwa Chu, and Ransleben, G.E., Jr., "Representation of Fuel Sloshing in Cylindrical Tanks by an Equivalent Mechanical Model", ARS J. 312, 1697-1705 (1961).

14. Mixson, J.S., and Catherine, J.J., "Experimental Lateral Vibration Characteristics of a 1/5-Scale Model of Saturn SA-1 with an Eight-Cable Suspension System", NASA TN-D-2214.

15. Lamb, H., "Hydrodynamics", Dover Publications, 1945.

16. Joglekar, M.M., "Dynamic Analysis of Clustered Booster Structures Using the Matrix Holzer Technique", M.S. Thesis, University of Rochester, June, 1965.